

# NOVEL VARIANT FOR APPLICATION AS A PROLONGED RELEASE DRUG DELIVERY SYSTEM

---

**TEBOHO KGESA**

A dissertation submitted to the Faculty of Health Sciences,  
University of the Witwatersrand, in fulfilment of the requirements for the degree of Master of  
Science in Medicine



**Supervisor**

Professor Viness Pillay, University of the Witwatersrand, Department of Pharmacy and  
Pharmacology, South Africa

**Co-Supervisors**

Professor Yahya E. Choonara, University of the Witwatersrand, Department of Pharmacy  
and Pharmacology, South Africa

**Co-Supervisors**

Dr. Lisa C. du Toit, University of the Witwatersrand, Department of Pharmacy and  
Pharmacology, South Africa

**2015**

## DECLARATION

I, Teboho Kgesa, declare that this dissertation is my own work. It has been submitted for the degree of Master in Medicine in the field of Pharmacy in the Faculty of Health Sciences at the University of Witwatersrand, Parktown, Johannesburg, South Africa. It has not been submitted before for any degree or examination at this or any other University.

.....

**This ..... day of**

## **ANIMAL ETHICS DECLARATION**

I, Teboho Kgesa hereby confirm that the research project received the approval from the Animal Ethics Screening Committee (AESC) of the University of the Witwatersrand with Ethics Clearance Number (2011/33/03).

## **RESEARCH PUBLICATIONS**

Review: Disulphide/Thiol Chemistry: A Versatile Tool for Implementing Contemporary Macromolecular Polymer and Material Design for Drug Delivery. Teboho Kgesa, Viness Pillay, Yahya E. Choonara, Valence M.K., Ndesendo, Lisa du Toit, Pradeep Kumar.

Research Paper I: Optimisation of the Novel Functionalised Thiol Drug Delivery Carrier System. Teboho Kgesa, Viness Pillay\*, Yahya E. Choonara, Valence M.K. Ndesendo, Lisa du Toit, Pradeep Kumar. To be submitted.

Research Paper II: Characterization of the Novel Thiol Functionalized Ovalbumin Polymer. Teboho Kgesa, Viness Pillay\*, Yahya E. Choonara, Valence M.K. Ndesendo, Lisa du Toit and Pradeep Kumar. To be submitted.

## **PODIUM PRESENTATIONS**

2013 Fifth Cross-Faculty Graduate Symposium. Thiol Chemistry: A Versatile Tool for Implementing Contemporary Macromolecular Polymer and Material Design for Drug Delivery. Teboho Kgesa, Viness Pillay\*, Yahya E. Choonara, Valence M.K. Ndesendo, Lisa du Toit and Pradeep Kumar.

## **PATENTS**

Novel Functionalised Thiol Drug Delivery Carrier System. Teboho Kgesa, Viness Pillay\*, Yahya E. Choonara, Valence M.K. Ndesendo, Lisa du Toit, Pradeep Kumar. To be submitted.

## **DEDICATION**

I dedicate this written dissertation to my parents, Petrus Kgesa and Ruth Sizakele Kgesa for their continuous love and support. Your dedication and support surpasses all.

## ACKNOWLEDGEMENTS

I acknowledge Prof. Viness Pillay, my supervisor, for providing me with an opportunity to study under his expert guidance.

Thanks to Prof. Yahya Choonara and Dr. Lisa du Toit for your constructive criticism of the research project and research papers.

To Dr. Ndidi Ngwuluka, Dr. Steven Mufamadi and Mr. Pradeep Kumar your help and guidance have been received with great appreciation.

To Dr. Charu and Dr. Lomas, thank you for your assistance in providing me with constructive criticism on submitted research papers.

I would like to thank Ass. Prof. Michael P. Danckwerts, head of the Department of Pharmacy and Pharmacology, University of the Witwatersrand, for the support he provided me as the head of department.

I thank the Animal Ethics Screening Committee (AESC) and members of staff of the Central Animal Services (CAS), University of the Witwatersrand who include; Prof. Graham Alexander, Ass. Prof. Kennedy H. Erlwanger, Dr. Leith Meyer, Ms. Mary-Anne Costello, Ms. Amelia Rammekwa, Ms. Kershnee Chetty, Ms. Lorraine Setimo, Mr. Patrick Selahle and Mr. Nico Douths, for the animal ethics approval and the technical assistance they provided me in performing my *in vivo* studies.

I thank Prof. Valence M.K. Ndesendo provided me with technical, scientific and research advice.

I thank the technical staff in the Department of Pharmacy and Pharmacology, University of Witwatersrand including; Mr. Sello Ramarumo, Mr. Bafana Themba, Mr. Kleinbooi Mohlabi, Ms. Busisiwe Damane for all the assistance they provided which made my work in the laboratories and office easier.

Last but not the least: To all of the Wits Advanced Drug Delivery Platform team, my sincerest gratitude to you. Without you, it would have been a long tedious journey. Your attitude, resilience, perseverance and sense of humour have been pivotal in motivating me to complete my research and attain my degree.

## ABSTRACT

The dissertation aims to discuss the disulphide and thiol chemistry for use in drug delivery. In particular it focuses on the use of the modified native ovalbumin polymer as a vehicle for the thiol containing captopril. The binding capabilities of thiols expand the area in which peptides and proteins can be used as potential therapeutic drug carriers. It is important that drug delivery systems enhance drug storage stability and *in vivo* particle stability while delivering the drug efficiently. As part of the developing novel drug delivery systems, thiol-based chemical reactions are distinctive role players in stabilizing disulphide bioconjugated nanostructures for use as efficient drug carrier vehicles *in vivo*. A review of the current approaches for designing, optimizing and functionalizing nanostructures and conjugates by thiol chemistry modifications was explored. Captopril (Cp) is an Angiotensin-Converting Enzyme (ACE) inhibitor, which acts as an anti-hypertensive, structurally contains a free reactive thiol that binds variably via the thiol/disulphide reaction. A single dose of captopril can regulate hypertension for up to eight hours and the duration of the antihypertensive action of a single dose of 35-75 mg would be taken at 8 hour intervals for 24 hours. Hence the necessities in developing a sustained controlled release ovalbumin carrier system to maintain relatively constant blood pressure levels for 24 hours. The research focused on the construction, characterization and optimization of the thiol conjugated complex for sustained oral drug delivery. The thiol/disulphide-functionalized captopril-ovalbumin conjugate complex was assessed in terms of the structural characteristics and the thiol-disulphide covalent substitution reaction. For analysis of the conjugation complex, the Fourier Transmission IR-spectroscopy (FTIR),  $^1\text{H}$  NMR and Differential Scanning Calorimetry (DSC) was performed and used to confirm conjugation. Preliminary studies focused on a comparative study of sodium alginate, polyvinyl alcohol and hydroxypropylmethylcellulose hydrogel formulations for the release testing and drug entrapment of the ovalbumin-captopril conjugate complex. Utilizing this data, a series of process variables were used to achieve an optimized formulation through a Box- Behnken statistical design. Furthermore the drug release profiles of the optimised formulation were then analyzed *in vitro* and *in vivo*. The captopril released from the formulation was high with a cumulative release of 82%. *In vivo* analysis was the final testing to verify the validity of the ovalbumin-captopril conjugate complex encapsulated in sodium alginate and utilized a pig model. Ultra Performance Liquid Chromatography (UPLC) blood analysis revealed increased blood levels of captopril ( $C_{\text{max}} \text{ Cp}=33.2\text{ng/mL}$ ) in relation to conventional dosage forms validating prolonged (24 hour) site-specific release and increased bioavailability. In conclusion, our validated method was successfully applied to the pharmacokinetic studies of captopril in the blood plasma samples.

## TABLE OF CONTENTS

---

---

	<b>Page</b>
DECLARATION	I
ANIMAL ETHICS DECLARATION	II
RESEARCH PUBLICATIONS	III
PODIUM PRESENTATIONS	III
DEDICATION	IV
ACKNOWLEDGEMENTS	V
ABSTRACT	VI
LIST OF FIGURES	XIII
LIST OF EQUATIONS	XVII

### CHAPTER 1

#### **Novel Application of Ovalbumin as an Effective Drug Delivery Vehicle**

1.1. Introduction	1
1.2. Rational and motivation	2
1.3. Novelty of the study	3
1.4. Aim and objectives of the study	4
1.5. Overview of the dissertation	5

### CHAPTER 2

#### **Disulphide/Thiol Chemistry: A Versatile Tool for Implementing Contemporary Macromolecular Polymer and Material Design for Drug Delivery**

2.1. Introduction	7
2.2. Thiol based click chemistry	11
2.2.1 Thiol-epoxy click reactions	14
2.2.2 Thiol-isocyanate nucleophilic addition click reactions	15
2.2.3 Thiol-halogen nucleophilic substitution click reactions	17
2.2.4 Thiol-ene/Thiol-yne Michael-type addition click chemistry	20



2.3. Thiol based defined architectures containing disulphide conjugates	22
2.3.1 Hyperbranched/Multiarmed star polymers	22
2.3.2 Micelles	23
2.3.3 Nanogels	25
2.3.4 Hydrogels	26
2.3.5 Thiomers	28
2.4. Bioconjugation for drug delivery	28
2.4.1 Disulphide bond linkages	29
2.4.2 Creating thiols via chemical and molecular approaches	30
2.4.3 Disulphide drug delivery systems	30
2.4.3.1 Macromolecular drug delivery uptake via endocytosis	30
2.4.3.2 Attachment by targeting moiety through thiols	31
2.4.3.3 Disulphide cleavage in the circulatory system	31
2.5. Mucoadhesion nanoparticle system	31
2.5.1. Improvising thiomers for better mucoadhesion	32
2.5.1.1 Formation of disulphide bonds with the mucus gel layer	32
2.5.1.2 In situ cross-linking process	33
2.5.2. Dosage forms of thiomers	33
2.5.3. Current sulfur conjugates	34
Concluding Remarks	

### **CHAPTER 3**

#### **Disulphide/Thiol Covalent Chemistry: A Method for Preparing Selectively Functionalised Captopril-Ovalbumin Drug Delivery Conjugates**

3.1.1. Introduction	36
3.2. Material and Methods	38
3.2.1. Materials	38

3.2.2. Methods	38
3.2.2.1. Purification and preparation of the native Quail hen eggs for analysis	38
3.2.2.2. Reduction of the disulphide bonds of the native ovalbumin into thiols	38
3.2.2.3. Characterization of the native ovalbumin and thiol modified ovalbumin	39
3.2.2.4. UV analysis for the determination of the thiol concentrations	39
3.2.2.5. Size and zeta-potential of the the native and modified ovalbumin	39
3.2.2.6. The conjugation of the modified thiol ovalbumin containing captopril	40
3.2.2.7. UV analysis for the determination of the thiol concentrations	40
3.2.2.8. UV analysis of the ovalbumin-captopril complex	40
3.2.2.9. ATR-FTIR analysis of the native, thiol and ovalbumin-captopril	40
3.2.2.10. H <sup>+</sup> NMR analysis of the native and thiol modified ovalbumin	41
3.2.2.11. Rheological analysis of the native, thiol and ovalbumin-captopril	41
3.2.2.11.1. Yield stress test of native, thiol and ovalbumin-captopril	42
3.2.2.11.2. Viscosity of the native, thiol and ovalbumin-captopril	42
3.2.2.11.3. Oscillatory stress sweep of the native, thiol and ovalbumin-captopril	43
3.2.2.11.4. Oscillatory frequency sweep of the native, thiol and ovalbumin-captopril	43
3.2.2.11.5. Oscillatory thermal analysis of the native, thiol and ovalbumin-captopril	43
3.2.2.11.6. Thermal characterization of the of the native, thiol and ovalbumin-captopril	43
3.3. Results and Discussion	44
3.3.1. Morphological characterization of the disulphide native ovalbumin polymer	44
3.3.2. Size and zeta-potential comparison of the ovalbumin polymer	44
3.3.3. ATR-FTIR spectroscopy of the native, thiol and ovalbumin-captopril	45
3.3.4. H <sup>1</sup> NMR Spectrum	48
3.3.5. Conjugation efficiency and captopril content	50
3.3.6. Thermal analysis of the variant ovalbumin complex	51
3.3.7. Thermal characterization of the native ovalbumin and its conjugate	52
3.3.8. Rheological analysis of the of the ovalbumin complex	55
3.3.8.1. Oscillation Stress Sweep	55

3.3.8.2. Frequency sweep	57
3.3.8.3. Oscillation Stress Sweep	58
3.3.8.4. Physicomechanical properties of ovalbumin	59
3.4. Concluding Remarks	

## **CHAPTER 4**

### **Sustained Delivery of Captopril from the Ovalbumin Drug Carrier System**

4.1. Introduction	61
4.2. Materials and Methods	64
4.2.1 Materials	64
4.2.2. Preparation of the thiolated ovalbumin conjugates	64
4.2.3. Preparation of nanoparticles	65
4.2.3.1. Synthesis of ovalbumin-captopril nanoparticles	65
4.2.4. ATR-FTIR spectroscopy of NaAlg, PVA, and HPMC hydrogel matrices	66
4.2.5. Thermal characterization of NaAlg, PVA, and HPMC hydrogel matrices	66
4.2.6. Drug encapsulation efficiency of NaAlg, PVA, and HPMC hydrogel matrices	66
4.2.7. Morphological characterisation of the each ovalbumin carrier hydrogel formulation	67
4.2.8. Weight Variation of the NaAlg, PVA, and HPMC hydrogel matrices	67
4.2.9. Swelling index of the NaAlg, PVA, and HPMC hydrogel matrices	67
4.2.10. Rheological characterisation of the NaAlg, PVA, and HPMC hydrogel matrices	67
4.2.11. <i>In vitro</i> Drug release of the NaAlg, PVA, and HPMC hydrogel matrices	68
4.3. Results and Discussion	69
4.3.1. Morphological studies of NaAlg, PVA, and HPMC nanoparticles	69
4.3.2. Size and swelling of the NaAlg, PVA, and HPMC particles	70
4.3.3. IR spectra for the NaAlg, PVA, and HPMC nanoparticles	72
4.3.4. Thermal analysis of the NaAlg, PVA, and HPMC nanoparticles	73

4.3.5. Newtonian Flow model for NaAlg, PVA, and HPMC nanoparticles	74
4.3.6. Captopril release of the NaAlg, PVA, and HPMC nanoparticles	77
4.3.7. Release order analysis of the NaAlg, PVA, and HPMC nanoparticles	77
4.4. Concluding Remarks	

## **CHAPTER 5**

### **Limiting Factors Affecting the Release of Captopril form the Ovalbumin-Captopril Carrier System**

5.1. Introduction	79
5.2. Analysis of the thermal effects on the sodium alginate nanoparticles	82
5.2.1. Materials and Methods	82
5.2.2. Materials	82
5.2.3. Methods	82
5.2.3.1. Effects of the pH and salt concentrations of the ovalbumin native polymer	82
5.2.3.2. Limiting factors affecting captopril release from the ovalbumin carrier system	82
5.2.3.2.1. Preparation of the sodium alginate ovalbumin captopril particles	82
5.2.3.2.2. Drug Release Analysis	83
5.3. Results and Discussion	83
5.3.1. Results	83
5.3.1.1. Effects of pH and salt on the denaturation of the ovalbumin protein	83
5.4.2. Drug Release Analysis	86
5.5. Concluding Remarks	

**CHAPTER 6**  
**Optimisation of the Ovalbumin Drug Carrier System**

6.1. Introduction	91
6.2. Materials and Methods	92
6.2.1. Materials	92
6.2.2. Methods	92
6.2.2.1. Preparation of the ovalbumin drug delivery hydrogel matrices in accordance with the Box-Behnken experimental design template	92
6.2.2.2. Preparation of the calibration curves for captopril in simulated intestinal fluid (pH 6.8)	95
6.3. Results and Discussion	96
6.3.1. Cumulative drug release profiles of the Box-Behnken experimental design	96
6.3.2. Elucidation of the variable responses using the Box-Behnken Design	99
6.3.2.1. Surface Plots	99
6.3.2.2. Comparative of the Box-Behnken formulations for size and zeta-potential	101
6.3.2.3. Response surface analysis of the mean dissolution time and drug entrapment efficiency	101
6.3.2.4. Residual Plots of the optimised ovalbumin-captopril formulations	103
6.4. Response Optimised	105
6.4.1. Fabrication of the optimised formulation	105
6.4.2. Application of the desirability functions for size and zeta-potential	105
6.5. Concluding Remarks	

**CHAPTER 7**  
**In Vivo Investigation and Analysis of the Optimised Ovalbumin Prolonged Drug Delivery System**

7.1. Introduction	109
7.2. Materials and Methods	112
7.7.2.2. <i>In vivo</i> ethics clearance	112
7.2.1. Materials	112

7.2.3. Habituation and housing	113
7.3. Jugular venous catheterization for blood sampling	113
7.3.1. Captopril gastric dosing and formulation testing	115
7.4. Ultra Performance Liquid Chromatography for blood analysis	117
7.4.1. Chromatographic method for detecting captopril and hydrochlorothiazide in blood plasma	117
7.4.2. Preparation of the hydrochlorothiazide and captopril calibration curves in plasma	118
7.4.3. Extraction of bioactives in blood plasma	117
7.5. Pharmacokinetic modelling and analysis of captopril and hydrochlorothiazide <i>in vivo</i>	118
7.6. Results and Discussion	119
7.6.1. Method Validation for captopril and hydrochlorothiazide in blood plasma	119
7.6.2. Recovery Efficiency of captopril and hydrochlorothiazide	119
7.6.3. <i>In vivo</i> blood analysis of captopril and hydrochlorothiazide	121
7.6.3.1. Captopril and hydrochlorothiazide analysis using Ultra Performance Liquid Chromatography (UPLC)	121
7.6.3.1.2. Comparison of the pharmacokinetics parameters of the ovalbumin captopril carrier system against the conventional	122
7.7. Concluding Remarks	122

## **CHAPTER 8**

### **Conclusion and Recommendations**

8.1. Conclusion	124
8.2. Recommendations	126
REFERENCES	127

## **APPENDICES**

A. Approvals	
A.1. Ethics Clearance Approval Certificate	
B. Publications	
B.1. Review Abstract	
B.2. Research paper abstract	

## LIST OF FIGURES

---

- Fig.1.1.** Schematic diagram representing the forms of ovalbumin
- Fig.2.1.** General thiol structures including multifunctional thiols
- Fig.2.2.** The covalent attachment reaction between epoxy and the thiolated proteins
- Fig.2.3.** Nucleophilic halogen substitution reaction
- Fig.2.4.** Preparation of glycopolymers from pentafluorostyrene (PFS) reaction with SH.
- Fig.2.5.** Microscopy images of layer-by-layer assembly of hydrogen bonded multilayers
- Fig.2.6.** a) Synthesis of the functionalised poly(n-butyl acrylate) star polymer
- Fig.2.7.** Synthesis of the thiol functionalised poly(pyridyldisulfide ethylmethacrylate)
- Fig.2.8.** a) The synthesis of branched Poly(BAC2-AEPZ1)-PEG
- Fig3.1.** Illustrates the conjugation of one ovalbumin cysteine
- Fig.3.2.** The IR spectra of captopril
- Fig.3.3.** IR-spectroscopy showing the comparison of the native unmodified OVA
- Fig.3.4.** IR-spectroscopy of the thiol modified Ova
- Fig.3.5.** The absorbance of modified OVA
- Fig.3.6.** Comparison of conjugate polymers dispersed in deionised water
- Fig.3.7.**  $^1\text{H}$  NMR Spectrum of N-OVA-disulphide
- Fig.3.8.** Differential scanning thermogram of the thiol containing Captopril
- Fig.3.9.** Comparative thermogram illustrating the change in the glass transition temperatures
- Fig.3.10.** Non-reversing and reversing heat flows derived from the ADSC ovalbumin
- Fig.3.11.** Frequency sweep of the conjugate complex, ovalbumin and captopril
- Fig.4.1.** The graphs represent the comparative size and zeta-potential values of the three nanohydrogels

**Fig.4.2.** Comparative FTIR spectra for captopril nanohydrogels

**Fig.4.3.** Comparative FTIR spectra for captopril nanohydrogels.

**Fig.4.4.** Differential scanning thermogram for the NaAlg-, PVA- HPMC-OVA microparticle

**Fig.4.5.** Calibration curve for captopril

**Fig.4.6.** Comparative drug release profiles of the three hydrogel composites

**Fig.4.7.** Comparative cumulative drug release profiles of the zero- and first order, Higuchi and Korsmeyers-peppas drug release orders

**Fig.5.1.** Comparative drug release profile of the ovalbumin (OVA) variable

**Fig.5.2.** Comparative drug release profile of the sodium alginate (NaAlg) variable

**Fig.5.3.** Comparative drug release profile of the calcium chloride (CaCl<sub>2</sub>) variable

**Fig.5.4.** Comparative drug release profile of the pH

**Fig.6.1.** Drug release profiles for F 1-4

**Fig.6.2.** Drug release profiles for F 5-8

**Fig.6.3.** Drug release profiles for F 9-12

**Fig.6.4.** Drug release profiles for F 13-15

**Fig.6.5.a.** 3-D Response surface showing average particle size of the nanoparticles

**Fig.6.5.b.** 3-D Response surface showing average zeta-potential of the nanoparticles

**Fig.6.5.c.** 3-D Response surface showing percentage drug entrapment efficiency.

**Fig.6.5.d.** Contour plot showing on the mean dissolution time

**Fig.6.5.e.** Contour plot showing the the mean dissolution time

**Fig.6.5.f.** Contour plot showing the on the cumulative drug release percentage

**Fig.7.1.** The structural formulae of captopril (I) and hydrochlorothiazide (II)

**Fig.7.2.** Catherter insertion surgery- showing the pre, mid and post-surgery

**Fig.7.3.** Preparation pre-oral administration of drug delivery system



**Fig.7.4.** Summary of the in vivo animal studies experimentation procedure

**Fig.7.5.** Separation of captopril and IS derivatives with hydrochlorothiazide

**Fig.7.6.** Separation of captopril and IS derivatives with hydrochlorothiazide from spiked plasma samples. (a) EIC characteristic to the specific product ion of captopril.

## LIST OF TABLES

---

**Table 2.1.** Examples of Thiol Reactions used in Polymer Synthesis.

**Table 3.1.** Drug content and conjugation efficiency of different captopril-ovalbumin conjugate.

**Table 4.1.** Hydrogel polymers and their intended application.

**Table 4.2.** Parameters for the formulation preparation.

**Table 4.3.** Compositions of the three hydrogel formulations.

**Table 4.4.** Compositions of the three hydrogel formulations.

**Table 4.5.** Average size distribution of the hydrogel nanoparticles before and after swelling of nanoparticles.

**Table 4.6.** Summary table for the thermal characterisation of the three hydrogel composites.

**Table 4.7.** Kinetics Parameters of Hydrogel Loaded with OVA microspheres and Pure Drug.

**Table 5.1.** Limit determinations of the upper and lower variables.

**Table 6.1.** Rationale for the selection of the compound employed in the formulation of the system.

**Table 6.2.** Levels of independent variables employed in the Box-Behnken design template.

**Table 6.3.** Box-Behnken Template for the preparation of each of the 15 formulations.

**Table 6.4.** Targets for the selected response parameters.

**Table 6.5.** Cumulative Results of the independent variables of the Box-Behnken Experimental Template.

**Table 7.1.** The amount of drugs to be used for the animal study.

**Table 7.2.** Statistic interpretation of pharmacokinetic parameters corresponding to captopril in tested pharmaceutical formulations against the reference (conventional) product.

## LIST OF EQUATIONS

---

Equation 3.1: Absorbance

$$E = \frac{A}{bc}$$

Where A=absorbance, b= path length in centimetres, c=concentration in moles/litre (=M).

Equation 3.2: Conjugation efficiency (%)

$$\text{Conjugation efficiency (\%)} = \frac{\text{weight of drug found conjugated}}{\text{weight of total drug used}} \times 100$$

Equation 3.3: Drug content (%<sup>w/w</sup> %)

$$\text{Drug content (\%}^w/w\text{)} = \frac{\text{weight of drug conjugated}}{\text{weight of conjugate}} \times 100$$

Equation 4.1: Drug encapsulation efficiency

$$\text{DEE} = \frac{M_i - M_d}{M_i} \times 100\%$$

Where  $M_i$  is the initial amount of ovalbumin-captopril dissolved in the hydrogel solution and  $M_d$  the amount of hydrogel mass measured in the gelling media ( $\text{CaCl}_2 \cdot 2\text{H}_2\text{O}$  solution).

Equation 4.2: Swelling ratio

$$Q_s = \frac{S_s - S_d}{S_d} \times 100$$

Where  $S_d$  is the weight of the capsule dry state.  $S_s$  the weight in the capsule's swollen state.

Equation 4.3: Zero-order model

$$Q_t = Q_0 + K_0 t$$

Where  $Q_t$  is the amount of drug dissolved in time  $t$ ,  $Q_0$  is the initial amount of drug in the solution (most times,  $Q_0 = 0$ ) and  $K_0$  is the zero order release constant expressed in units of concentration/time. Values of  $0.5 < n < 1$  indicate non-Fickian or anomalous mechanism due to both diffusion and polymer chain relaxation.

Equation 4.4: First order model

$$\frac{dC}{dt} = -kC$$

Where  $k$  is first order rate constant expressed in units of  $\text{time}^{-1}$ . Equation (5) can be expressed as:  $\log C = \log C_0 - kt / 2.303$  (6) where  $C_0$  is the initial concentration of drug,  $k$  is the first order rate constant, and  $t$  is the time.

Equation 4.5: Higuchi model

$$Q = A \sqrt{D} (2C_0 - C_s) \sqrt{C_s t}$$

Where  $Q$  is the amount of drug released in time  $t$  per unit area  $A$ ,  $C_0$  is the drug initial concentration,  $C_s$  is the drug solubility in the matrix media and  $D$  is the diffusivity of the drug molecules (diffusion coefficient) in the matrix substance.

Equation 4.6: Korsmeyer-Peppas model

$$M_t / M_\infty = Kt^n$$

Where  $M_t / M_\infty$  are a fraction of drug released at time  $t$ ,  $k$  is the release rate constant and  $n$  is the release exponent. The  $n$  value is used to characterize different release for cylindrical shaped matrices.

Equation 6: Mean Dissolution Time (MDT).

$$MDT = \int_0^\infty \frac{(M - M(t))}{M} dt$$

Where  $M_t$  is the fraction of dose released at time  $t_i$ .  $t_i = (t_i + t_{i-1})/2$  and  $M_\infty$  corresponds to the loading dose.

## CHAPTER 1

### Novel Application of Ovalbumin as an Effective Drug Delivery Vehicle

---

#### 1.1. Introduction

It is important that drug delivery systems enhance drug storage stability and *in vivo* particle stability (Leach et al.,2005), while delivering the drug efficiently. The use of natural polymers has become of interest in recent years, with a shift from the usual use of synthetic polymers and surfactant polymers. In research studies, questions on the toxicity of the synthetic polymers and surfactants have been investigated but have not yet been fully resolved (Leach et al.,2005). Some studies have investigated possible substitutes to the synthetic and surfactant polymers (Mantalva et al.,2008). One of which being the use of natural polymers, where in some instances such as in protein nanotechnology, or so called biopolymers, are used in drug delivery systems (Randolph et al.,1997; Judge et al.,1996; Sakai et al.,1999; Sobotka et al.,1961). Some of these biopolymers are used as supplements and agents for carrying vitamins and oils. The choice of polymer is dependent on biopolymer strength, rigidity and the ability to form a matrix.

In a study performed by Aimi et al., (2009), casein was investigated for its ability to deliver different active agents for uses such as transdermal, digestive and disease treatment agents Andrews et al.,2000. From the above findings, biopolymers can be used as efficient drug delivery systems for various drugs, at low cost to the manufacturer. The challenge has been in designing a natural polymer for use for drug delivery applications, following a simple, reproducible biopolymer or like that is biodegradable, increases bioavailability and has little or no toxicity and side effects on patients. Factors such as drug loading, particle size and shape, water-air interface and adhesion relative to drug molecules must be superior to commercially available drug delivery vehicles. The encapsulation of the drug delivery vehicle must enhance particle storage while enhancing increased drug stability and target site delivery of the drug.

In the oral administration of drugs, it is important that drug delivery vehicle becomes entero-soluble and absorbable by the intestinal mucosa. Properties such as mechanical strength, resistance to enzyme degradation and resistance to fluid moisture must be efficient. The type of protein used in the synthesis of the biopolymers determines the characteristics of the polymer vehicle.

Proteins found in egg white for example, can be formed into drug delivery vehicles. Whey protein has been researched for its foaming, emulsifying and stability characteristics (Banta,

2007). It has been reported that the difficulty experienced with the structural properties of whey protein, has been with whey protein converting into a poor strength gel when exposed to slightly high pH (Challa et al.,2005). This is attributed to the most abundant protein found in whey protein, ovalbumin. Ovalbumin, a 45kDa monolithic protein, was also tested in high temperatures, where numerous results showed that ovalbumin is water-insoluble, and forms aggregates or lamellar sheets under increased heat of 80°C (Creighton, 1993). It was reported that the aggregates formed micelles when they were exposed to salts such as sodium, potassium, or the like (Huntington et al.,1997). Physicochemical and physicomachanical studies later revealed that ovalbumin had increased surface pressure and hydrophobicity characteristics due to its foaming abilities (Gupta et al.,2005). This has since led to the investigation of ovalbumin providing stable modes of drug delivery to certain sites in the animal model. The possibility of ovalbumin contributing to the stability and crosslinking with other polymers in drug delivery, to stabilise, increase tertiary structure strength and provide a versatile drug delivery vehicle polymer exists.

## 1.2. Rationale and Motivation

The design of the polymeric drug carrier system should:

- Ensure thiol to thiol conjugation between the polymer and the bioactive.
- Be site specific in the release of the bioactive without chemically modifying the bioactive.
- Release from the vehicle easily by unbinding to form a free thiol.
- Demonstrate the versatility of the thiol binding sites and their potential use as drug carrier systems.
- Demonstrate the reversible covalent binding properties *in vivo* of the disulphide-thiol chemistry reaction.

Polymer therapeutics has proven to be effective in conjugating biocompatible polymers to therapeutic proteins or drugs for improved drug, protein or gene delivery. Biocompatible polymers are extensively used and have important role in modern pharmaceutical sciences; nonetheless there is a demand for the ever-increasing application of more efficient polymer chemistry to innovate new and diverse pharmaceutical polymers (Roper et al.,2004).

Thiols are formed through various ways, some of which include the exogenous exposure to enzymatic cleavage and chemically reducing or oxidizing disulphide interactions. The most common way of producing thiols is the use of enzymes which act by cleaving the disulphide bonds between two cysteine residues (Li et al.,2009).

The limitations of using the above mentioned chemicals have been the instability. The approaches for the degradation of the disulphide bonds ensure that the thiols are available for interactions in shorter periods of time. Thiols can reversibly be cleaved in the presence of reducing agents such as dithiothreitol (DTT), tris(2-carboxy-ethyl) phosphine (TCEP), 1-ethyl-3-(3-dimethylaminopropyl)carbodiimide (EDC), 2-iminothiolane, thioglycolic acid and hexandithiol (HDT) (Chan et al.,2009; Lowe et al.,2009) to mention a few.

These modifications exhibit the potential binding sites of thiol groups found in all natural and some synthetic protein polymers. The advantages of using thiols as binding sites for biopharmaceutical bioactives is that (1) they have demonstrated increased structural stability in the process of polymer synthesis, (2) have shown multifaceted reactions that thiols can form, (3) demonstrated the versatility of the thiol binding sites and their potential use as drug carrier systems. The novelty of thiol reactions has been their reversible covalent binding properties *in vivo*.

The rationale was to synthesize of a multifunctional drug carrier system was to enable the bioconjugation of any thiol containing bioactive while remaining stable *in vitro* and *in vivo*. The novel ovalbumin polymer was to be used as the carrier because of its natural internally buried disulphide bonds that would provide excellent potential sites for bioconjugation.

The success of an effective drug delivery system may be evaluated completely by stability studies. The sole purpose of stability testing is to obtain a stable product which maintains its efficacy to the maximum shelflife at specific storage conditions and maintain peak drug release profiles. The advantages of a stable formulation are:

- Prolonged residence time at the site of action
- Localization of dosage form at a specific site
- Increased drug concentration gradient across the intestine, increasing contact of the drug particles with the mucosa
- Direct contact with the intestinal cells, which precedes particle absorption (Rashid et al., 1990).

### **1.3. Novelty of the Study**

The novelty of the study was the use of a native polymer, namely ovalbumin, that contained thiol binding sites for bioconjugation. The ovalbumin polymer when modified provided reactive thiol sites for the conjugation of the thiol-based bioactives such as captopril, which make ovalbumin a novel drug carrier system. The functional novelty of thiol reactions has

been their reversible covalent binding properties *in vivo*. The benefits of using ovalbumin thiol-based chemistry in the delivery of drugs include;

- Thiols demonstrate increased structural stability in polymer synthesis.
- Improved patient compliance thus aiding in the reduction of frequency in the oral administration of captopril thus aiding in the control of hypertension.
- The possibility of using native polymers such as ovalbumin in the fabrication of pharmaceutical dosage forms for sustained delivery of drugs.
- The generation of scientific data for publication in high-impact peer reviewed journals and presentation at conferences.

#### **1.4. Aim of the Study**

The aim of the study was to design an efficient, target specific drug delivery vehicle that would enhance the delivery of thiol-based bioactives. This was achieved by designing modified ovalbumin vehicles for oral administration and intra-mucosal absorption. The chemically modified ovalbumin vehicles were manipulated to achieve the desired dosage form by meeting the following objectives;

1. Characterization and the assessment of the native ovalbumin properties such as the thermal response, and physical stability in response to pH, salt and temperature variations.
2. Analyse the chemical characteristics of the functional groups and assess the potential sites for possible interactions with crosslinking polymers and the properties of the bonds formed.
3. Elucidate the conjugation efficiency, morphological characteristics, zeta-potential and size and thermal properties of the complex conjugate.
4. Compare different hydrogel polymers suitable for the encapsulation of the ovalbumin drug carrier system. Furthermore determine the Fourier transform infrared spectroscopy and thermal properties of the hydrogel ovalbumin particles.
5. Determine parameters affecting the dissolution rates of the chemically modulated modified ovalbumin particles and the bioavailability of captopril.
6. Fabrication and optimization of the composite polymeric vehicle carrier system in the capsule dosage form, comprising of ovalbumin, sodium alginate and calcium chloride.
7. Performance of *in vivo* animal studies in the Large White pig model to determine release and bioavailability of captopril.



## 1.5. Overview of the dissertation

**Chapter one** introduced the prospect of a new material for use as a drug delivery carrier. It exemplifies the use of natural polymers for the purposes of drug delivery and the challenges associated with the use of natural polymers. A chemical altering technique was proposed and rationalized to create a highly stable vehicle matrix with increased surface area to efficiently control the release of the drug from the system. The design of the polymer would be manipulated to enhance drug release and achieve the desired drug release profiles. The aims, objectives and technology proposed for designing the drug carrier vehicle were provided in this chapter.

**Chapter two** was a review that highlights recent interests and applications of disulphide and thiol chemistry in creating contemporary macromolecular designs for drug delivery. Due to the chemical nature of disulphides and thiols a wide range of chemical species react with these functional groups to yield a variety of polymers extending their applications in chemical, biological, physical, material engineering and material sciences. The review aimed to illustrate the versatility and demonstrate the potential of thiol-based chemistries. The focus is on exploring bio-cleavable disulphides and linking by “clicking” thiols via thiol/other functional group exchange reactions.

**Chapter three** demonstrated the thiol conjugation of the natural polymer to a bioactive. The research was aimed to analyse the ovalbumin polymer after disulphide modification. The chapter was aimed to assess the thiol/disulphide functionalization of the captopril-ovalbumin interaction, the structural characterization and mechanical properties of the conjugate complex and to report on the thiol-disulphide covalent substitution reaction. The ATR-FTIR, differential scanning calorimetry, rheological analyses were employed to assess the chemical and physicochemical properties of the captopril-ovalbumin conjugate complex as a drug carrier system. The results demonstrated the stability and functionality of the native polymer in carrying and stabilising the bioactive, without chemically compromising the bioactive and its pharmacodynamics.

**Chapter four** provided a comparison of the three hydrogels used to encapsulate the captopril-ovalbumin conjugate complex. The aim of the chapter is to examine the pharmacokinetics of three main hydrogel polymers known for their controlled release properties namely, sodium alginate, 2-hydroxy propyl methyl cellulose and poly vinyl alcohol. These above mentioned hydrogels exhibited bioadhesive properties that could potentially increase the release of the bioactive across the intestinal mucosa. The results verified the best encapsulating hydrogel for the captopril-ovalbumin conjugate complex. It resulted in the high percentage drug release, drug encapsulation and prolonged release of the captopril.

**Chapter five** was an assessment of the parameters affecting the pharmacokinetics of the ovalbumin drug carrier system. These parameters gave insight on the preformulatory factors affecting the release of captopril, by exploring the responses of the lower and upper limits of the components that synthesized the captopril-ovalbumin drug delivery system. The parameters also provided insight into the interactions between the polymers and the salt concentrations. The limits of the parameters were, but were not limited to, the polymer concentrations and salt concentration. The responses demonstrated the resultant effect on drug release. The results showed that the higher the salt concentrations, the less drug was released. The variation in the polymer concentrations showed that no statistical significant difference was found between the upper and lower limits of the polymer concentrations.

**Chapter six** described the optimisation procedure of the drug delivery system. The Box-Behnken design for optimisation of the drug delivery system was assessed and reported on. The interactions assessed the responses of each component of the drug delivery system on the effects of accumulated drug release, particle size, zeta-potential and mean dissolution time. The results were reported on and the suitable combination of polymer concentration and salt were chosen for the optimized ovalbumin drug carrier system.

**Chapter seven** describes the *in vivo* assessment undertaken on the ovalbumin drug carrier system. The pig model was used to assess the pharmacokinetics and pharmacodynamics of the system. Blood samples were analysed using the UPLC to determine the concentrations of the captopril released *in vivo*. A validation method was also determined and applied for the quantification of the model drug, captopril.

**Chapter eight** summarises the conclusions of the ovalbumin drug delivery system and recommendations for further studies.

## CHAPTER 2

### Disulphide/Thiol Chemistry: Macromolecular Design and Synthesis of Polyfunctional Material for Drug Delivery

---

#### 2.1. Introduction

Polymer therapeutics is a term largely used to describe polymeric drugs, polymer conjugates in the form of polymer-drug or -protein conjugates, polymeric micelles or gels to which drugs are covalently bound (Duncan, 2003). Polymer therapeutics has proven to be effective in conjugating biocompatible polymers to therapeutic proteins or drugs for improved drug, protein or gene delivery. Biocompatible polymers are extensively used and have important role in modern pharmaceutical sciences; nonetheless there is a demand for the ever-increasing application of more efficient polymer chemistry to innovate new and diverse pharmaceutical polymers (Roper et al., 2004). One interesting and fast advancing tool used in polymer science is the use of thiol chemistry in polymer synthesis.

Thiols are formed through various ways, some of which include the exogenous exposure to enzymatic cleavage and chemically reducing or oxidizing disulphide interactions. The most common way of producing thiols is the use of enzymes which act by cleaving the disulphide bonds between two cysteine residues (Li et al., 2009). Enzymatic cleavage of the covalent disulphide bonds results in the complete separation of the two amino acid strands which results in a longer duration of separation. The problem with using enzymes has been the reformation of disulphide bonds with other proteins especially in redox plasma environments, such as at cellular and plasma levels. Enzymatic cleavage causes a transformational change in the protein which results in rebinding on the protein (Judy, 2011; Bumcrot et al., 2006). The other ways of cleaving the disulphide bonds is by oxidising or reducing the bonds using, for example, performic acid or 2-mercaptoethanol and iodoacetic acid. The limitations of using the above mentioned chemicals have been the instability and the duration required for the bonds to separate. Both approaches for the degradation of the disulphide bonds ensure that the thiols are available for interactions in shorter periods of time.

In some instances for example in, lactoglobulins which have three thiol groups, and in ovalbumin four thiol groups are buried in the interior of the protein (Onda, 1997). The thiol groups (SH), are formed spontaneously when exposed to air. As mentioned above, thiols are produced either by partial heating of the protein, by acid induced denaturing of the disulphide bonds or by salt induced denaturation. These external stressors modify the ovalbumin protein by chemically separating the disulphide bonds; in some instances by

causing partial unfolding of the primary structure, exposure of the hydrophobic bonds, oxidation or reduction of covalent bonds and introduction of the hydrogen bonds. The above mentioned modifications ultimately result in either the disintegration of the tertiary structure or varying the degrees of denaturation of the protein. The half-life of the reaction  $RS-SR + 2e \rightarrow 2RS^-$  has a standard reduction potential of 0.25V and therefore oxidation could be carried out in mild conditions (Roth et al., 2011). Unfortunately the thiol chemistry of macromolecular proteins such as ovalbumin have not yet been extensively reported and researched, hence this review seeks to explore the other thiol related chemistry of polymers.





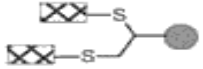

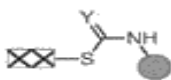
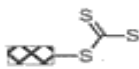
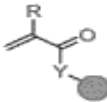
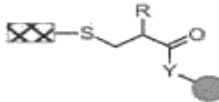
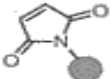
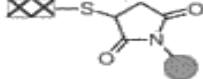
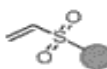
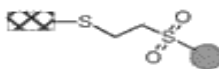



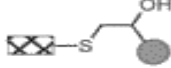

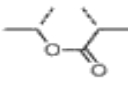
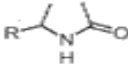
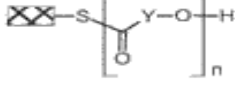

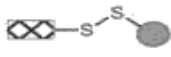


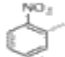
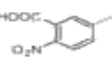
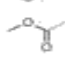
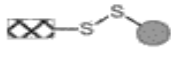
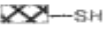

Polymers that contain thiol groups have generally been referred to as thiomers. Thiols can reversibly be cleaved in the presence of reducing agents such as dithiothreitol (DTT), tris(2-carboxy-ethyl) phosphine (TCEP), 1-ethyl-3-(3-dimethylaminopropyl)carbodiimide (EDC), 2-iminothiolane, thioglycolic acid and hexandithiol (HDT) (Chan et al.,2009; Lowe et al.,2009) to mention a few. In some instances thiols have been expressed in proteins using DTT for example, creating stability or improving drug binding efficiency to the delivery systems as will be demonstrated in the review. Thiomers are mostly used due to their ability to act as very good mucoadhesive polymers. The covalent bonds in the form of disulphide bonds enable the thiomers to bind mucus surfaces of the mucosa of the gastrointestinal wall. The thiomers act by binding onto proteins, glycoproteins, drugs and carbohydrates through the disulphide covalent bonds. Binding capabilities of thiols expand the area in which peptides and proteins can be used as potential therapeutic drug carriers.

Proteins and peptides have been used as the primary bases for protein drug delivery especially in the advancement of gene therapy, genetic engineering, molecular biology and also to improve drug binding efficiencies. The benefits of using macromolecular peptides and proteins in drug delivery are encompassed in the fact that they are readily available, are endogenously biodegradable and can be produced in commercial quantities. Proteins are also important as they are employed in the regulation and integration of life systems at nucleic and organ level. Enzymes, hormones and antibodies are for example highly specific in their binding sites on both receptors and antigens. The specificity of the binding sites in these proteins, enable peptides and proteins to specifically bind to a limited number of sites without compromising the efficiency and effectiveness of the bond formed in terms of both excellence and enhancement of stability. To date, different peptides have been used in drug delivery. Proteins and peptides continue to display the importance as future drug delivery carriers because of the ever increasing advancement in molecular biology, identification and discovery of hormones, their usefulness and broad application as biopharmaceuticals and lastly their regulatory roles in human pathophysiology. The present review also aims to explain the potential binding sites of thiol groups found in all natural and synthetic proteins.

Overall this review provides a detailed account on the advantages of using thiols as binding sites for biopharmaceutical bioactives, illustrate their functionality in polymer synthesis, show the multifaceted reactions that thiols can form and lastly demonstrate the versatility of these binding sites and their uses in drug delivery systems.

Some of the reactions will be briefly discussed because they are not the focal points in this review. The main reactions that will be discussed are those that are relevant in thiol-based chemistry used primarily in thiol polymer synthesis, modification and functionalization. Table 1 shows some examples of thiol chemistries and illustrate some of the thiol chemistry reaction classifications. The specific examples used in this review aim to illustrate the versatility, functionality and speciality of thiols being used in drug delivery and material science.

**Table 1. Examples of Thiol Reactions used in Polymer Synthesis** [Reproduced with permission from Roth et al., 2011, © WILEY-VCH Verlag GmbH & Co. KGaA, Weinheim].

Reactions of Thiols  -SH with	Product
<i>radical additions</i>	
 radicals	
 radicals	
<i>nucleophilic additions</i>	
$Y=C=N$  Y = O or S	 Y = O or S
$S=C=S$ base, $-H^+$	
 R = H or CH <sub>3</sub> Y = O, NH or NR	 R = H or CH <sub>3</sub> Y = O, NH or NR
	
	
<i>nucleophilic Substitutions (carbon, carbonyl)</i>	
$X-R$  X = Cl, Br, I R = alkyl	 R = alkyl
 (Lewis acid)	
 base Y =  or 	
<i>nucleophilic Substitution (sulfur)</i>	
$R-S(=O)_2-S$  R = -CH <sub>3</sub> R = -ONa	
$EWG-S-S$  EWG =    	
<i>other</i>	
 -SH	
metals, metal oxides (atoms, nanoparticles, surfaces)	complexes, self-assembled monolayers

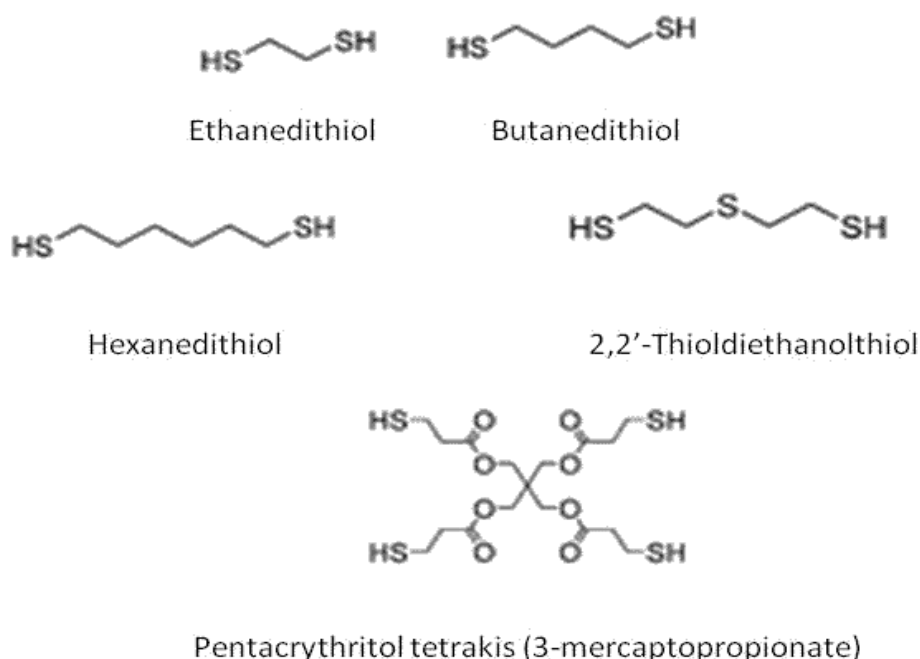
## 2.2. Thiol-based click chemistry

As part of the developing a realm of novel drug delivery systems, researchers have recently recognized several thiol-based chemical reactions as 'click' chemistry reactions. The strength of many thiol chemistries are based on the ability of the highly inherent reactive groups to react readily with a wide array of functional groups under a variety of experimental conditions, that do not necessarily affect the bond formed. The main challenge that was postulated for the thiol-based chemistries in polymer and material science, was the modification of the conditions or 'masking' of the thiol reaction to produce thiol bond formation at the specific regions required on the polymer or material. The term 'click' chemistry, first coined by Kolb et al.,(2001) referred to as a series of simple reactions that were facile, rapid, and quantitative and site specific (Hein et al.,2008). According to Kolb et al., in order for the reactions to be considered as 'click' they have to meet six basic requirements as follows: i) the use of cheap, readily available material; (ii) maintain ease of execution; (iii) be able to form a high quantitative yield in drug delivery that meets the requirements to be classified as click chemistry reactions, even though there has been scepticism about the consideration of thiol-based chemical single target product; (iv) be environmentally friendly; (v) require non-chouromatographic purification at the last stage; and lastly (vi) have regiospecific targeting.

Kolb et al. also noted that the orthogonality of thiols, facile and high reactivity were generally compromised, hence Lowe and Harvison (2010) pointed out that the thiol click chemistry's strength was also its weakness in chemistry. This has been evident in the reduced number of publications that link thiol-click chemistry with polymer or material science. In the following sections thiol-chemistry will be discussed in the context of polymer synthesis, functionality and modification in drug delivery systems. The thiol-chemistry reactions used throughout the review are those that were conducted in the absence of possible competitive functional groups and side-reactions and under appropriate conditions with characteristic click thiol-based-chemistry environments.

There are three main types of thiols; namely the thiolate, thiol ion and the thiyl radicals that exist. Hoyle and Bowman (2010) distinguished four basic structures of thiols reported in literature, namely alkyl thiols, thiophenols, thiol propionates, and thiol glycolates. These above mentioned thiol structures influence the chemistry of thiols, which determines whether they are catalysed before reactions or are in a radical state for reactions to occur. The chemical natures of the thiol functional groups provide interesting reactivity in that they readily react with very useful and available organic substrates. Thiols react with alkynes, electron poor enes (Michael Addition), isocyanates (carbonyl addition), epoxies (SN2 ring

opening) and halogens (SN2 nucleophilic substitution) and especially the electron rich enes (radicals). Figure 1 depicts the general thiol structures with multifunctional thiols.

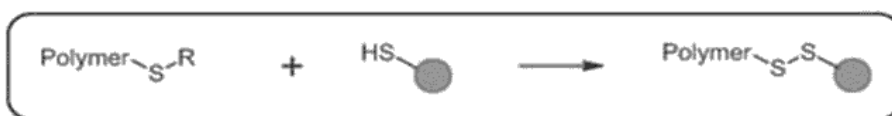


**Fig. 2.1.** General thiol structures including multifunctional thiols [Reproduced with permission from Lowe et al., 2010 © The Royal Society of Chemistry].

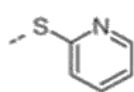
Two general forms of disulphides are known namely, the asymmetric and the symmetric disulphides (Scheme 1). The asymmetric disulphides are disulphides obtained by using thiol/disulphide exchanges while symmetric disulphides are obtained by oxidising the disulphide bond using oxidising reagents such as iodine, iron chloride and oxygen (Roth et al., 2011). The readily reactive thiol groups permits for the creation, functionalization and modification of a range of polymers with a diverse array of physical, chemical and mechanical properties for use in drug delivery that meet extensive biological and bioactive delivery requirements. The use of multiple thiol click reactions support the original concept of click chemistry reactions of synthesising a wide array of chemical and more elaborate materials within a short period of time under chemically and friendly environmental conditions.



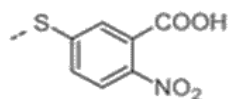
### Asymmetric Disulfides



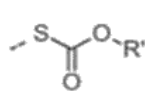
R =



(1)



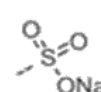
(2)



(3)

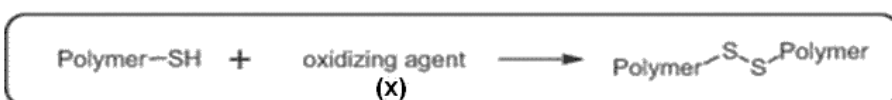


(4)



(5)

### Symmetric Disulfides



X =



(1)



(2)



(3)

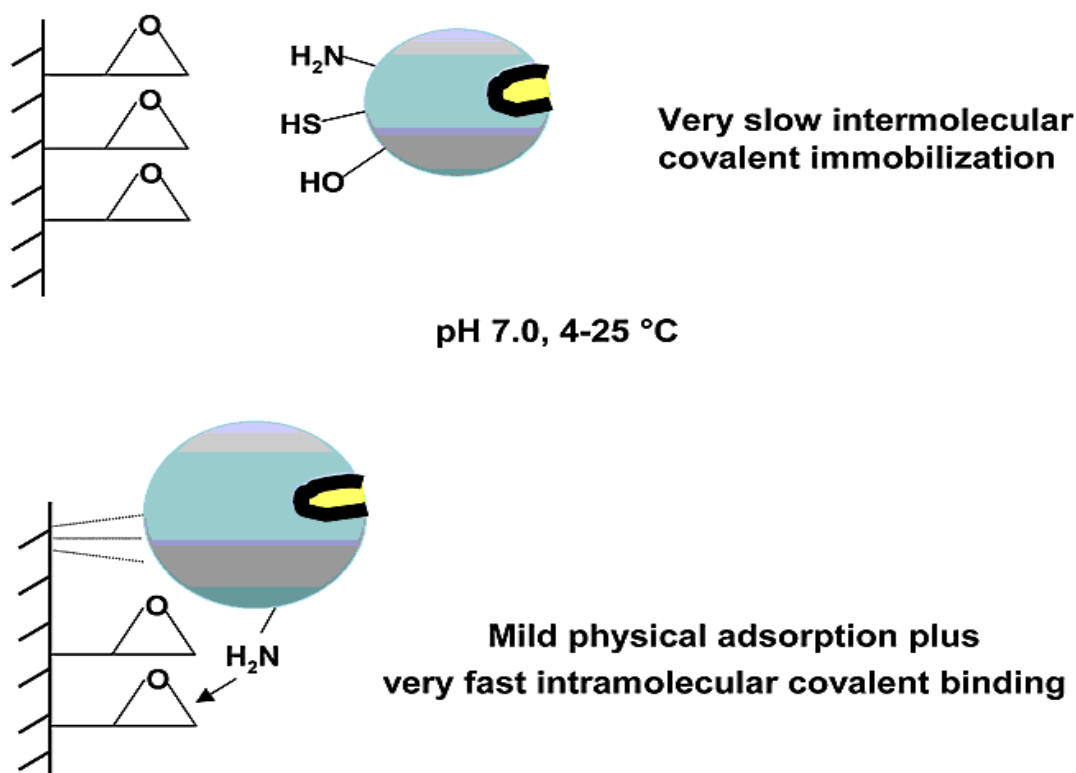
**Scheme 1.** Structure and synthesis of asymmetric and symmetric disulphides [Reproduced with permission from Roth et al., 2011 © WILEY-VCH Verlag GmbH & Co. KGaA, Weinheim].

The most well-documented thiol-based click chemical reactions in drug delivery are the multiple carbon-carbon bonds. Two specific multiple carbon-carbon click reaction groups, the thiol-ene and thiol-yne reactions dominate in polymer sciences especially in drug delivery. Other thiol-based click reactions such as the thiol-epoxy, thiol-isocyanate, thiol-halogen nucleophilic substitution and thiol nucleophile-mediated Michael addition click chemistries exist. Nucleophilic thiol reactions rely on the nucleophilicity of the thiol reactive group, and tend to proceed at rates that are determined by the substrate and its proclivity for the nucleophilic attraction by either the thiols or the thiolate anions (Killpos et al., 2008; Lowe et al., 2010; Hoyle et al., 2004; Gress et al., 2007). In some instances the rates of the above mentioned reactions become determined by the choice of catalysts, which accelerate the reactions to achieve high conversions. Most of these nucleophilic reactions are initiated by strong nucleophilic bases. The above mentioned thiol click chemistry will be discussed briefly hereunder.

### **2.2.1. Thiol-epoxy click reactions**

Hoyle et al., (2004) described the epoxy-thiol click reaction, used in many important biosynthetic and biomedical applications, as a straightforward ring opening nucleophilic reaction by the thiolate anion. The consecutive step involves the protonation of the alkoxide anion by the quaternary ammonium, originally formed by the base catalyst and the thiol to generate a thiol anion. The reaction is catalysed by a variety of strong bases through deprotonation of the thiol.

An example of the functionality of the epoxy-thiol reaction is the formation of Sepabeads to stabilise the enzymes on the surfaces of proteins using the epoxy-thiol supports. The science behind the formation of the Sepabeads demonstrated by Mateo et al., (2007), illustrate the stabilisation of proteins that support the retardation of the enzyme, to promote adsorption of the enzyme and create a rigid protein that allows the retardation of the enzyme whilst promoting enzyme binding or attachment. The key purpose of this work was to create a heterofunctional enzyme, penicillin G acylase (PGA) that would ultimately assist enzyme attachment and re-use of the enzyme. By modifying the enzyme to generate multiple covalent attachment points using dithiothreitol, ensured the disulphide exchange between the two thiol surfaces. Sodium sulphide was also introduced onto the enzyme as an additional thiol additive at pH 7 to create the rigid thiolated enzyme surface structure. The outcome was an improved specific immobilisation of the enzyme by the exchange in thiols between the enzyme and the protein disulphide bonds of the modified protein (Figure 2.2). It was reported that the stabilization factor for the PGA complex increased by 12-15 fold compared to previous counterparts.



**Fig.2.2.** The covalent attachment reaction between epoxy and the thiolated protein [Reproduced with permission from Mateo et al., 2003 © American Chemical Society].

The thiol-epoxy reactions continue to be of interest in drug synthesis and drug delivery material synthesis as they continue to develop rapidly in applications of drug synthesis, bioactives and biological processes of numerous synthetic materials. The ring-opening reactions especially those involving thiols and epoxy have been reported to be important in industry because of their adhesive and highly functional coatings used in synthons and in optical fields.

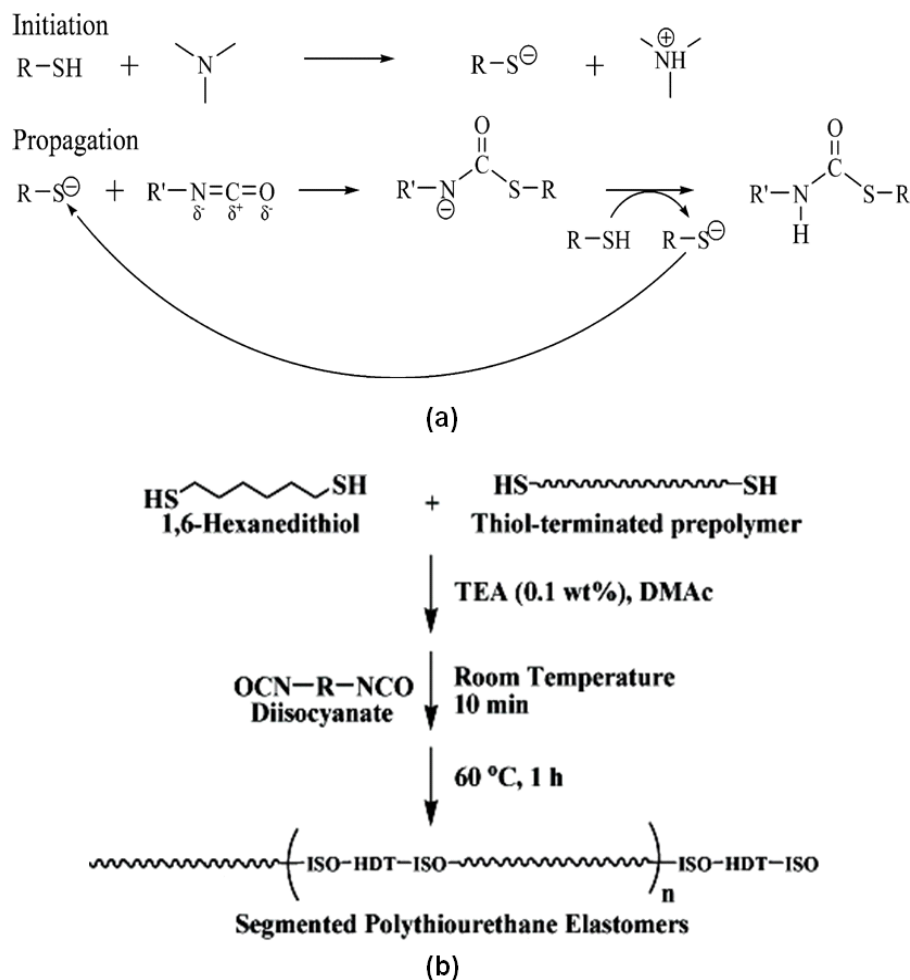
### 2.2.2. Thiol-isocyanate nucleophilic addition click reactions

This sulphur analog of the polyurethanes, polythiourethanes, have been ineptly explored as potential drug delivery materials in past years. The polythiourethanes have mostly been used in industry and recently in polymers for improved high macromolecular weight polymer architect synthesis (Matsushima et al., 2010) in the last two decades. The nucleophilic addition of the thiols to isocyanate groups has been reported to yield high products within seconds of reacting the monomers, dimers and trimers. Very few articles have been published that show the versatility of the polythiourethanes; but their use as efficient optical materials has been exemplified. Their use in optical materials on a commercial and industrial

scale expanded primarily due to the high refractive index properties that the polythiourethanes exhibit.

Shin et al., (2010), explored the mechanical and viscoelastic properties of the polythiourethanes using multifunctional thiols and diisocyanates. The reaction was either photochemically or thermally initiated to achieve controlled sequence thiol-ene photopolymerization. Triethylamine (TEA) and 2,2-dimethoxy-2-phenyl acetophenone (DMPA) were used to initiate the formation of the thiol-isocyanate in the presence of the base catalyst tributylamine 3 tetraphenylborate (TBA-3-HBPh<sub>4</sub>). The nucleophilic addition of thiols to isocyanate groups in the presence of a strong base catalyst is depicted in Scheme 2a. The thiol-isocyanate coupling kinetics of the hybrid were analysed and found to yield quantitatively rapid and efficient conversions of >90%, within minutes and seconds of exposure to one another. The glass transition temperature of the hybrid increased from -5 to 35°C, as a function of the thiourethane content because of the higher covalent hydrogen bond which ultimately resulted in enhanced mechanical properties. The hybrid network structure formed highly uniform and dense network structures. These results are indicative of the relationship between chemical composition and physical mechanical properties, specifically those of calorimetry, hardness, thermal and tensile properties of the hybrid network.

Shin et al., (2009) do, however, emphasise the rate of reaction between the thiolate anion and isocyanate with use of the correct catalyst as being slow. They highlight the fact that strong bases, with higher conjugate acid pKa values, are essential for the formation of the thiolate anion and affect the outcome of the thiol-isocyanate coupling reaction rate. The investigators illustrated an example of a sequential thiol-isocyanate reaction, and also characterized the thermal and mechanical properties of the polythiourethane elastomers. In this specific example 1,6-hexanedithiol (HDT) was reacted with butenediol diacrylate, in presence of catalyst, Me<sub>2</sub>PPh, which resulted in the formation of a flexible, soft polythiourethane oligomeric polymer. Scheme 2b depicts the synthetic pathway of the novel polythiourethane elastomers employing the segmented thiol-isocyanate coupling. The thermal and 'dynamic' mechanical property was evaluated based mostly on the chemical composition following polymerization. It was noted that the glass transition and cross linking density decreased with the increase in the thiol content. The tensile properties were dependant on the micro-separation and mixing of the phases.

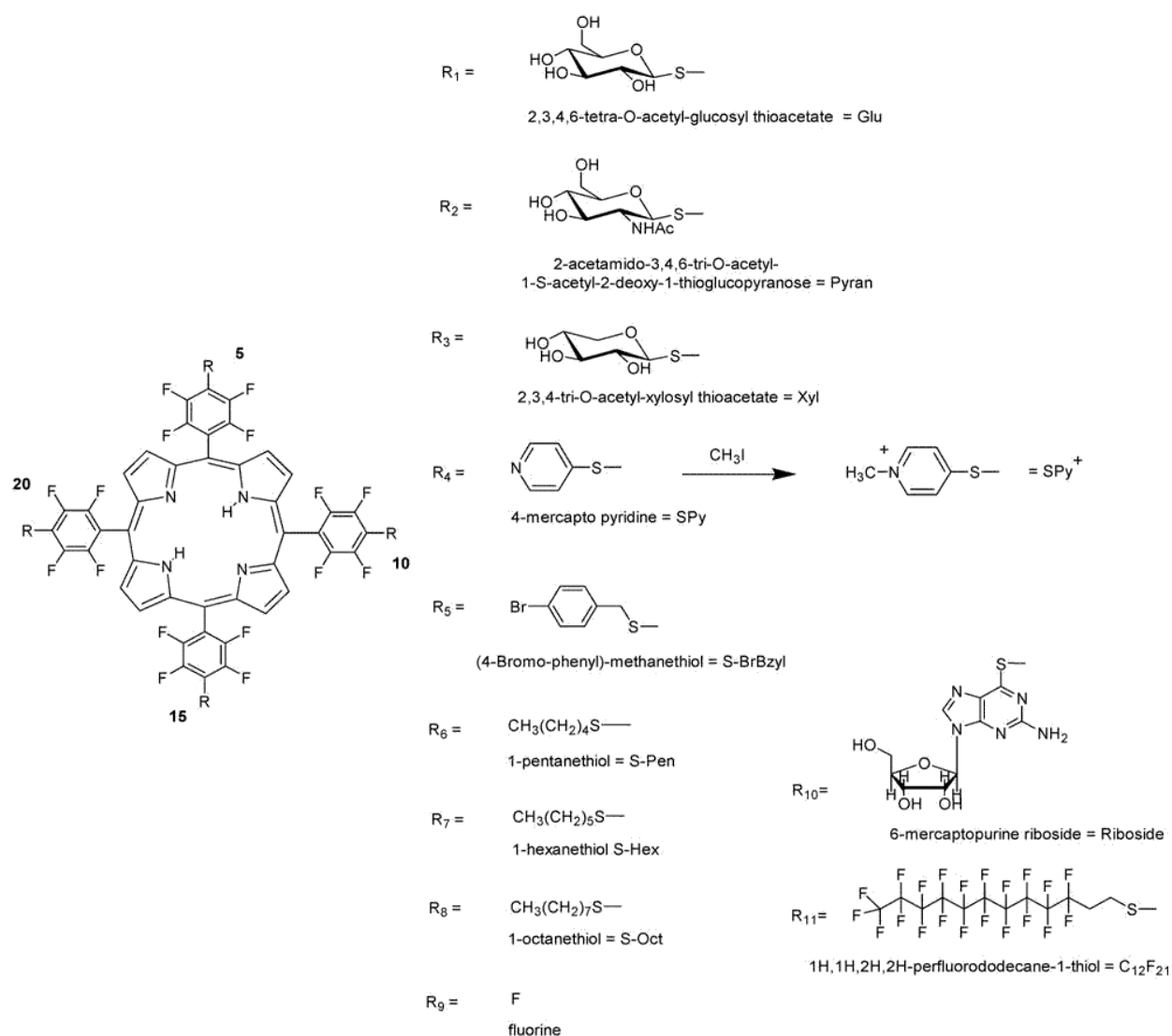


**Scheme 2.** (a) Tertiary Amine Catalyzed Thiol-Isocyanate Nucleophilic Coupling Reaction Mechanism [Reproduced with permission from Shin et al., 2010 © American Chemical Society]. (b) Synthesis of novel polythiourethane elastomers employing the segmented thiol-isocyanate coupling. Adapted from Materials Chemical [Reproduced with permission from Shin et al., 2009 © American Chemical Society].

### 2.2.3. Thiol-halogen nucleophilic substitution click reactions

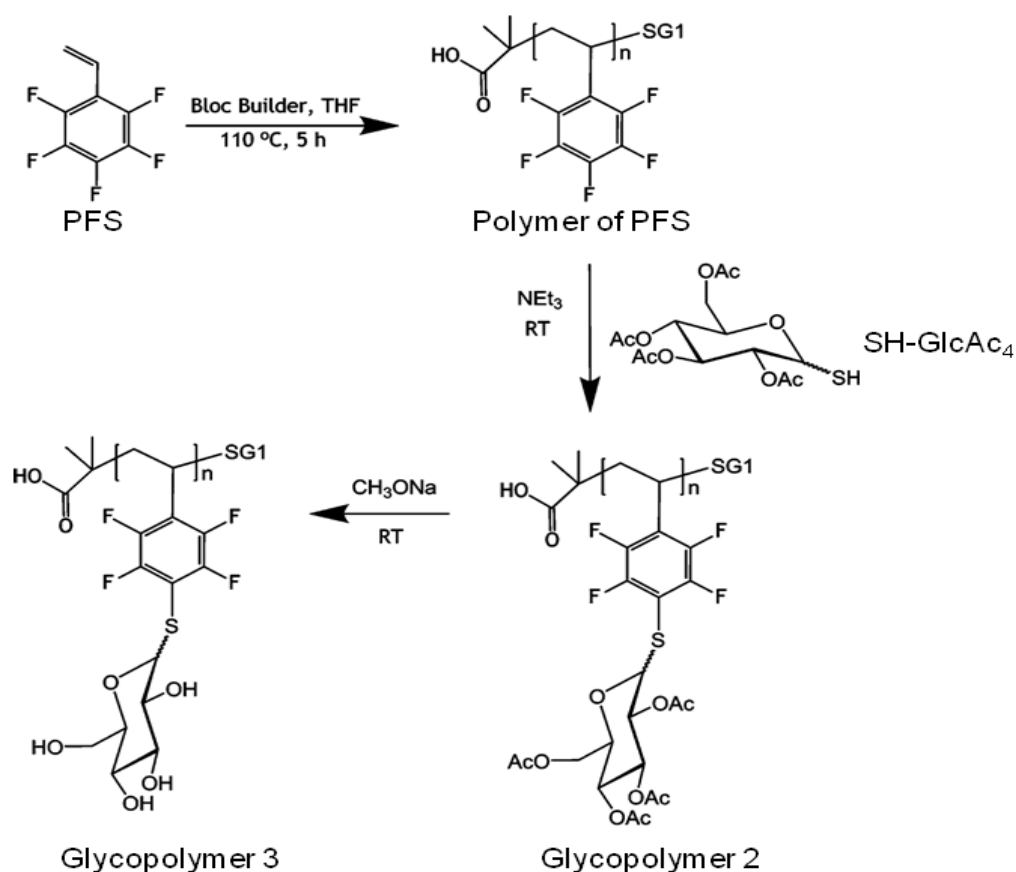
Thiols are generally soft nucleophiles, which makes their substitution rapid and efficient by readily displacing groups such as halogens, and form thiol-halogen nucleophilic reactions. Rosen et al., 2010, illustrated that the nucleophilicity of the thiol in 2-mercaptoethanol was very high compared to other thiol-dialcohol species added on halogenated and functionalised polymers and other halogen containing polymers. This illustrated that the thiol-halogen ion affects the orthogonality of the nucleophile thiol-halogen reaction, because the thiol anion displaced the halogen even in the presence of high concentrations of alcohol groups and aliphatic amines.

An astute example of the nucleophilic halogen substitution reaction that was demonstrated by Samaroo et al., (2007) which involved four para fluoro groups on 5,10,15,20-tetrakis-(2,3,4,5,6-pentafluorophenyl)-porphyrin (TPPF20) that were used to bind biopolymers such as DNA and small proteins that could be taken up by cells and nuclei in cancer cells. In this specific study TPPF20 was used to create motifs to assist in inducing breast cell apoptosis and necrosis. The results show that the 20-30nm size particles that were formed were found to be able to cross the blood brain barrier. The reaction yield was high and demonstrated the successful binding of the thiols onto the para fluoro. The entire reaction is illustrated in Figure 2.3.



**Fig. 2.3.** Nucleophilic halogen substitution reaction using Para fluoro for conjugation to small biopeptides [Reproduced with permission from Samaroo et al., 2007 © American Chemical Society].

Becer et al., (2009) synthesized glycoproteins constituting homopolymers styrene and pentafluoro (PF). The thiol-glycoside was created by using a catalyst, to create pentafluorostyrene (PFS), and the resulting self-assembled nanospheres had an average diameter of 70-720nm when using the nanoprecipitating method. For the addition of thiols on the backbone of PFS, a thiol-glycoside (2,3,4,6-tetra-O-acetyl-1-thio-D glucopyranose), was used to exchange the thiol with the para-fluoro to the polymeric backbone of the PFS moieties (Figure 2.4). The reaction was reportedly monitored by  $^1\text{H}$ ,  $^{13}\text{C}$   $^{19}\text{F}$  NMR spectroscopy and size exclusion chromatography. The synthesis of glycopolymers via the nucleophilic substitution of the para fluoro click displacement reaction proves that the free thiol fluorine could be used as a method of preparation in dendrimer and bioorganic functionalization of the nanoparticles for the application in a wide range of tailor made macromolecules suited for drug delivery, nanotechnology and catalysis.



**Fig. 2.4.** Preparation of glycopolymers from pentafluorostyrene (PFS) reaction with SH-GlcAc<sub>4</sub> (2,3,4,6-tetra-O-acetyl-1-thio-β-d-glucopyranose) [Reproduced with permission from Becer et al., 2009 © American Chemical Society].

#### **2.2.4. Thiol-ene/Thiol-yne Michael-type addition click chemistry**

There has been immense interest in thiol-ene and thiol-yne click chemistry especially in their application and functionalization in polymer and material science. The progress in this area has been due to unique polymer functionalization and regiospecificity advantages when compared to previous traditional coupling and functionalization strategies. The newly invented methods for the formation of materials in drug delivery are attributed to the robust nature of the thiol-ene and thiol-yne chemistry for the synthesis of well defined materials, with few structural limitations and synthetic requirements. In the following section the formation of thiol-enes, network and dendrimer formations and modification by accessorising three-dimensional objects are discussed.

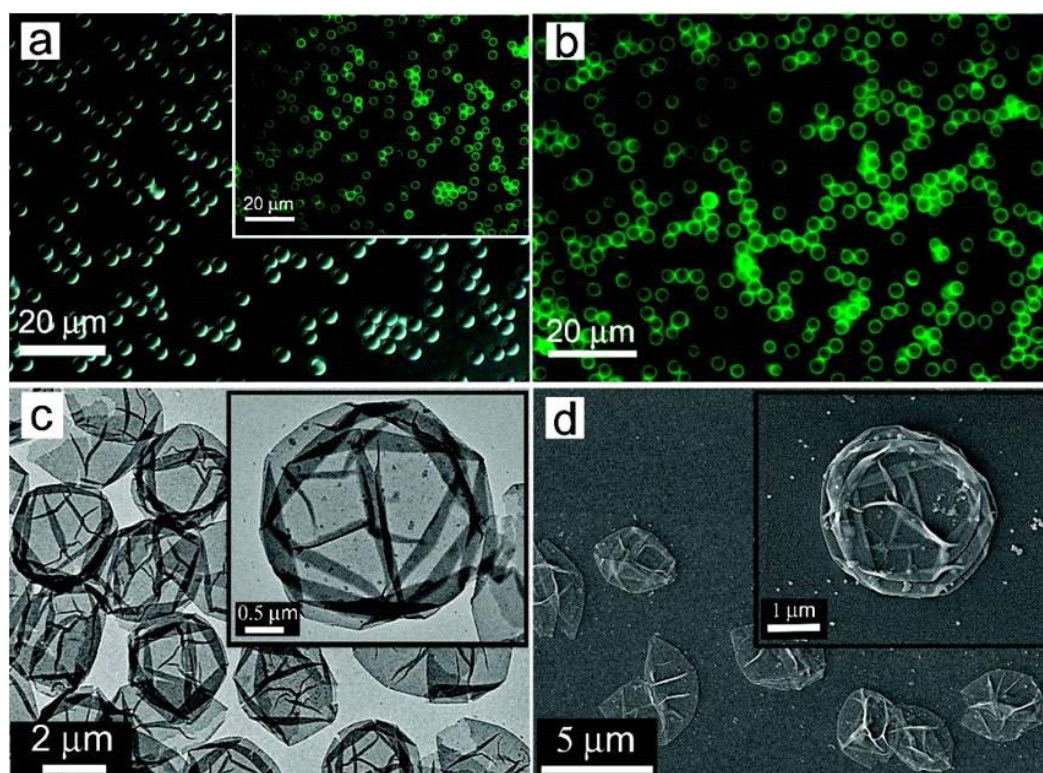
The thiol-ene/thiol-yne reaction has been known for over a 100 years and is simply defined as the hydrothiolation of the carbon=carbon bond. Previously thiol-enes/thiol-yne were used to prepare near-perfect networks and films to be used in polymer or drug delivery because of the attractive and versatile chemical features that they exhibit. Kade et al., (2010) noted that data had shown that the structural regularity of the thiol-ene and thiol-yne were more regular than those networks formed by diacrylates. A number of factors attribute to the thiol-ene/thiol-yne reaction being facile, versatile and attractive as a future drug delivery tool. Lowe (2010) highlighted three main features associated with thiol-ene/thiol-yne versatility. The hydrothiolation reactions were ensued in a variety of conditions including radical pathway, catalytic processes by nucleophiles, acids and bases and supramolecular catalysis using, for example, cyclodextrins. Thiol-enes/thiol-yne generally serves as suitable substrates for activated and inactivated functional group species and as 'multiple-substitution olefinic bonds' (Mather et al., 2006; Yu et al., 2009). Lastly, any free radical thiol can be employed depending on the sulfur-hydrogen bond strength and cleavage mechanism, whether homolytic or heterolytic lysis. As part of click chemistry features the reactions occur rapidly in mild conditions and in the presence of oxygen and the resulting product, the 'thioether', improves regiospecificity. The thiol-ene and thiol-yne are the radical thiols that are generally used by photopolymerization to form complex networks used in polymer science.

Heredia et al., (2010) synthesised a heterotelechelic biotin-maleimide cleavable disulphide bond by RAFT polymerization for reversible surface modification with proteins. The incorporation of cleavable disulphide bonds in this example illustrated that the 'cleavable handle' provided for capture and release of the protein and substrate. Chain transfer agents containing disulfide bond mediated the polymerization of NIPAAm to  $\alpha$ -biotin disulfide,  $\omega$ -trithiocarbonate-pNIPAAm. Trithiocarbonate was coupled radically to a maleimide initiator



which resulted in a heterotelechelic  $\alpha$ -biotin disulfide,  $\omega$ -maleimidepNIPAAm. The method of synthesis used the retro-Diels Alder reaction. The polymer was then conjugated using the disulfide bond to either bovine serum albumin or mutant V131C T4 lysozyme (T4L) and anchored onto streptavidin- or neutravidin-functionalized surfaces. The reversibility of the polymer conjugate was demonstrated by surface-anchored protein maintained activity towards antibodies.

Connal et al., (2009) stabilized and functionalized polymer multilayers and capsules using the thiol-ene click chemistry. They reported the synthesis of the layer-by-layer assembly of hydrogen bonded multilayers and deposition of methacrylic acid which contained thiol groups (PMA<sub>thiol</sub>). Poly(vinylpyrrolidone) (PVP) was combined with PMA<sub>thiol</sub> to form coated PVP/PMA<sub>thiol</sub> nanoparticles which were subjected to UV-light. Figure 5 depicts the transmission and scanning electron microscope images of the PVP/PMA<sub>thiol</sub>-ene nanoparticles.



**Fig. 2.5.** Microscopy images of layer-by-layer assembly of hydrogen bonded multilayers by alternately depositing poly(methacrylic acid) containing either thiol groups (PMA<sub>thiol</sub>) or ene functionality (PMA<sub>ene</sub>), with poly(vinylpyrrolidone) (PVP), at pH 4, (PVP/PMA<sub>thiol</sub>/PVP/PMA<sub>ene</sub>)<sub>2</sub>/PVP on silica particles and resulting thiol-ene PMA (PMA<sub>T-E</sub>) capsules upon selective removal of the core and exposure of the particles to

pH 7. (a) Phase contrast image of UV-irradiated coated particles at pH 4 and the corresponding fluorescence microscopy image (inset). (b) Fluorescence microscopy image of UV-irradiated PMA<sub>T-E</sub> capsules at pH 7. (c) Transmission electron and (d) scanning electron microscopy images of PMA<sub>T-E</sub> capsules at pH 7. PMA was labelled with AF488. [Reproduced with permission from Connal et al., 2009 © American Chemical Society].

## 2.3. Thiol-Based Defined Architectures Containing Disulphide Conjugates

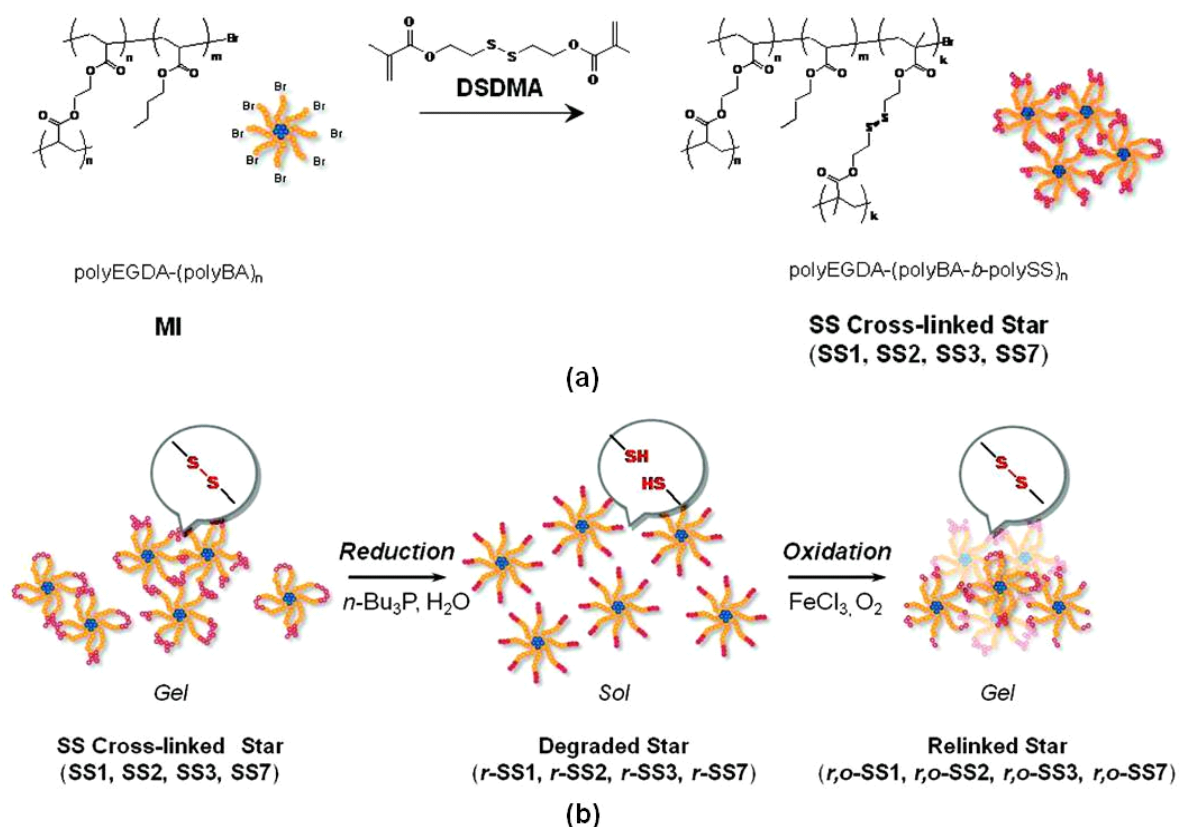
### 2.3.1. Hyperbranched/Multiarmed star polymers

Hyper branched polymers are generally used to encapsulate and isolate functional groups from external media that may easily conjugate to free moieties from. The main idea was to isolate the functional groups from reacting with the surrounding organic functional groups and for biomedical applications (Helms et al., 2005). Various methods have been used in the synthesis of these hyper branched polymers, where use of disulphide linkers which target either the arm or the cores of the polymer structure were employed. Initially the arm approach was easier to achieve since the target was generally on the extremities of the polymer. The assembly of the hyper branch required the pre-synthesis of the primary linear chains which were consequently coupled to the functional core or polymerised and linked using a cross-linker to achieve highly functional hyper branched polymers. Different methods have been used to prepare, for example, multi armed star polymers such as hetero-Diels Alder reactions (Barner et al.,2006), alkyne-azide reactions (Gao et al.,2009) thiol-ene reactions (Liu et al.,2008), and thiol-pyridal disulphide reactions (Iha et al.,2009).

Roth et al.,(2011) described the synthesis of multi armed star polymers is achieved using three different strategies namely, the “core first” approach, the “arm first” approach and the “coupling to” approach. Iha et al., (2009) explained the approaches as follows: i) the core first approach was when the arms of a star polymer were developed from multifunctional initiators; ii) the arm first approach was when the coupling of pre-synthesised macro-initiators or macro-monomers with a cross linker to form a star occurred; while iii) the coupling approach entailed the process when pre-synthesised polymer chains were added onto multifunctional cores. The core and arm first approached were generally employed to add functionality to a polymer by using functional monomers, from pre-synthesized block copolymers. In comparison to the coupling approach the synthesis of the star polymer is limited by the efficiency and selectivity of the reaction used in the conjugation step.

Kamade et al., (2011) synthesised poly(n-butyl acrylate)-based star polymer consisting of the monomers n-Butyl acrylate (BA) and ethylene glycol diacrylate (EGDA). The polyEDGA-(polyBA) was synthesised using the atom transfer radical polymerization method by

employing the core first approach. The above mentioned complex was further polymerized using the arm first approach to produce a disulphide cross-link star polymer. In this specific example the use of arm and core first approaches are conjugated to form a redox responsive star polymer. The addition of thiols by the cross-linker bis(2-methacryloyloxyethyl) produced the disulphide functionality, which was cleaved via reducing reactions, resulting in individual stars with thiol ends. The thiol ends were reversible by repetitive oxidation and reduction. The diameter of the star polymers was 20nm and the mechanical properties were conclusive of the oxidation and reduction conditions. The authors concluded that such stimuli responsive polymers had a great potential application in self-healing materials. Figure 6 illustrates the redox behaviour of the thiol/disulphide star polymer.

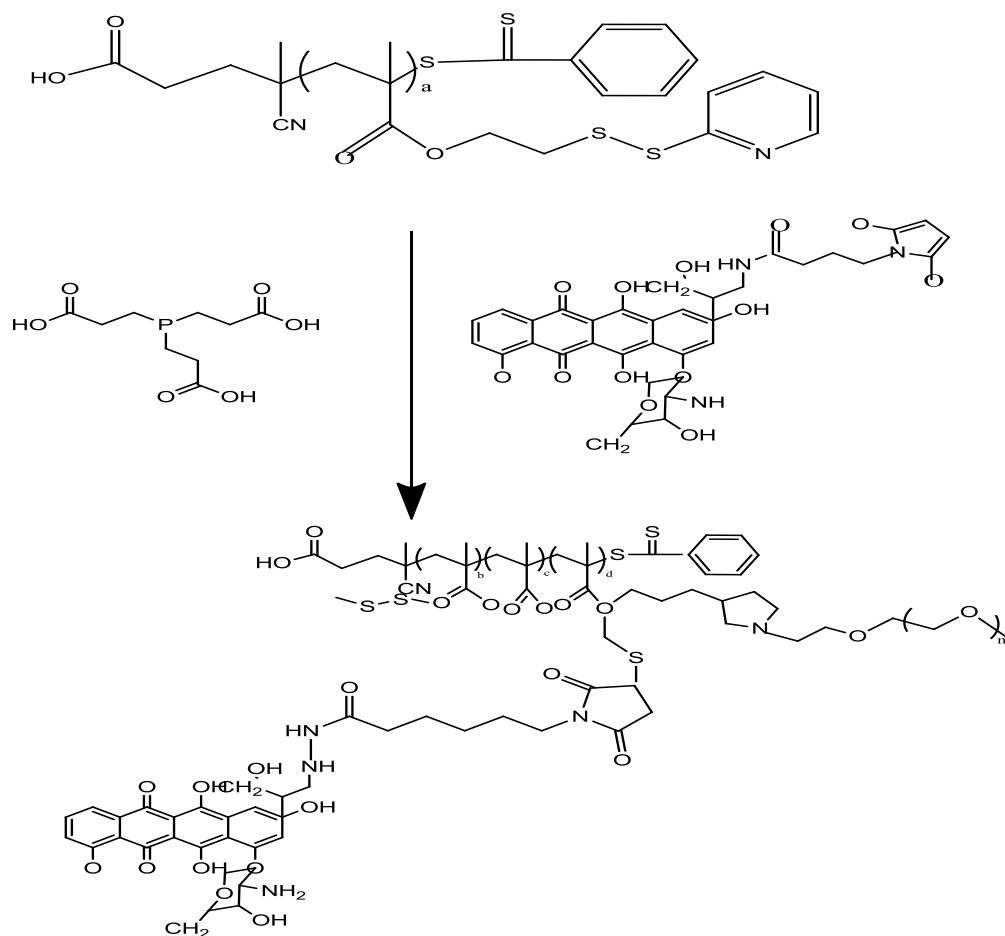


**Fig. 2.6.** a) Synthesis of the functionalised poly(n-butyl acrylate) star polymer; and b) Reduction and oxidation of the disulphide/thiol functionalised star polymer [Reproduced with permission from Kamada et al., 2010 © American Chemical Society].

### 2.3.2. Micelles

Wong et al., (2008) used an anticancer drug, doxorubicin for grafting onto RAFT-synthesized poly(pyridyldisulfide ethylmethacrylate) PPDS polymer. The method employed was the thiol-ene and thiol-yne click addition reactions which provides efficient drug delivery vehicles. The Dox-PEG complexes were covalently conjugated to thiol groups on the PPDSM in the

presence of disulphide reducing agent, dithiothreitol (Figure 2.7). The average size of the micelles was 192nm. The micelle nanoparticles were viable in inhibiting human cervical carcinoma cells. Roth et al., (2011) noted that micellar instability had become a limitation for *in vivo* applications as micelles only function and maintain stability above their critical micellar concentration (CMC). To bypass this limitation, micelles were crosslinked with linkers such as adding cleavable bonds, using pH sensitive chemical functional groups that are easily reduced or modified to assist in the reversibility of the bonds formed.



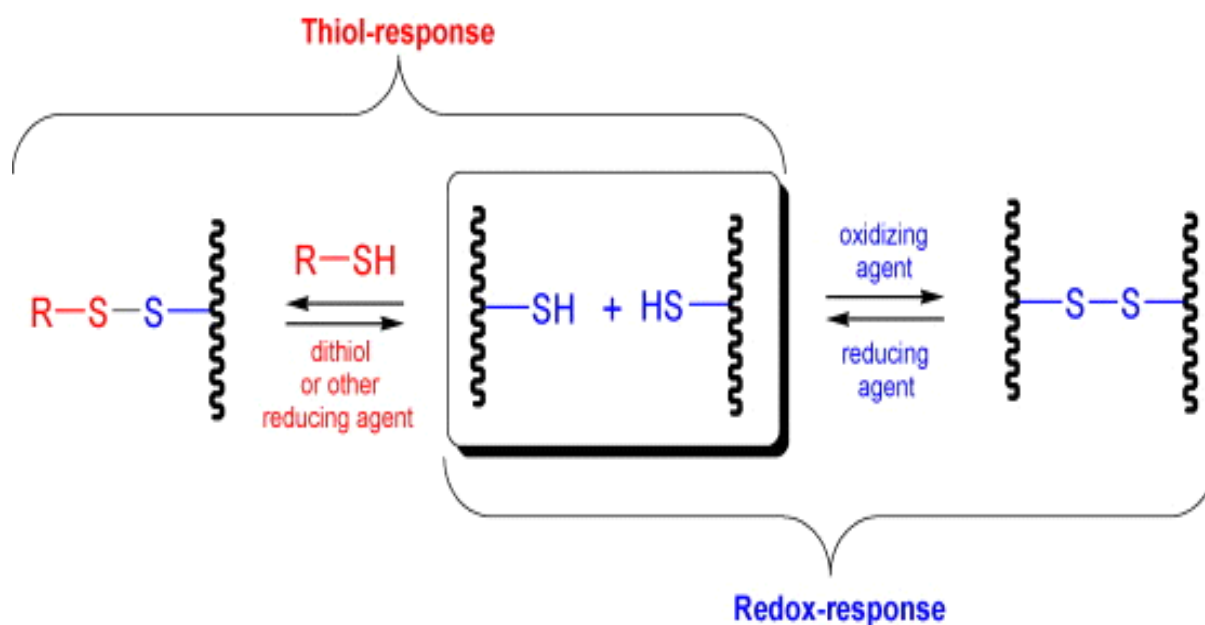
**Fig. 2.7.** Synthesis of the thiol functionalised poly(pyridyldisulfide ethylmethacrylate); Doxorubicin-conjugated complex with PEGylated disulphide crosslinked particles prepared by RAFT polymerization [Reproduced with permission from Wong et al., 2008 © American Chemical Society].

Micelles are normally cross-linked using biodegradable linkers, such as disulphides or pH-sensitive groups, because cleavable linkers such as disulphides have proven to provide reversible stabilisation. Dufresne et al., (2005) synthesised surface modified colloids for selective interactions with biological surfaces as drug delivery systems. Poly(ethyleneglycol)-

block-poly-(2-(N,N-dimethylamino)ethyl methacrylate) was synthesised with a thiol end. The micelles were designed to specifically recognise streptavidin. Mucoadhesion was also assessed through the formation of disulphide groups with the surface mucins. The efficiency of the system was conveyed by the ability of the intermicellar disulphide bonds generated under oxidative stress to promote the formation of stimuli responsive micellar networks.

### **2.3.3. Nanogels**

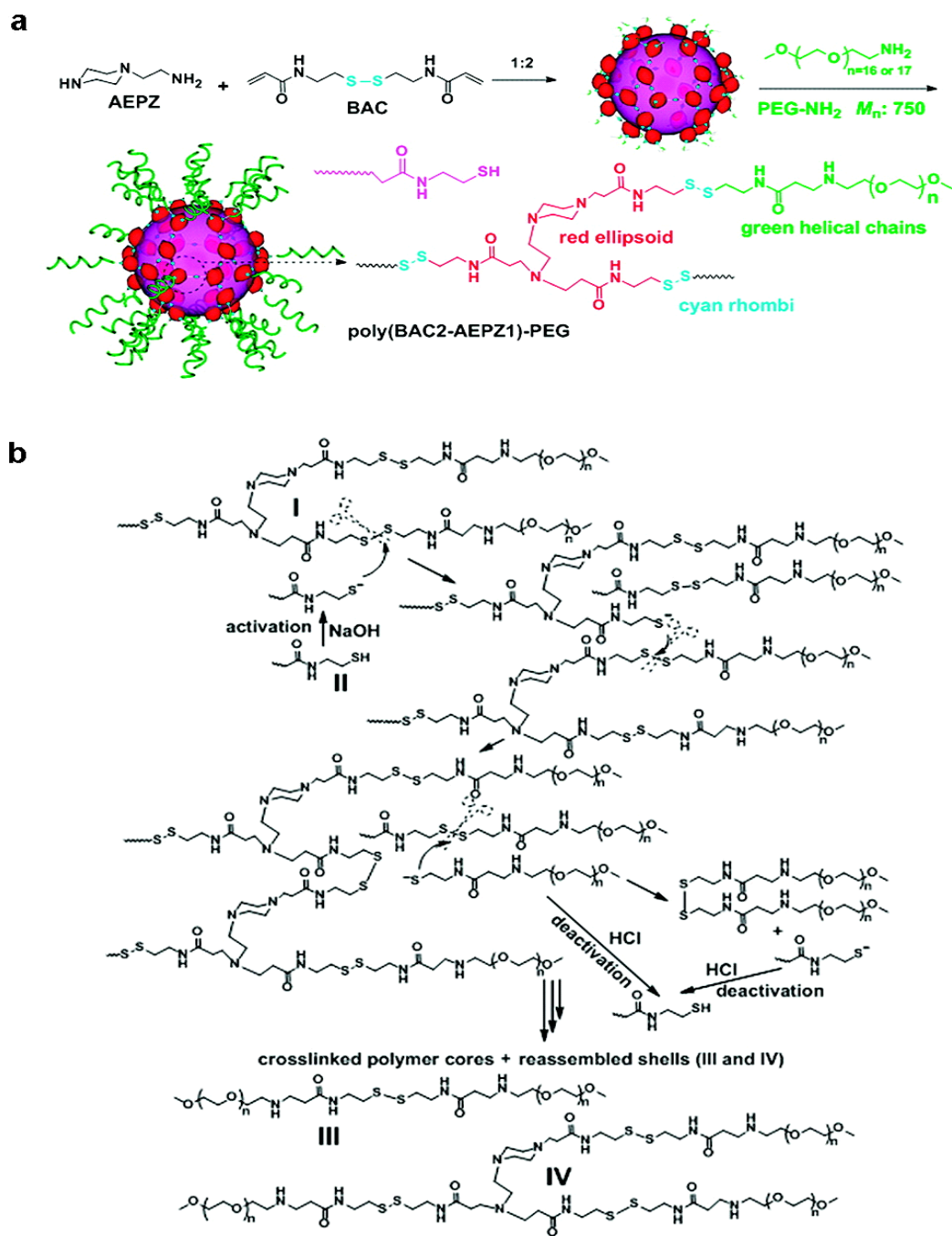
Nanogels are potential drug delivery systems especially in their applications in drug and gene delivery. Nanogels are networks with interior and exterior properties that allow water or physiological fluid to distend the network structure which has similar characteristics to hydrogels and nanoparticles (Oh et al., 2008). Tan et al., (2011) explain that nanogel sizes offer additional properties advantageous to nanogel networks such as increased surface area for bioconjugation, entrapment of biomolecules such as drug, proteins, carbohydrates, and DNA, and the immediate response to external stimuli. Nanogels have attracted attention in material science for use in cosmetics, biotechnology and medicine. Morimoto et al.,(2008) prepared dual responsive nanogels which were able to alter their responses to redox and temperature conditions. Poly (N-isopropylacrylamide) (PNIPAM)-grafted polysaccharides were prepared with end thiols. The PNIPAM chains were grafted with pullulan which was treated with sulfanylthiocarbonylsulfanyl (STS), to functionalize the conjunction between PNIPAM and STS. The PNIPAM-grafted pullulan was then aminolysed to thiols. The nanogels were found to swell slightly on cooling and the nanogel sizes were approximately 102nm, in water and upon reducing the disulphide bonds, the average size of the particles were approximately 55nm at a temperature of 50°C. Tan et al., (2011) synthesised thiolated hydroxypropyl cellulose (HPC-SH) as a means of preparing dual-sensitive self assembled fabricated nanogels. The HPC-SH maintained the thermosensitivity of the HPC and the thiol groups were oxidised to form disulphide bonds. The oxidation of the thiol groups was to help the HPC-SH to stabilize the association structure. The HPC-SH was easily disassociated by reducing the disulphide bond using dithiothoureitol (DTT) and the temperature affected the hydrodynamic radius of the HPC-SH architect. Scheme 3 depicts the basic concept of thiol thermo/redox responsive mechanism (Roy et al., 2010).



**Scheme 3.** Basic concept of thiol thermo/redox responsive mechanism [Reproduced with permission from Roy et al., 2010 © Elsevier B.V. Ltd].

#### 2.3.4. Hydrogels

Synthesis of biodegradable gel can be achieved by two methods: i) the copolymerisations of monomers in the presence of disulphide-containing crosslinkers; and (ii) the oxidation of multi-thiol containing polymers such as di/trifunctional telechelic thiol polymers. Wu and co-workers [69] demonstrated the synthesis of “living” controlled *in situ* gelling system which uses the thiol-disulphide exchange reaction. The branched “living” hydrogel was synthesised by the Michael addition polymerization binding 1-(2-aminoethyl)piperazine (AEPZ) with N,N'-bis(acryloyl)cystamine (BAC) to yield a core-shell branched polymer, poly(BAC<sub>2</sub>-AEPZ<sub>1</sub>)-PEG (BAP). The formation of the “living” *in situ* hydrogel caused the activation, interruption, termination and reactivation by manipulating the pH of the system. The resultant hydrogel as described by Wu et al., (2010) were biocompatible, biodegradable, easily fabricated with certain desired shapes, size and properties (Figure 2.8). The thiol-disulphide exchange reaction was in this instance used to countercheck whether the rearrangement brings forward the intended meaning-otherwise correct as it may be appropriate so as to ultimately manage to control the formation of the gel, which acted as an on and off function.



**Fig. 2.8.** a) The synthesis of branched Poly(BAC2-AEPZ1)-PEG (BAP); and b) the thiol-disulfide exchange reaction which causes the formation of cross-linked Poly(BAC2-AEPZ1) cores [Reproduced with permission from Wu et al., 2010 © American Chemical Society]

### **2.3.5. Thiomers**

The uniqueness of using thiol-based polymers is their ability to form mucoadhesive polymers capable of forming covalent bonds with cysteine rich residues from other proteins. The ease of forming covalent bonds with various surfaces such as the mucosa achieves various effects. Some of which enhance contact to the absorptive mucosa that favour drug absorption and bypass enzymatic degradation. Bernkop et al., (2005) also noted that the prolonged retention time of short biological half-life of certain biopharmaceutics was improved and resulted in better patient compliance for drug delivery systems.

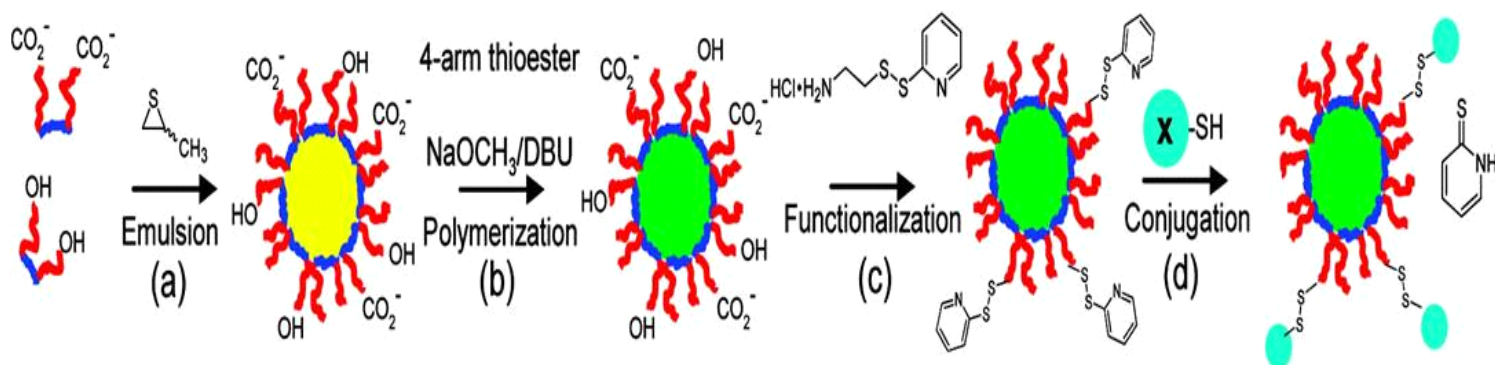
The most common thiolated polymer researched for most drug delivery systems was thiolated chitosan (Bernkop et al., 2005; Bravo-Osuna et al., 2006, Bravo-Osuna et al., 2007; Bravo-Osuna et al., 2007). Some other researched polymers include the hydrophilic polymers poly(acrylates) (Greimel et al., 2006; Palmberger et al., 2007; Greindl et al., 2006; Iqbal et al., 2006) or deacetylated gellan gum (Krauland et al., 2003; Narkar et al., 2010; Cao et al., 2009). The above mentioned polymers contain thiol groups on their side chains. The unique characteristic of the disulphide bond especially as a tool in drug delivery is its reversibility and its relative stability in plasma.

### **2.4. Bioconjugation for drug delivery**

Bioconjugation strategies have been employed in many drug delivery systems via the use of linkers Kamada et al., (2010). Proteins moieties and molecules have been used to form protein-protein, protein-molecules and protein-drugs interactions. The attachments of cellular and subcellular moieties, drug delivery enhancing molecules and the functional groups to the drugs have become essential and important in modern day drug delivery. The success of the linker between the bioactive and the drug delivery system determines the degree of success of the system and its effect. The problems highlighted by Saito et al., (2001) associated with the above mentioned linkers have been in the increase of the drug weight especially in macromolecular carriers, pharmacokinetics of the drug delivery system and metabolism of the macromolecule. As previously explained, Dharap et al., (2005) had used the LHOVRH peptide to create a polymer drug delivery carrier which targeted the ovalbumin, breast and prostate cancer cells. The drug delivery carrier was designed to firstly induce apoptosis, secondly to target moieties and enhance penetration, and lastly to carry the anti-cancer drug to the specific tumor site. The LHOVRH results showed that the hormone enhanced the above mentioned and targeted responses. Vlies et al., (2010) synthesised pyridyl functionalised nanoparticles for small molecules, peptides and proteins. The nanoparticles were designed to carry thiol reactive groups, to which other thiol containing antigens and biomolecules would bind in non-thiol competitive environments. The pyridyl functionalised



nanoparticles were 25nm in size and permitted efficient release of the antigen intracellularly. Hydroxyl and carboxylic polymers were used in the emulsion with propylene sulphide. 4-arm thioester was added and polymerised and functionalised by adding iodoacetamide (Figure 2.9).



**Fig.2.9.** Conjugation of the carboxylated nanoparticles and pyridyl disulphide yielding Ovalbumin protein biologically-functionalized: (a) Hydroxyl-Pluronic and carboxylate-Pluronic are used to make an emulsion with propylene sulfide. (b) To the emulsion is added four-arm thiol initiator, and polymerization is started by addition of base. After polymerization, particles are exposed to air to cross-link, and the remaining thiolates are end-capped with iodoacetamide. (c) The carboxylate-nanoparticles are reacted with pyridyl disulfide cysteamine to yield thiol-reactive functionalizable nanoparticles. (d) Conjugation of thiol-containing biotin, AcSDKDSLKCGOH peptide, and ovalbumin protein gives biological-functional nanoparticles. [Reproduced with permission from Vlies et al., 2010 [85] © American Chemical Society].

#### 2.4.1. Disulphide bond linkages

Covalent linkages have been commonly used for the reversibility and stability of these bonds in drug, molecular and protein interactions (Madea et al., 2009). The recent focus has been in utilizing covalent disulphide bonds in creating stably expressed drug delivery systems. The unique characteristics of the disulphide bond are its reversibility and relative stability in the plasma. Saito et al., noted that the high redox potential difference between the oxidizing extracellular space and the reducing intracellular space has made the disulphide bond feasible as a successful delivery tool. The application of these thiol-based conjugations have achieved targeted bioactive delivery, enhanced cellular cytosolic delivery, improved pharmacokinetics and also an improved stability of the formed bond. Cayot et al., (2002) used electrochemical modifications of proteins in order to cleave the disulphide bonds. It was reported that at pH 10 and 11 the disulphide bonds were reduced.

### **2.4.2. Creating thiols via chemical and molecular approaches**

The conjugation of two molecules via disulphide bonds need two free sulfhydryl groups that are either exogenously introduced or found readily existing between two cysteine amino groups. Many approaches have been adopted in drug delivery to create these thiol groups, some of which include incorporating thiol group moieties onto the polymer or chemically modulating the polymer to express its own thiol groups as mentioned above. The former is achieved by introducing cysteine derivatives onto the polymer and the latter is achieved by the chemical modification of the polymer, such as using oxidation or reduction to expose the buried thiol groups, considering modification of any polymer generally result in a slight decline in its efficacy. The other way that thiol groups could be introduced onto a polymer is by using hetero-bifunctional linkers. These linkers are found exposed on the surfaces of lysine residues or the N-terminal residues. Some examples of these linkers are 2-imithiolane and N-succinimidyl S-acetylthioacetate (SATA) (Frandsen et al., 2012). Conjugating approaches such as site specific conjugation of cysteines introduced into recombinant expressed protein are achieved by directing the amino acid to a specific site for amino acid substitution. This approach has been beneficial especially with the use of newly genetically modified proteins for enhanced drug delivery (Olas et al., 2010). Weber et al., (2000) prepared surface modified nanoparticles by introducing exogenous thiols onto the surface of human serum albumin (HSA). The thiol groups were introduced by reducing the aldehyde residues with dithiothreitol or 2-imithiolane for attachment onto the surface HSA nanoparticles, which resulted in well defined characterised thiol surface. The thiols were highly stable with a half-life of 28.2 days.

### **2.4.3. Disulphide drug delivery mechanisms**

There are three main approaches in disulphide linkages that are generally employed by drug delivery systems, the first being the employment of macromolecule for endocytosis across the plasma membrane (i.e. in the cells), secondly cytosolic delivery of macromolecules and lastly cleavage of the disulphide in the systemic circulation, which are briefed as under.

#### **2.4.3.1. Macromolecular drug delivery uptake via endocytosis**

The uptake of macromolecular drugs by endocytosis has proven to be beneficial and effective as a mode of drug delivery. One example includes the use of antibody targeted chemotherapy drugs that use disulphide bonds to release anti-carcinogenic drugs upon cellular internalisation (Singh et al., 2008). Endocrine glands such as the pancreas, liver and stomach are generally known to have the ability to cleave disulphide bonds or oxidise the bonds utilising hormone cleavage. In cells, the cellular compartments have been targeted such as the Golgi apparatus, endosomes, lysosomes and the plasma membrane. These

sub-cellular organelles show potential thiol interaction sites because of their free thiol group moieties which enable easy disulphide formation creating improved binding and stability between the drug-drug for the drug delivery vehicle to be efficient.

#### **2.4.3.2. Attachment by targeting moiety through thiols**

Moieties provide good sites for attachment. The free accessible thiol groups are increased in number and show improved number of stably expressed thiol groups that can bind strongly onto a linker, conjugate complex or a hydrogel. The creation of moieties occurs by the addition of the thiol moiety which can be controlled by synthesizing stably expressed conjugates that are stable in the systemic circulation (Chi et al., 2003).

The importance of using interchangeable disulphide bonds is that they create stability in the drug delivery system as a whole; they also create relatively stable covalent bonds to modulate the stability of the formulation in an aqueous environment (Pitaressi et al., 2008). Disulphide bonds are also important in stabilising and assembling small proteins such as genes, viruses and bacteria. It has however been noted in a study done by Pitarresi et al., that the increase in disulphide interactions between drug delivery system and the mucosa of the intestine was decreased due to strong bonds that were not easily cleaved thus resulting in reduced drug release profiles.

#### **2.4.3.3. Disulphide cleavage in the circulatory system**

Blood plasma generally has an oxidising environment and the reduction of disulphide bonds occurs frequently in the systemic circulation because of the low concentrations of cysteines present in the body. The disulphide bonds are eventually cleaved resulting in increased release of the drug or polymer in blood circulation. The bioconjugate or linker is also designed to decompose the amino component ensuring biodegradability of the polymer or carrier to enhance drug release.

### **2.5. Mucoadhesive nanoparticulate system**

Biohesion onto the intestinal mucous membrane was popularised by Longer et al. in 1985. Longer et al., (1985) were the first to prove that intestinal mucosal bioadhesion improves drug absorption by increasing the drug residence time. This led to a delayed gastrointestinal transit which improved drug absorption and controlled the drug released from the drug delivery device. The most common dosage form used for mucoadhesion was in a tablet or a capsule form. This was achieved by coating the tablet with Carbopol and hydroxypropyl-methylcellulose. Bern-Schurp and co-workers (Bravo-Osuna et al., 2007; Cevher et al., 2008; Cevher et al., 2008; Chopra et al., 2008; Davidovich-Pinhas et al., 2009) adopted

chitosan as a mucoadhesive polymer and have since proven that chitosan provides good mucoadhesive properties. Chitosan has also been used in an array of drug delivery systems for example transdermal patches (Grabovac et al., 2008) because of its permeation enhancer properties (Imam et al., 2003). It has even been used in transfection (Loretz et al., 2007) as well as a cysteine conjugate (Schimtz et al., 2008; Werle et al., 2007; Werle et al., 2007; Reinwarth et al., 2012; Werle et al., 2006). Furthermore Chitosan has been utilised for its application in oral non-viral gene delivery (Martein et al., 2007) and nasal delivery of bioactives (Krauland et al., 2006). Notably, bioadhesive polymers have become important in delivering poorly absorbable drugs since their inception in the 1990s.

Peptide drugs are gastroenterologically poorly absorbed owing to their high molecular weight and hydrophilicity, not to mention their quick biodegradability by gastric enzymes (Hamman et al., 2005). The concept of delivering peptide drugs orally would have been ideal if they could bypass enzyme degradation in the stomach and remain intact until when they become absorbed or released. This concept has been applied to other delivery systems such as pulmonary (Luppi et al., 2009), vaginal (Bernkop-Schnurch et al., 2003), nasal (Sharma et al., 2010) and ocular (Vijay et al., 2008) drug administration systems via the mucous membranes.

### **2.5.1. Improvement of thiomers for enhanced mucoadhesion**

To improve mucoadhesion in animal models two basic concepts have been adopted, the first one being targeting of the mucus gel layers in the pulmonary, ocular and the vaginal systems, while the second one is the *in situ* cross-linking process:

#### **2.5.1.1. Formation of disulphide bonds with the mucus gel layer**

Disulphide bonds form between two thiol groups between the thiomers and the mucus gel. Mucins in particular the mucus glycoproteins, exhibit cysteine rich subdomains that provide desirable potential sites for thiomers attachment. The rate of disulphide bond formation between two surfaces depends on the concentration of the thiolate anions between the two or three potential binding sites. The concentration of the thiolate anions has been reported to be mainly affected by the pKa of the thiol group, the pH of the thiomers and the pH of the surrounding medium (Peppas et al., 2009). The pKa of the thiol group mostly affects the polymer backbone and the chemical structure of the conjugate by causing instability in the backbone. The pH of the thiomers such as in ionic thiomers, which are commonly used, display high buffer capacity (Albrecht et al., 2007). It has also been noted that the reactivity of the thiomers can be controlled by adjusting the pH of the polymer to a certain level. The higher the pH of the polymer the more thiol reactivity and vice versa. The pH of the

surrounding medium determines the reactivity of the thiols on the surface of the polymer (Bernkop-Schnurch et al., 2006). The mucus layer in this instance has a pH of 7, allowing the thiols to react and penetrate the mucus layer efficiently.

#### **2.5.1.2. *In situ* cross-linking process**

The other mechanism used to improve the mucoadhesive properties of thiomers has been the cross-linking properties. The mechanism works on the basis of thiol bonds forming additional disulphide bonds within the polymer itself after cross-linking with the gel. This has led to an improved anchorage of the polymer with the gel layer which results in the stabilization of the drug delivery carrier (Ho et al., 2010; Sreenivas et al., 2008)). The mechanism improves the adhesive properties by improving penetration of the polymer device and increasing the stability process. It has been demonstrated that thiols oxidised at physiological pH-values result in the formation of inter- and intramolecular disulphide bonds (Jauhari et al., 2006; Wang et al., 2009). These findings were confirmed by rheology, diffusion, gel permeation and mucoadhesion studies. It was also found that the rheological properties of thiolated polymers helped to improve the elasticity of the gel because of the immobilized thiol groups which resulted in higher elastic modulus (i.e.  $G'$ ). In the case of anionic thiomers, the tensile properties were improved by 2 to 20-fold while viscosity correlated to *in situ* cross-linking (increased by 10-fold). The intestinal residence time was also improved by 3-fold.

#### **2.5.1.3. Dosage forms of thiomers**

Shaji et al., (2008) reported that thiolated nanoparticles easily disintegrate because of the oxidation of the sulphate ion, but when calcium ions and sulfonate ions were bound to them they tended to inhibit disintegration. This led to stabilisation of the cross-linking process; however this caused a reduction in the mucoadhesive properties of the nanoparticles. The immobilisation of the thiol groups in turn resulted in the improvement of the mucoadhesive properties by forming disulphide bonds within the thiomers and the mucin surface thus increasing the stability of the drug delivery system. The double binding of thiols resulted in the particles not disintegrating easily under physiological conditions. The size of the particles also contributed to the prolonged residence time.

Thiomer matrices are useful for intraoral, peroral, ocular and vaginal administration. The cross-linking properties of thiomers guarantee the cohesiveness and stability of the carrier matrix (Loretz et al., 2007). The dry matrix tablet adheres and interpenetrates more easily depending on the swelling behaviour of the delivery system. The hydration state of the tablet will determine the cohesiveness of the drug delivery system, hence targeting moist or well

hydrated areas permits for better adhesion and penetration behaviour of the system (Malik et al., 2007). In addition, thiomers provide advantageous controlled drug delivery systems which have been previously proven to be effective and sufficient, in this example by homogenising the thiomers with a drug and compressing the system to a tablet form yielded guaranteed zero order release delivery system for several hours. The formation of thiomers tablets are predominately controlled by hydration states of the environment in which they are to be administered and the diffusion process between the administration layer and the thiomers. The vagina and nasal cavity provides an attractive alternative for drug delivery systems compared to the oral delivery of drugs. The vagina and nasal cavity permit for peptides, protein carriers and drugs to attach covalently on the mucus surfaces resulting in efficient residence time on the mucosa (Morishita et al., 2006).

Challenges surrounding liquid formulations as novel drug delivery systems have always been rather obvious because of residence time that the drug delivery system has in contact with the adhesion surface. A comparison between tablet and liquid formulations that involved mucoadhesion microdisc engineered for ophthalmic drug delivery, revealed that liquid formulations were previously inefficient as drug delivery systems due to their shortened residence time (Thompson et al., 2011). Thus, most of the ophthalmic formulations were improved by adding mucoadhesive polymers that could enable them attach easily and quickly on the surface.

#### **2.5.1.4. Current sulfur conjugates**

An interesting recent expansion of the use of thiols has been the in conjugating thiols to metal atoms. Clusters of the thiol-metal conjugates such as gold conjugated to p-mercaptobenzoic acid ( $\text{Au}_{102}(\text{p-MBA})$ ) and  $\text{Au}_{25}(\text{SCH}_2\text{CH}_2\text{Ph})_{18}$ , have been successfully synthesised in neutral and anionic charge states (Gupta et al., 2009; Heaven et al., 2008). In a recent study performed by Kacprzak et al., (2010) and Seib et al., (2006) the thiolate ion was conjugated to copper, silver and gold. These metal-thiolate complexes containing flexible bond motifs demonstrate structural monocyclic rings, catenanes and helix structures which often compete in energy when analysed using structural, vibrational and electronic studies. Of the three metal-thiolates, copper was found to be the strongest metal to sulphur bond (Cu-S), followed by gold (Au-S) and lastly by silver (Ag-S). The most interesting feature of vibrational analysis was the covalency between the Au-S bond, whereas the Cu-S bond was the most polar of the three. This vibrational result shows the ability of the covalent thiolate to bond better with a polar motif than a covalent metal, in this case Au. Unfortunately due to poor solubility the applications of metal-sulfur complexes are relatively few.

## **2.6. Concluding Remarks**

The review illustrated the potential versatility of synthetic and natural approaches for designing, optimizing and functionalizing nanostructures and conjugates by thiol chemistry modifications. The examples used in the review illustrate the power and adaptability of thiols for site specific functionalization, the construction of complex macromolecules and the generation of both biodegradable disulphides and non-biodegradable bonds. In addition, the ability of thiols to react with various functional groups found in various polymer science materials and peptide related structures were demonstrated. In spite of the fact that research efforts in thiol chemistry is still in the initial stages, it is likely that its true potential has yet to be discovered. It is however anticipated that thiol chemistry will be used as an effective tool in drug delivery and as a drug carrier systems.

## CHAPTER 3

### Disulphide/Thiol Covalent Chemistry: A Method for Preparing Selectively Functionalised Captopril-Ovalbumin Drug Delivery Conjugates

---

#### 3.1. Introduction

Polymer therapeutics is a term largely used to describe polymeric drugs, polymer conjugates in the form of polymer-drug or -protein conjugates, polymeric micelles or gels to which drugs are covalently bound (Hein et al., 2008). Polymer therapeutics has proven to be effective in conjugating biocompatible polymers to therapeutic proteins or drugs for improved drug, protein or gene delivery. Biocompatible polymers have played very important roles in modern pharmaceutical sciences; nonetheless there is demand for the ever-increasing more efficient polymer chemistry to innovate new and diverse pharmaceutical polymers (Cramer et al., 2004; Li et al., 2009; Roth et al., 2011; Bumcrot et al., 2006). One interesting and fast advancing tool used in polymer science is the use of thiol chemistry for polymer synthesis, functionalization and conjugation.

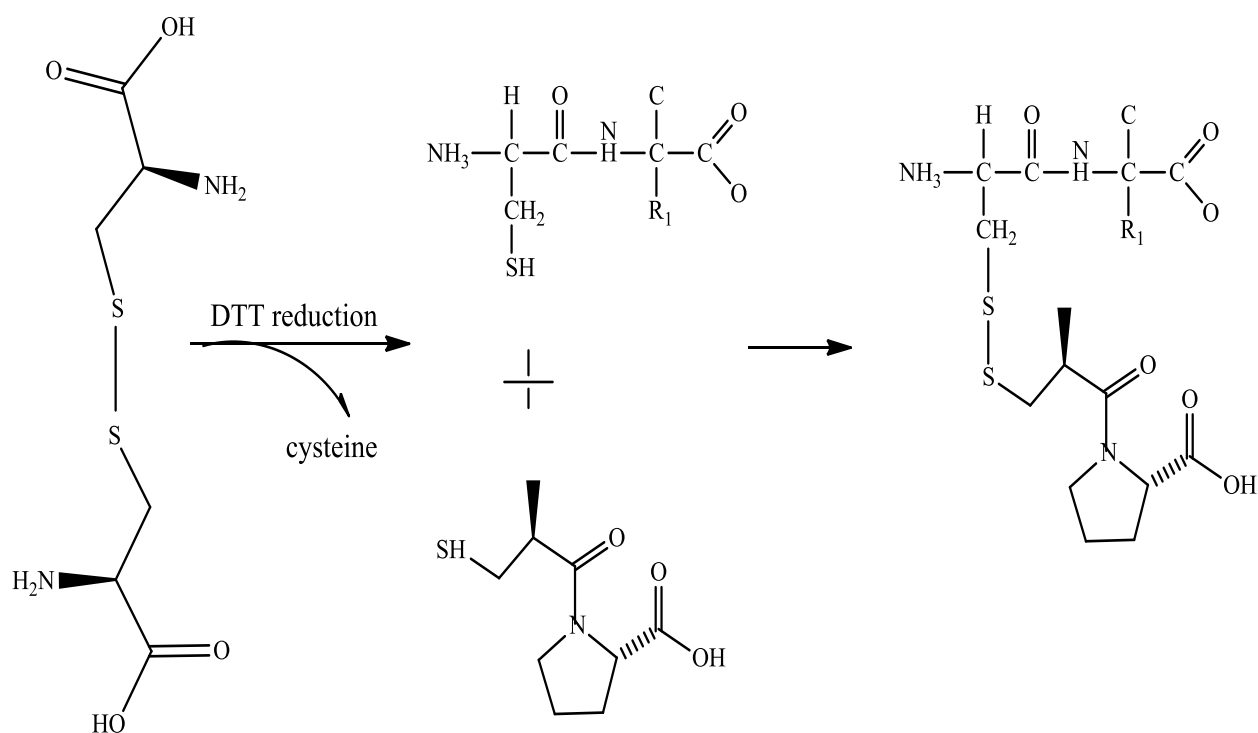
Disulphide groups are known to degrade into sulfhydryl groups in the presence various reducing agents. The sulfhydryl groups otherwise known as thiol functional groups (SH) are formed spontaneously when exposed to air by autoxidation or reduction (Judy, 2011; Kosters et al., 2003). When reduced the resulting thiols can rebond to form disulphide bonds. Thiols can also be produced by either partial heating of the protein (Alting et al., 2002), by acid induced denaturing of the disulphide bonds or by salt induced denaturation (Alting et al., 2000; Alting et al., 2003; Moad et al., 2011). The majority of thiol chemistries used for polymer science material and in drug delivery were performed on the ends of Reversible Addition Fragmentation Chain Transfer (RAFT) polymers, derived by reacting thiol containing compounds to form the self assembled multi-arm polymers (Boyer et al., 2009; Back et al., 1979).

A different approach that can be adopted in polymer science is to polymerise protected thiols and expose them in the presence of thiol-reducing reagents. Naturally occurring proteins such as ovalbumin generally have disulphide groups buried in the interior of the protein which makes these proteins attractive alternatives to the use of synthetic polymers. Ovalbumin is one of the major egg-white proteins (60-65%) with a molecular weight of 42.7kDa (Huntington et al., 1997). The protein is a non-inhibitory member of the serine inhibitor (serpin) super-family and has secondary structure elements of  $\alpha$ -helix and  $\beta$ -sheet



(Smith et al., 1965). Ovalbumin has one 'solvent-accessible' disulfide bridge and four free sulfhydryl groups buried in the interior of the protein.

External stressors can modify the ovalbumin protein by chemically separating the disulphide bonds, in some instances by causing partial unfolding of the primary structure, exposure of the hydrophobic bonds, oxidation or reduction of covalent bonds and introduction of the hydrogen bonds. These modifications would ultimately result in either the disintegration of the tertiary structure or varying the degrees of denaturation of the protein. The half-life of the disulphide/thiol reaction  $RS-SR + 2e^- \rightarrow 2RS^-$  has a standard reduction potential of 0.25V and therefore oxidation could be carried out under mild conditions (Huntington et al., 2001).



**Fig. 3.1.** A schematic illustrating the conjugation of one molecule of ovalbumin cysteine conjugating to captopril yielding biologically-functionalized ovalbumin vehicle carriers.

These modifications exhibit the potential binding sites of thiol groups found in all natural and some synthetic protein polymers. The advantages of using thiols as binding sites for biopharmaceutical bioactives is that (1) they have demonstrated increased structural stability in the process of polymer synthesis, (2) have shown multifaceted reactions that thiols can form, (3) demonstrated the versatility of the thiol binding sites and their potential use as drug

carrier systems. The novelty of thiol reactions has been their reversible covalent binding properties *in vivo*. One such covalent reaction includes the thiol containing bioactive pharmaceutical captopril. Captopril (Cp; 1-[(2S)-3-mercapto-2-methylpropionyl]-L-proline) (Cp) is an Angiotensin-Converting Enzyme (ACE) inhibitor, which acts as an anti-hypertensive and binds to proteins via the thiol/disulphide interactions (Cotarelo et al., 2006). The properties of the reaction include the reversibility of the sulphide bond in comparison to other drug-protein interaction in the presence of reducing agents such as dithiothreitol.

The thiol chemistry of macromolecular proteins such as ovalbumin has not yet been extensively reported on, hence the aim of the research is to analyse the ovalbumin polymer after disulphide modification. The chapter was aimed to assess the thiol/disulphide functionalization of the captopril-ovalbumin interaction (Figure 3.1), the structural characterization and mechanical properties of the conjugate complex and to report on the thiol-disulphide covalent substitution reaction.

## **3.2. Material and Methods**

### **3.2.1. Materials**

Quail hen eggs were purchased from Pick 'n Pay Hypermarket. Purified lyophilised ovalbumin (OVA), Dithiothreitol (DTT), 2-Mercaptoethanol (2-ME) and 5'5 Dithio-bis nitrobenzoic acid (DTNB) and captopril were purchased from Sigma (Sigma Aldrich, Missouri, USA). Ethanol, Tris EDTA salt, NaCl<sub>2</sub>, Potassium phosphate monobasic and Disodium hydrogen phosphate were purchased from Merck (Merck KGaA, Darmstadt, Germany). All the chemical agents were analytic grade and used without further purification. It should be noted that no differences were found between the Sigma obtained ovalbumin and the self purified native ovalbumin. For model polymeric studies we used three short homopolymers: lyophilised native ovalbumin (45kDa), modified ovalbumin and drug conjugated ovalbumin.

### **3.2.2. Methods:**

#### **3.2.2.1. Purification and preparation of the native Quail hen eggs for analysis**

The purification method for native ovalbumin was adopted from literature for the purification of ovalbumin (Takahashi et al., 1996; Vachier et al., 1995). Briefly Quail hen eggs, lyophilised ovalbumin was prepared by treating ovalbumin with a solution of ammonium sulphate. The ovalbumin was then washed three times in deionised water and frozen to -70°C and lyophilised for 24 hours. Native ovalbumin (OVA) was then stored at 25°C or at

room temperature until further analysis. Briefly 250mg of modified lyophilised ovalbumin was dissolved in 10mL of 100mM of dithiothreitol buffer solution and incubated for 4 hours. The reduced ovalbumin solution was then washed in deionised water and then stored at 2°C until further analysis

#### **3.2.2.2. Reduction of the disulphide bonds of the native ovalbumin into thiols**

100mM of dithiothreitol solution was prepared for ovalbumin disulphide (SS) modification. 100mg of lyophilised ovalbumin powder was dissolved in 10mL of 100mM dithiothreitol solution and incubated for 4 hours. The polymer solution was then centrifuged and washed three times with deionised water, frozen at -70°C in a refrigerator and lyophilised for 48 hours.

#### **3.2.2.3. Characterization of the native ovalbumin and thiol modified ovalbumin**

The surfaces of the native disulphide ovalbumin and thiol modified ovalbumin were analyzed using the scanning electron microscope (SEM) (PHENOM™ Desktop SEM, FEI Company, Oregon, USA) operated at 10KV in the electron imaging mode. Briefly the ovalbumin samples were mounted on specimen stubs and gold coated using a SPI-Module™ sputter coater (SPI Supplies, STRUCTURE PROBE INC, West Chester, Pennsylvania, USA) and then observed at 600X magnification.

#### **3.2.2.4. Ultraviolet spectrophotometry for the determination of thiols**

Ovalbumin (0.2mg/mL) was incubated at 37°C for 125 minutes in Tris-EDTA buffer. 0.01 volume of 0.4mMol dithio-bis nitrobenzoic acid was added to the sample. After 1 hour at room temperature the absorbance, at 413nm was measured and reactive thiols were determined on the basis of a molar extinction coefficient of 13,600 M<sup>-1</sup>/cm<sup>-1</sup>.

$$E = \frac{A}{bc} \quad (1)$$

Where A=absorbance, b= path length in centimetres, c=concentration in moles/litre (=M).

#### **3.2.2.5. Size and zeta-potential measurements of the native and modified ovalbumin**

The particle size and zeta-potential of the unmodified and thiol reduced ovalbumin were analyzed using the NanoZS instrument (Malvern Instruments (Pty) Ltd., Worcestershire, UK). Briefly, the ovalbumin solutions were dispersed in double distilled water, and filtered through the 0.22µm pore filter. The 10mm quartz cuvette containing the ovalbumin solutions were separately analysed by filling the cuvette with 1mL of the filtered ovalbumin

solution. The zeta-potential was determined using a capillary cell after diluting the solution by a factor of 1:10.

### **3.2.2.6. The conjugation of the modified thiol ovalbumin with thiol containing captopril**

Predetermined captopril, (50mg) was added to the 100 mM disulphide reduced ovalbumin solution and incubated for 1 hour for thiol-thiol binding saturation. The ovalbumin-captopril conjugate solution was then centrifuged and washed three times with deionised water, frozen at -70°C and lyophilised for 24 hours.

### **3.2.2.7. UV analysis for the determination of the thiol concentrations**

Stock solutions were prepared by separately dissolving 10mg of Captopril HCl in 100mL of Phosphate Buffered Saline (PBS) (pH 6.8). From the stock solution a series of dilute standard solutions of the following concentrations: 0.125, 0.25, 0.50, 0.75, 1.0 and 1.25 mg/mL were prepared. The absorbance of each standard solution was determined at the maximum wavelength of absorption ( $\lambda_{max}$ ) of 271nm for captopril hydrochloride.

### **3.2.2.8. UV analysis of the ovalbumin-captopril complex**

Ovalbumin protein, (100mg) was incubated with 50mg captopril for 24 hours at room temperature. Quantification of captopril was achieved via spectrophotometry at 271nm (Cecil CE 3021, 3000 Series, Cecil Instruments, Cambridge, England). The conjugation efficiency of the OVA-captopril conjugates was calculated using the following equations:

$$\text{Conjugation efficiency (\%)} = \frac{\text{weight of drug found conjugated}}{\text{weight of total drug used}} \times 100 \quad (2)$$

$$\text{Drug content (\%}^w/w) = \frac{\text{weight of drug conjugated}}{\text{weight of conjugate}} \times 100 \quad (3)$$

### **3.2.2.9. ATR-FTIR analysis of the native, thiol and ovalbumin-captopril**

Attenuated total reflection Fourier transform infrared spectroscopy (ATR-FTIR) is used to study molecular surface interactions. It is an advantage in the analyses of a whole IR spectrum, especially in mid-IR region where the molecular-specific fingerprint region occurs. The powdered samples of the three ovalbumin variants, namely native, thiol modified and captopril conjugate complex of ovalbumin were analysed using the the Perkin Elmer 2000

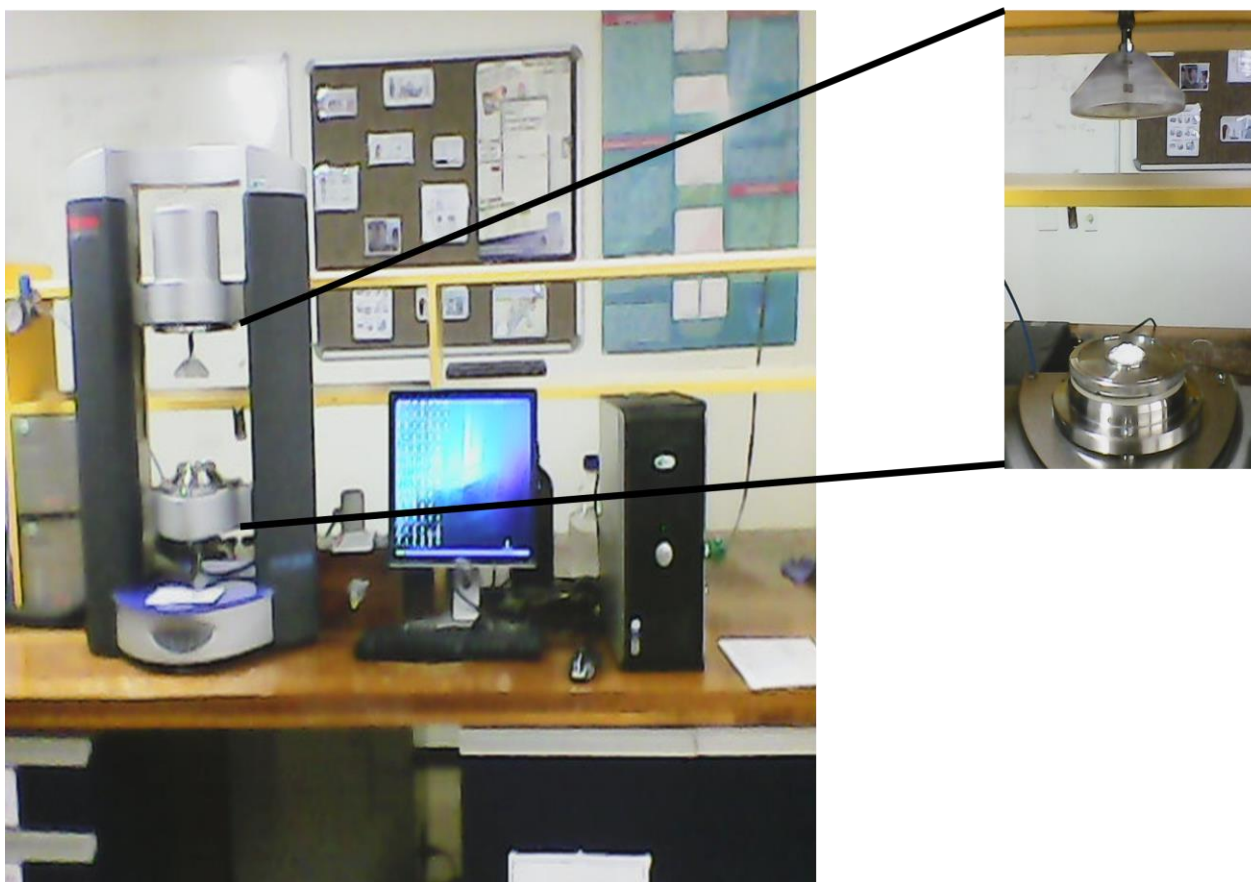
FTIR spectrometer that was fitted with a MIRTGS detector (PerkinElmer Spectrum 100, Llantrisant, Wales, UK). The three ovalbumin variants were analyzed at a wavelength number of  $650\text{-}4000\text{cm}^{-1}$  with a resolution of  $4\text{cm}^{-1}$ . The absorbance was also measured at a wavelength number of  $0\text{-}0.75\text{nm}$ .

#### **3.2.2.10. H<sup>+</sup> NMR analysis of the native and thiol modified ovalbumin**

Thiol functional groups bind readily to metal ions and form hydrogen bonds, which stabilize the secondary and tertiary structures of proteins [detection of sulfhydryl groups 3,4]. The unique feature of thiol groups is their low proton/deuteron fractionation factors ( $\text{SD}/\text{SH}=0.5$ ), making thiols of cysteine residues to preferentially bind to protons, rather than deuterons in a mixture of water and deuterated water.

#### **3.2.2.11. Rheological analysis of the native, thiol and ovalbumin-captopril**

The viscosity ( $\eta$ ), storage and loss modulus ( $G'$  and  $G''$  respectively) were analysed using the modular advanced rheometer (HAAKE MARS Modular Advanced Rheometer, Thermo electron Corporation, Karlsruhe, Germany). The native, thiol modified and captopril conjugated aqueous samples were measured at different sampling points to assess the rheological changes affecting inter and intramolecular changes that occurred during analysis. All samples were analysed at room temperature except for the thermal analysis response of the samples at high temperatures of  $90^\circ\text{C}$  summary the sample solution was poured onto the parallel-plate geometry (50 mm in diameter) and a small amount of silicone oil was applied at the periphery of the solution to prevent evaporation. The dynamic storage modulus ( $G'$ ) and loss modulus ( $G''$ ) were examined as functions of temperature. The specific viscosity of ovalbumin solutions (100mg/mL 20mM phosphate buffer, pH 7.0, containing 0.1 M NaCl, filtered through a  $0.45\mu\text{m}$  filter) that had been subjected to 1 hour at  $37^\circ\text{C}$  and cooled at  $25^\circ\text{C}$ . The Haake viscometer was calibrated with the ovalbumin solution before heating.



**Fig.3.1.1.** Image of the captopril conjugated ovalbumin which was placed between the two parallel plates for rheological analysis.

#### **3.2.2.11.1. Yield stress test of the native, thiol and ovalbumin-captopril**

5mL of aqueous ovalbumin solutions, namely native, thiol modified and captopril conjugated ovalbumin was placed between the two parallel plates (Figure 3.1.1). To prevent evaporation, silicon oil was added to the ovalbumin solution to seal it. Since the silicon oil was non-reactive under experimental conditions, its viscosity would not change with temperature during measurement. The sealed fixture was then covered with a conical silicon cover to mitigate solvent evaporation and ensured uniform temperature distribution.

#### **3.2.2.11.2. Viscosity of the native, thiol and ovalbumin-captopril**

Viscosity was analysed to determine the resistance to flow of the native, thiol modified and captopril conjugated ovalbumin in aqueous solution. The samples were subject to a shear rate range of 0 – 200 1/s over 180 seconds.

#### **3.2.2.11.3. Oscillatory stress sweep of the native, thiol and ovalbumin-captopril**

The analysis of the viscosity and elastic behaviour of the native, thiol modified and captopril conjugated ovalbumin aqueous solutions and the network structure formed by drug/particle-particle interactions, an oscillation frequency sweep test was performed. Oscillation stress sweep tests were carried out at a constant frequency of 1Hz in a stress range of 100 Pa. Oscillation frequency sweep tests were performed over a frequency range from 0.1 to 10 Hz at constant stress amplitude of 1 and 5 Pa, respectively.

#### **3.2.2.11.4. Oscillatory frequency sweep of the native, thiol and ovalbumin-captopril**

A frequency sweep test is a dynamic test measuring the response of a system as a function of frequency at constant stress amplitude. It demonstrated that the storage modulus  $G'$  (elastic response), the loss modulus  $G''$  (viscous response) and the complex viscosity of a sample. The shear stress of each sample was dependant on the on the yield value obtained from the yield stress measured.

#### **3.2.2.11.5. Oscillatory thermal analysis of the native, thiol and ovalbumin-captopril**

The linear viscoelastic region of the systems was first determined the oscillatory stress sweep. Temperature ramps were performed over the range 20–90 °C, at a frequency of 1 Hz, with an oscillatory torque of 500 Nm. During the frequency sweep, a solvent trap polycarbonate cover was used to prevent sample drying and evaporating as this would affect the rheological properties of the ovalbumin solutions.

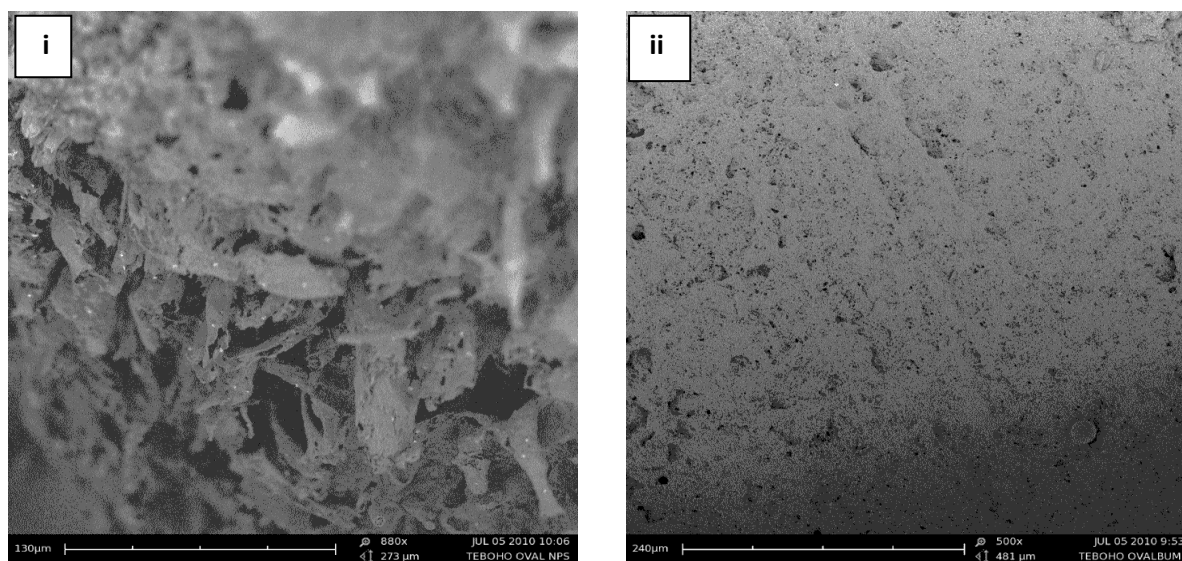
#### **3.2.2.11.6. Thermal characterization of the native, thiol and ovalbumin-captopril**

The thermal characterisation of the native, thiol modified and captopril conjugated ovalbumin were performed on a Differential Scanning Calorimetry (DSC) (1 STAR<sup>e</sup> system, Mettler Toledo, Schwerzenbenbach, Switzerland). 50mg/ml of native ovalbumin, modified ovalbumin and captopril-SS-ovalbumin were heated from 25 to 100°C at 1 °C/min. The denaturation temperature ( $T_d$ ) was evaluated using STAR<sup>e</sup> software. The total enthalpy change and the enthalpy changes of the polymers and drug were determined by integration of the peak area upon deconvolution of the recorded thermogram of the three native, thiol modified and captopril conjugated components.

### 3.3. Results and Discussion

#### 3.3.1. Morphological characterization of the disulphide native ovalbumin polymer

Ovalbumin proteins undergo significant conformational changes, when subjected to extreme pH conditions which in turn affect the structural integrity and biological activity. These proteins, molten globule, maintain a relatively compact structure i.e., preserve most of secondary structure but lose some of their tertiary structure. Molten globule by definition is an ensemble of structure related molecules that are rapidly interconverging, but slowly change into a single unique conformation which results in greater flexibility of the protein. It was demonstrated that incubation of lyophilised Quail egg ovalbumin (Figure 3.2.i) at extreme acidic pH, resulted in a molten globule state as visualised in Figure 3.2.ii. The conversion of ovalbumin molten globule to unfolded state was energetically small and rapid which was followed by the unfolded state. The end of the unfolded state was characterized by the decomposition of hydrogen, disulphide and electrostatic bonds. In the unfolded state ovalbumin showed greater flexibility and increased folding caused by the interconverging of hydrophobic bonds which resulted in the aggregation of ovalbumin [3].



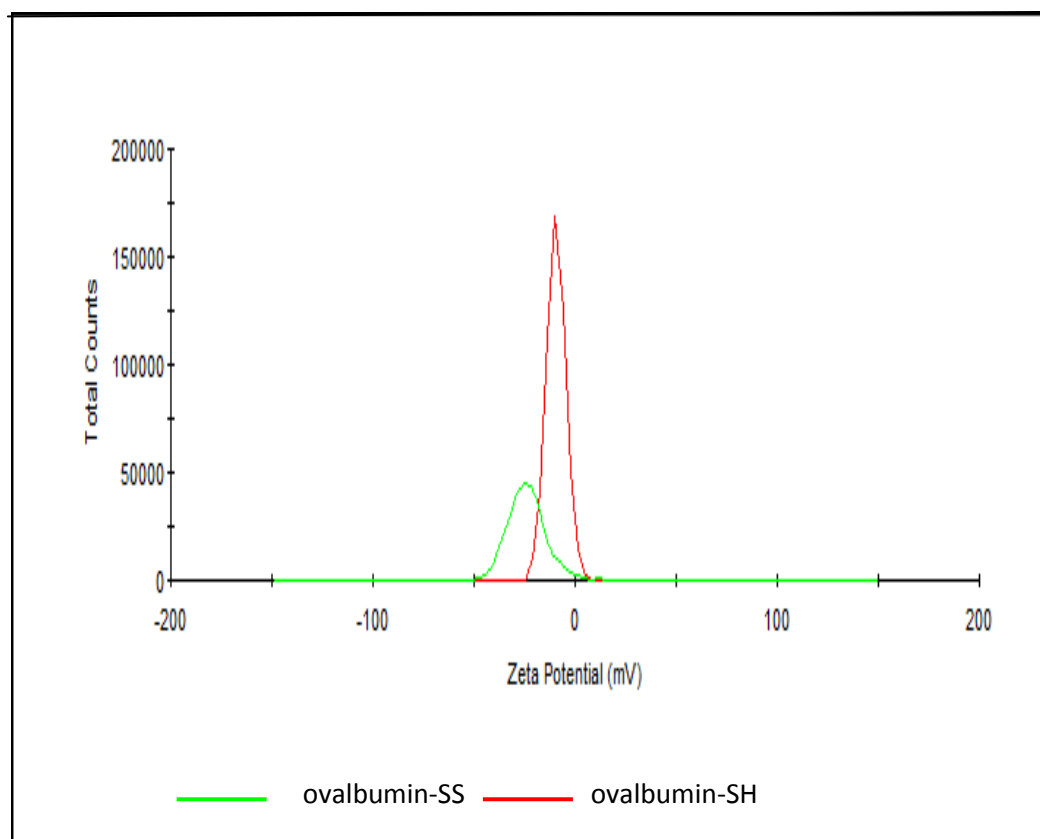
**Fig.3.2. (i)** Surface analysis of the unmodified native lyophilised ovalbumin. **(ii)** Morphology of disulphide reduced ovalbumin yielding a smooth porous surface.

#### 3.3.2. Size and zeta-potential comparison of the ovalbumin polymer

In comparison to the native ovalbumin which had an average particle size of 226.9nm, the sizes of the modified ovalbumin fragments were 6nm after a 4 hour of reducing treatment with dithiothreitol. The reduction of the ovalbumin protein was a time and concentration dependant reaction. The predetermined optimal concentration of dithreitol chosen for this



specific study was 30mM which yielded the best total free and bound thiols in solution. An average of 0.264mM of 100mg was obtained which bound on 30mg of drug. The zeta potential, shown in Figure 3.3, was greater in native lyophilised ovalbumin than in modified lyophilised ovalbumin. This could be because of the greater hydrogen ion concentration in solution from the reduced disulphide bonds yielding a value of -10mV and the native ovalbumin yielded a value of -26mV.

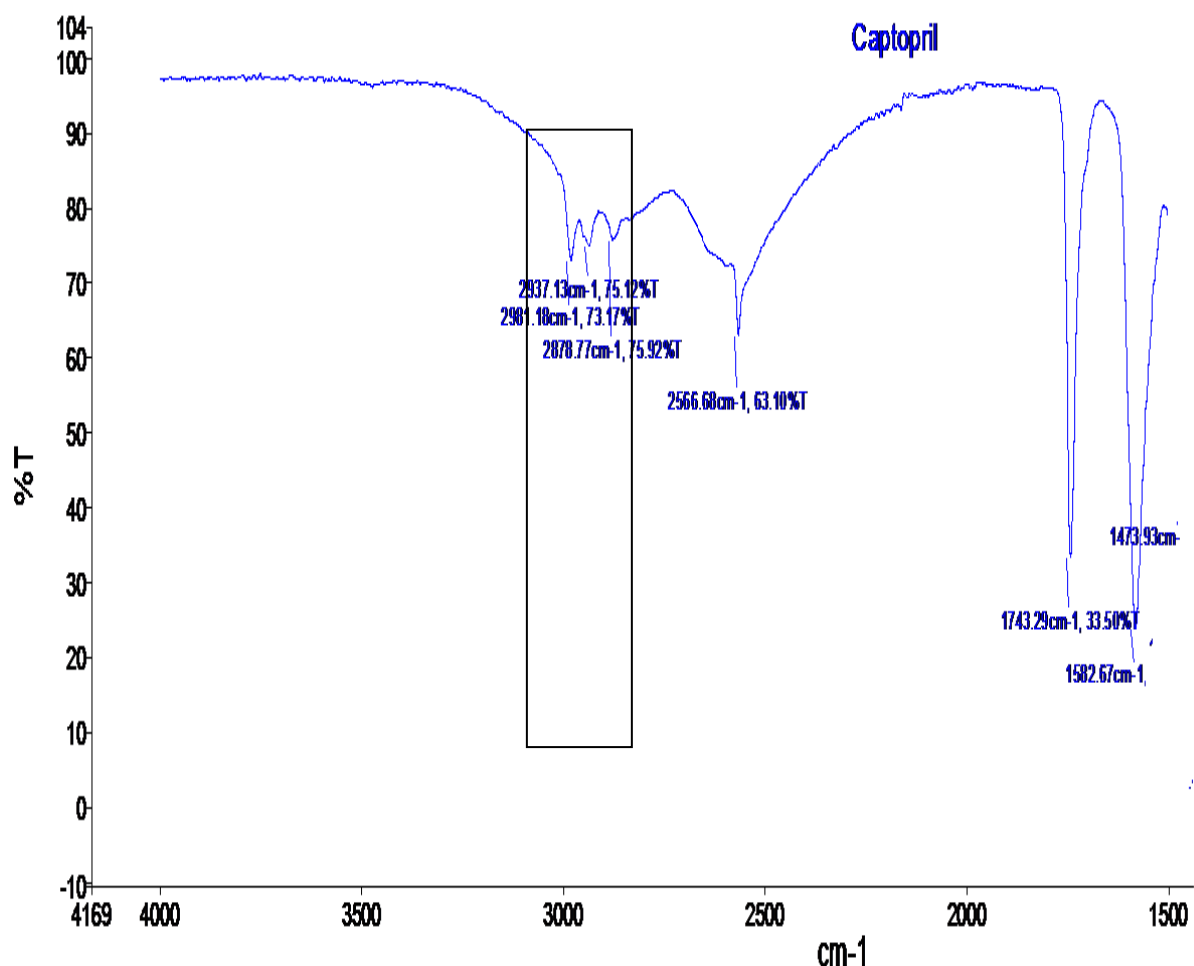


**Fig.3.3.** Zeta Potential of unmodified and thiol modified ovalbumin dispersed in deionised water measured by DLS: ovalbumin-SS and ovalbumin-SH.

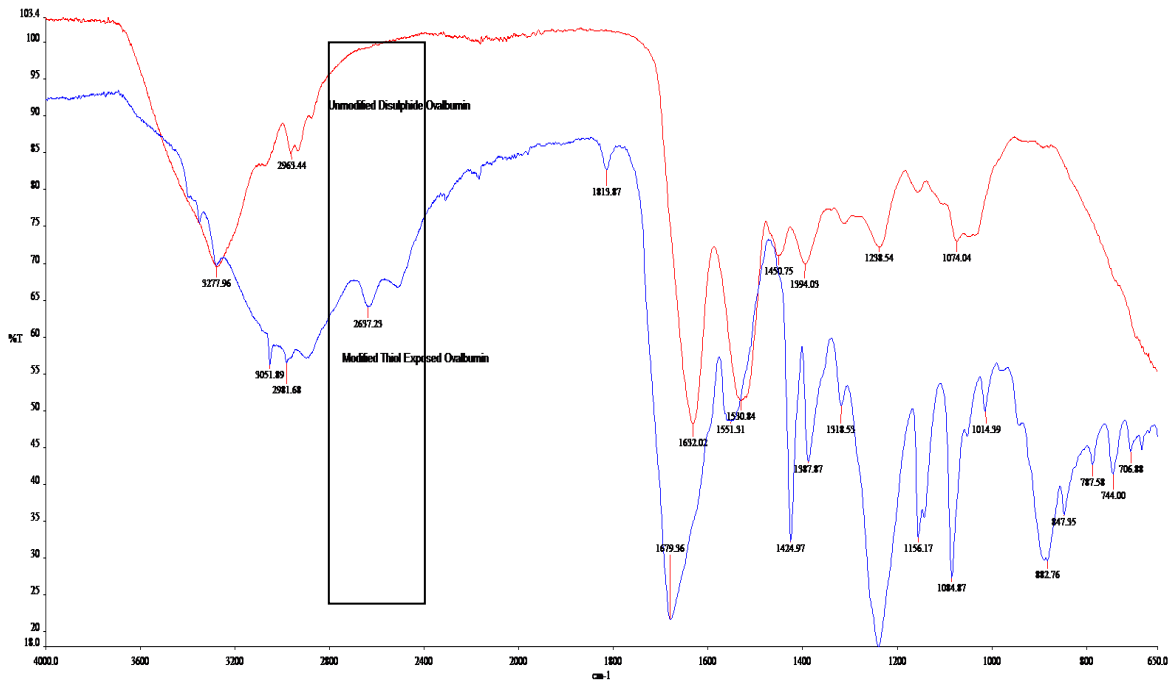
### 3.3.3. ATR-FTIR spectroscopy of the native, thiol and ovalbumin-captopril

The kinetic studies of reduction and oxidation processes by IR-spectroscopy are useful in determining the presence of disulfide and thiol functionalities. The IR spectra of SS ovalbumin, degraded ovalbumin, and cross-linked drug ovalbumin are shown in the traces in Figures 3.4 and 3.5. Figure 3.7. Illustrates the absorbance of the SS and SH of ovalbumin before and after reduction of the SS of ovalbumin. In the spectrum of unmodified ovalbumin (Figure 3.6), the  $\nu_{SS}$  band at  $513\text{cm}^{-1}$  are observed, indicating the existence of the SS bonds. After degradation, the bands disappeared and new bands at  $2637\text{cm}^{-1}$  ( $\nu_{SH}$ ) are detected (Figure 3.6).

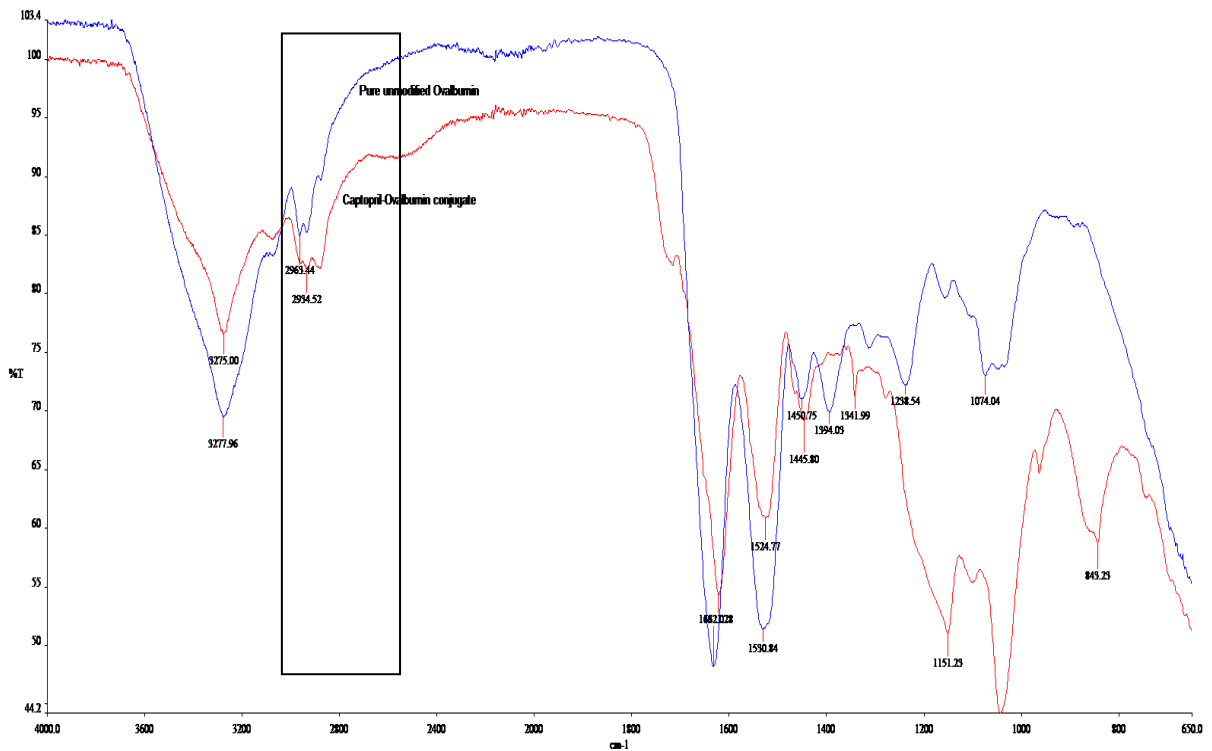
These results reveal the degradation of the SS bond and the formation of SH groups (Alting et al., 2000; Alting et al., 2003). The results prove the cleavage and reformation of disulphide bonds in response to the redox conditions occurred. The absorbance of the modified ovalbumin at  $2637\text{cm}^{-1}$  was 0.275. These results correspond to those reported by Pinhas-Hamiel, (1996) and Lin *et al.* (2001). Fleming, (1989), reported that the S-H absorption as being typically weak and occurring at lower wavenumber (frequency) because of the higher atomic mass of sulphur, they also note that the  $k$  was smaller with a value of  $340\text{kJ mol}^{-1}$ . It should be noted however that the SH wavenumber is generally stronger when using Raman spectroscopy. The IR spectra also showed OH stretching at  $3277.96\text{cm}^{-1}$ , C-H  $2987\text{cm}^{-1}$ , C-O at  $174\text{cm}^{-1}$  3, C=C  $1679\text{cm}^{-1}$ , amide I and II at  $1632\text{cm}^{-1}$ , C=N at  $1551\text{cm}^{-1}$ , C-O of  $\text{COO}^-$  at  $142\text{cm}^{-1}$  4, -CH at  $1387\text{cm}^{-1}$  and C-O-H stretching  $1156\text{cm}^{-1}$ .



**Fig.3.4.** The IR spectra of captopril the versatile and reactive thiol group at  $2566.66\text{cm}^{-1}$ .



**Fig.3.5.** IR-spectroscopy showing the comparison of the native unmodified ovalbumin against the modified of ovalbumin-disulphides prepared in 20mM phosphate buffer.



**Fig.3.6.** IR-spectroscopy of the thiol modified ovalbumin in comparison to the Captopril bound ovalbumin samples.

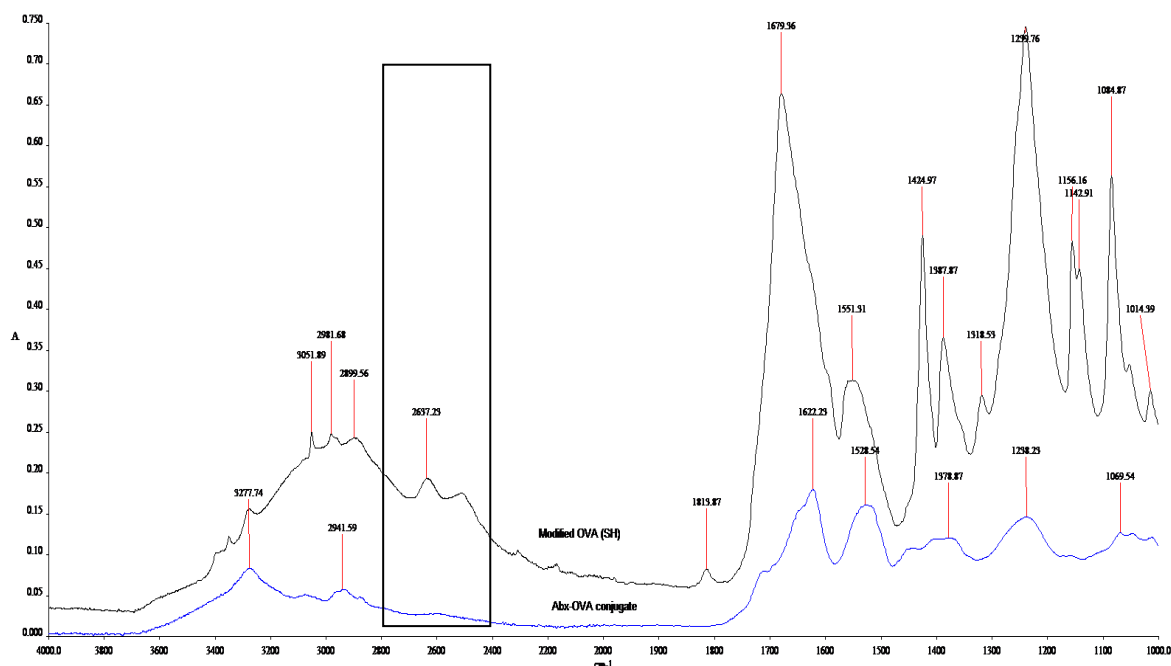
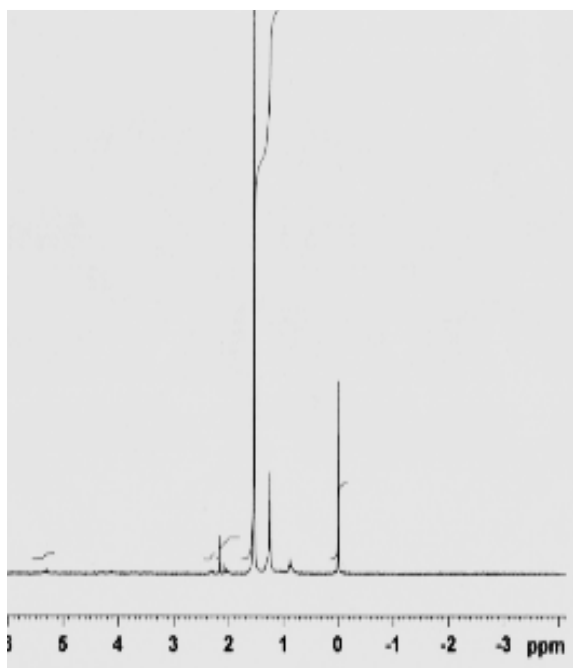


Fig.3.7. Spectra indicating the absorbance of modified ovalbumin and captopril bound ovalbumin samples were indicated.

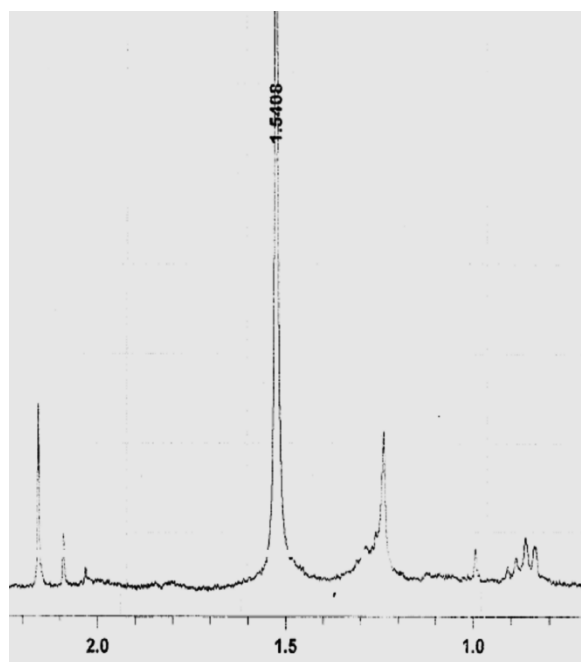
### 3.3.4. $^1\text{H}$ NMR Spectrum

The thiol concentration was determined directly to be 264  $\mu\text{mol}/100\text{g}$ . The conversion of ovalbumin to ovalbumin-thiol would result in 528 $\mu\text{mol}/\text{g}$  of thiol concentrate. The resultant structure was analyzed by NMR. In the  $^1\text{H}$  NMR two types of stabilizing thiols were found in the ovalbumin structure after modification with dithiothreitol. The expected surface dithiols with protected  $\omega$ -thiol functionality were detected and the linked dithiols could also be found. The combination of the two dithiols provided ovalbumin with increased stability. The destabilisation of ovalbumin caused by the disintegration of disulphide bridge resulted in the formation of linked dithiols. In Figure 3.8, represented (i) pure captopril and (ii) the dithiothreitol modified ovalbumin containing free thiol motifs and (iii) the ovalbumin-captopril conjugate complex. There are definite peaks in Figure 3.8 (i) that are not present in Figure 3.8 (ii and iii). There were free thiols with thiol functionality and double surface linked thiols. The broadness of the signal signified the restriction of mobility of the double linked thiols and the narrow signals were the easily accessible thiols (Masihul et al., 2002).

i.



ii.



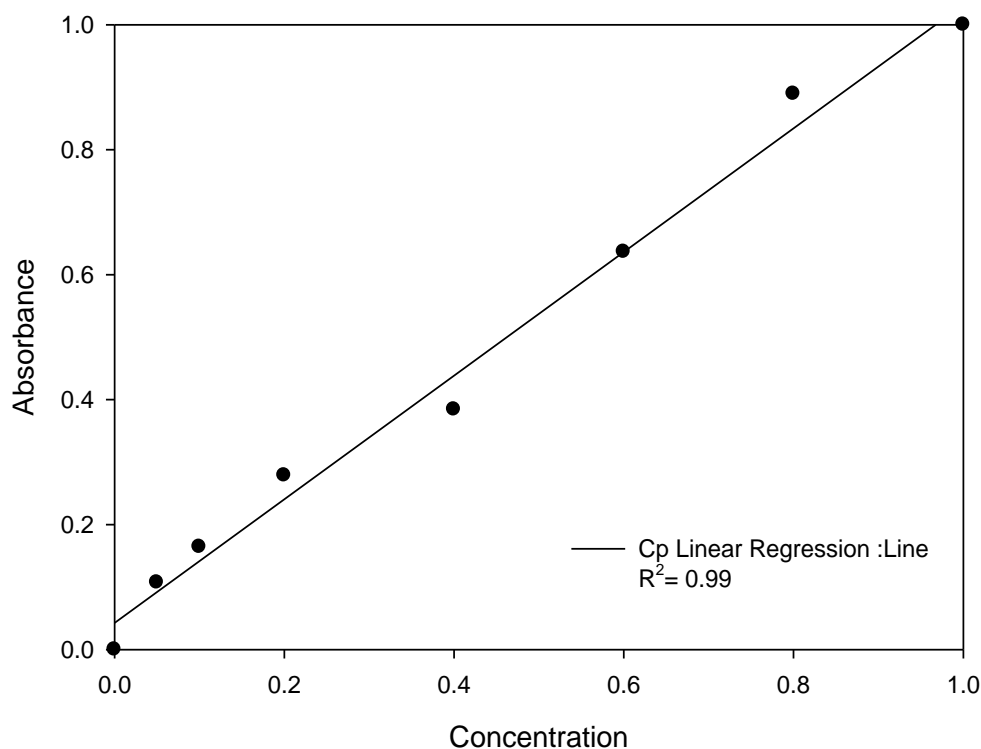
iii.



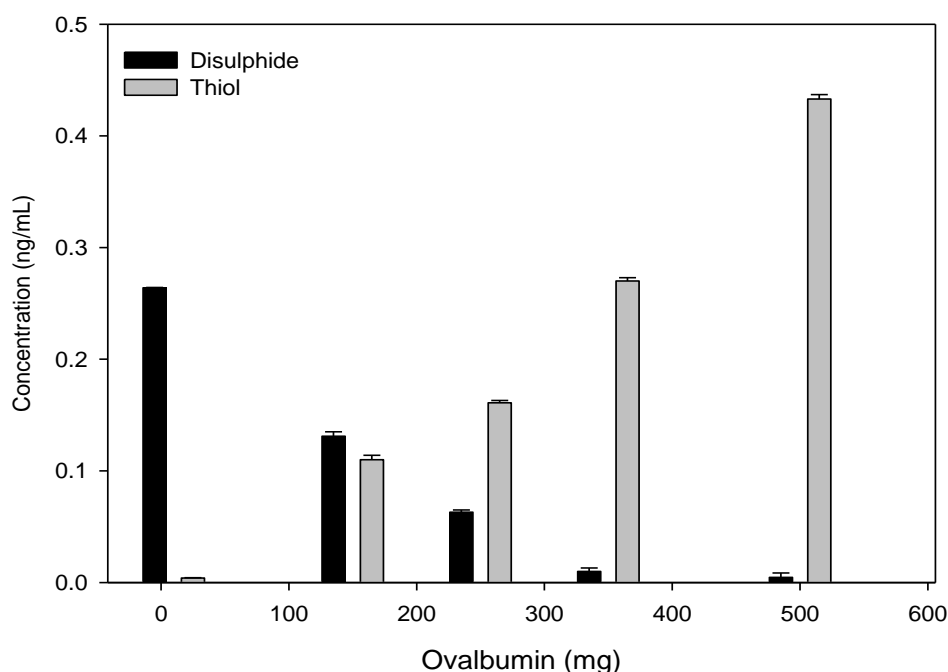
**Fig.3.8.**  $^1\text{H}$  NMR Spectrum of (i) Captopril (ii) modified ovalbumin containing free thiol motifs and (iii) ovalbumin-captopril conjugate in 100% deuterated  $\text{CdCl}_3$ .

### 3.3.5. Conjugation efficiency and drug content

In polymer conjugation, two necessities that are required for click chemistry based on the philosophy can be defined, for which polymer reactions must be tested to assess their ability for practicable modular transformations: (i) end group alteration without any presence of reduced side products and (ii) high conjugation efficiency when at least two polymer/molecules are coupled to each other, and that the completion of the reaction on a equitable time scale without using an excess of one reaction polymer (Madurai et al., 2011; Kim et al., 2008). The violation of any of the above two requirements would ultimately lead to complex product combinations that in the worst case are non-separable. The drug conjugation efficiency of ovalbumin and captopril measured was 79%. The thiol concentration was extrapolated from the L-cysteine calibration curve which had a correlation coefficient of  $R^2=0.99$ , (Fig.3.9). The conversion of disulphides to thiols when treated with dithiothreitol, were shown in Fig.3.10. The conversion was a linear relationship, i.e. with increasing thiol concentration was a direct decrease in the disulphide bond concentration.



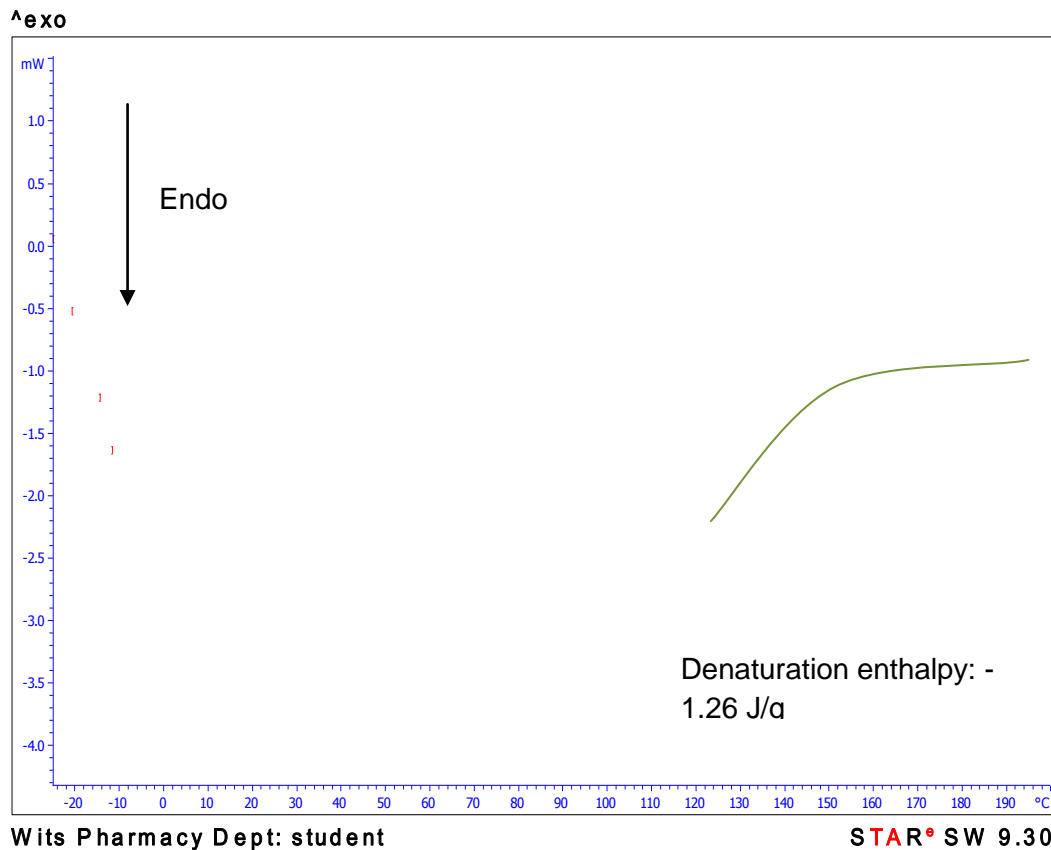
**Fig. 3.9.** Calibration curve for L-lysine cysteine for thiol quantification.



**Fig.3.10.** Thiol conversion from the unmodified ovalbumin into the reduced thiol groups treated with dithiothreitol.

### 3.3.6. Thermal analysis of the variant ovalbumin complex

Pharmaceutical compounds exhibit polymorphic characteristics that influence stability and bioavailability. The glass transition ( $T_g$ ) is an important parameter in characterizing pharmaceutical compounds (Hornof et al., 2003; Sachan et al., 2012). The glass transition ( $T_g$ ) of ovalbumin was  $72.25^\circ\text{C}$ , Fig 3.11, which corresponded to the glass temperature range reported by Cramer et al., (2004) of about  $75.0^\circ\text{C}$ . The degree of crystallisation or immobilisation of the ovalbumin protein was due to other interactions that affect stabilisation of the secondary ordered structures. Covalent crosslinkages between disulphide bonds and other interchain interactions called hyper tanglements (Ferguson et al., 1980) contributed directly to the increase of glass transition (Figure 3.11). These included the van der Waals, hydrophobic, and electrostatic interactions, and hydrogen bonds which were disrupted by the increase in heat, resulting in a shift of the glass transition. It was evident that as the glass transition temperature was increased, the crosslink's between the disulphide bonds were reduced in size and width, thus directly increasing the viscosity.

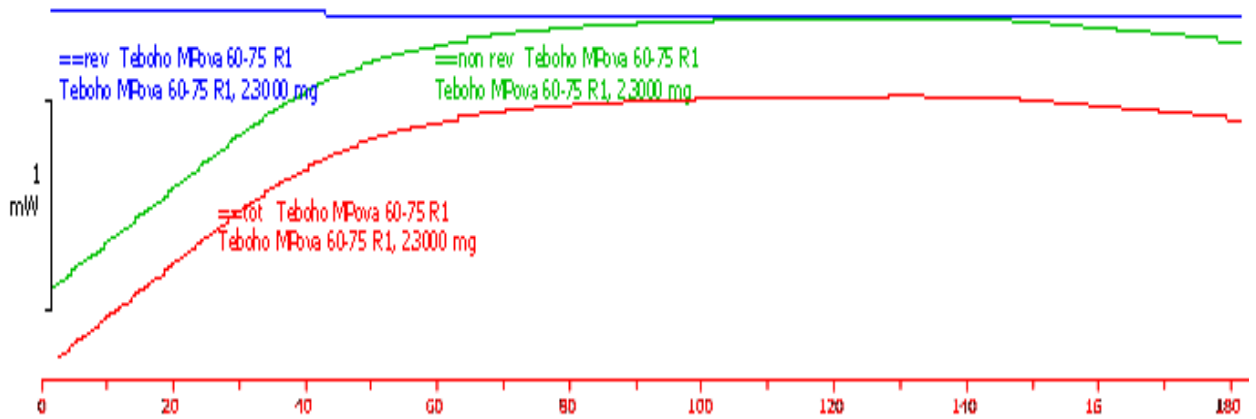


**Fig.3.11.** Comparative thermogram illustrating the change in the glass transition temperatures of pure unmodified ovalbumin at 72.25°C and Cp-Ovalbumin was measured as 90.15°C.

### 3.3.7. Thermal characterization of the native ovalbumin and its conjugate

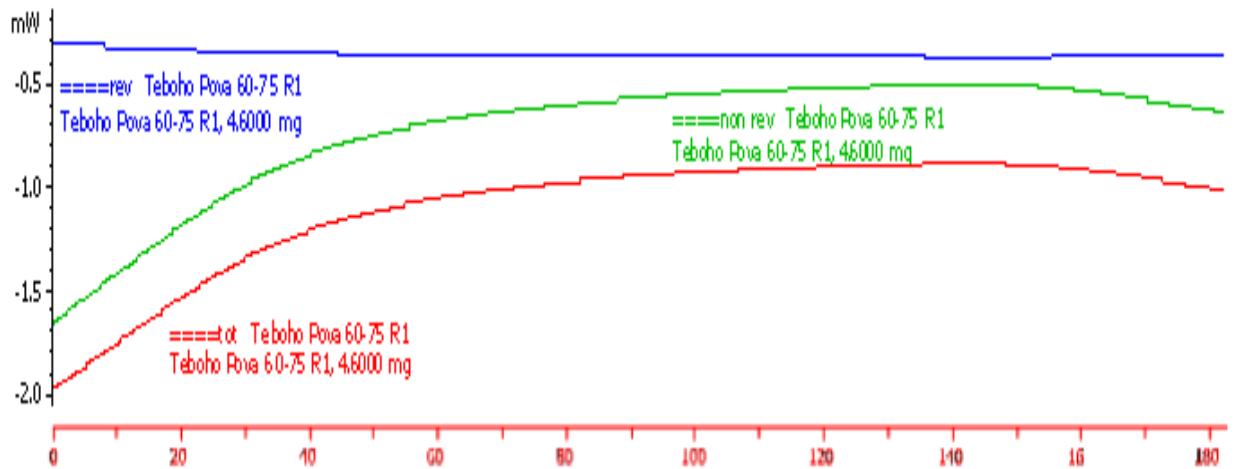
In order to further identify the different thermal transitions observed, temperature modulated differential scanning calorimetry was employed. In this specific modulation technique, the total heat flow was measured. The non-reversing heat flow was the difference of the total heat flow and the reversing heat flow. In Figure 3.12.i. the three heat flows of the ovalbumin polymer were separate, symbolising the polymer in its native state under quasi-isothermal conditions.



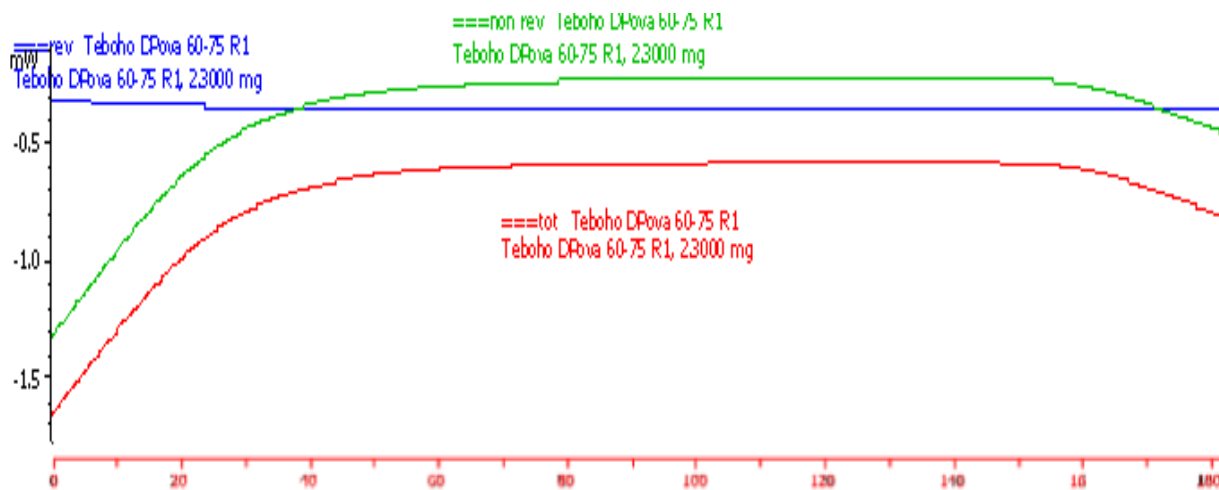


**Fig.3.12.i.** Non-reversing and reversing heat flows derived from the ADSC of (A) unhydrated native ovalbumin.

On modification of ovalbumin by addition of the pharmaceutical compound captopril the non-reversing heat flow increased, because of the disruption within the polymer associated with the exposure of the thiol groups, (Figure 3.12.ii).



**Fig.3.12.ii.** Non-reversing and reversing heat flows derived from the ADSC of (B) the conjugate captopril to ovalbumin. iii. The total heat flow remained constant but there was an overlap between the non- and reversing heat flows, because of the addition of the high crystalline structure captopril. The overlap was an indicator of glass transition and crystallization.



**Fig.3.12.iii.** Non-reversing and reversing heat flows derived from the ADSC of (C) thiol modified ovalbumin.

Up to a temperature of about 40°C the ovalbumin solutions were fluid, with a viscosity of minimum 72.9Pa s. During this heating phase the properties of the solution did not change, it is believed that the protein retained its native, folded structure (Liu et al., 2006) However when the temperature reached about 40-60°C, small white precipitates appeared which indicate the definite change in the protein structure. The heating of the ovalbumin solution to 77°C lead to secondary thermal transitions, thus increasing the viscosity. The region was identified as the irreversible denaturation of the ovalbumin solution. By fitting it in a linear background slope of the curve before and after the thermal transition, the melting temperature ( $T_m$ ) was determined for the ovalbumin solution. This value corresponded to the melting temperature recorded by the differential scanning calorimetry. The viscosity continued to increase beyond 74°C, saturating around 79-80°C before diminishing slightly at greater temperatures. Upon cooling the viscosity increased but never recovered confirming the proteins irreversible denaturation.

When the protein macromolecules in solution were heated, the weaker bonds between the amino acids holding the tertiary folded structure were the first to disintegrate. As the structure deformed the internal functional groups specifically the thiol groups were exposed to the buffer solution and began to form bonds with ions and water, forming new hydrogen bonds in the peptide structure of ovalbumin. Additional rebinding within ovalbumin by interverconging hydrogen, disulphide and electrostatic bonds had formed, which resulted in the formation of aggregated ovalbumin microstructures. This unfolding and the subsequent disulphide interactions affected the ovalbumin solution's viscosity thereby changing the ovalbumin protein's rheological properties around melting temperature. Disulphide bonds

directly affected the mechanical properties (viscosity, tensile, strength, hardness) of ovalbumin and were correlated to the degree of disulphide bonding.

Slow decomposition of ovalbumin began at 200°C and accelerated at 245°C. The conjugate complex ovalbumin and captopril started to decompose vigorously at 245°C (data not shown). The ovalbumin-captopril complex contained more water molecules that were strongly conjugated than ovalbumin at 18°C and 7°C, respectively. The peaks of the evolution of absorbed water appeared in the thermograms at 62°C and 53°C respectively. Regardless of their composition their relatively fast decomposition began at 200°C and proceeded slightly more readily for complexes with excess of the ovalbumin-captopril complex, whereas the complex with excess of ovalbumin decomposed more slowly.

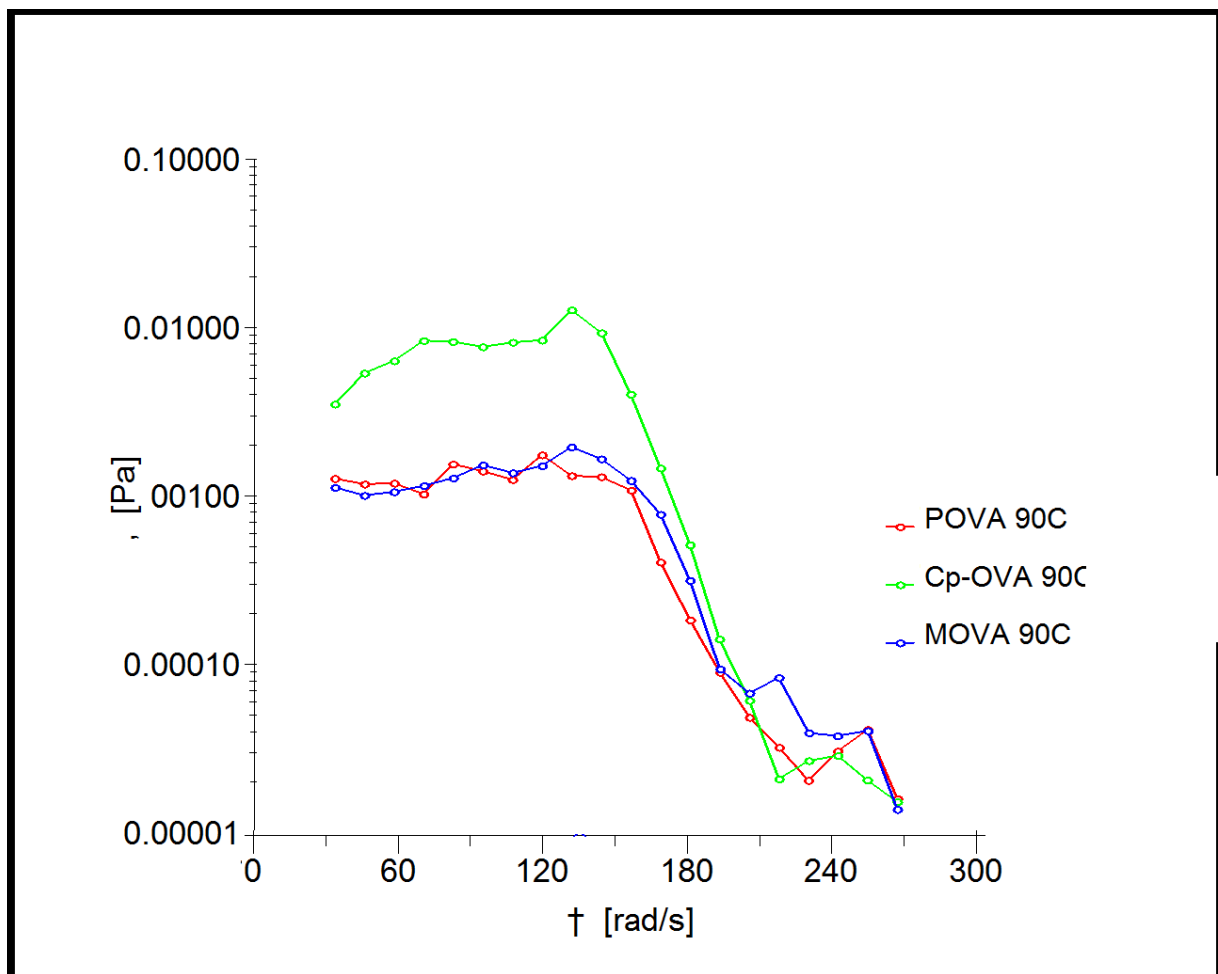
### **3.3.8. Rheological analysis of the ovalbumin complex**

In general, the viscoelasticity of a protein or colloidal solution is a manifestation of both the increased resistance to flow that originates from the friction experienced by the dispersed moieties, and from the strength of interactions that must be overcome to cause any deformation from an undisturbed state. The degree of crosslinking correlates to the increase in yield stress and the extension of the visco-elastic region.

#### **3.3.8.1. Oscillation stress sweep**

Interfacial shear rheology provides a sensitive tool to study aging kinetics, which can be affected by numerous parameters such as diffusion and adsorption behaviour, rearrangement, physical gelation, secondary adsorption and S-H to S-S exchange in ovalbumin molecules. To get comprehensive information on the rheological state of the formulation, oscillation measurements yielding information about viscosity and elastic properties of the investigated system were performed. Oscillation tests are dynamic methods for determining the viscoelastic properties of the tested material in its rheological ground state. When determining the oscillation measurements of a solid formulation, the viscoelastic region must be measured first by a stress sweep at constant frequency. By definition, a stress sweep test is a test where the complex modulus  $G^*$  is measured as a function of stress at a constant frequency. The range of stress over which  $G^*$  is independent of the applied stress is called the linear viscoelastic region. Over the linear region, the complex structures of the macromolecules remain intact, despite them displaying different behavioural patterns. A value of 1 Pa was chosen as the stress amplitude in the subsequent studies since it lies in the viscoelastic region for both tested systems. A decrease of the elastic modulus was indicative of the viscoelastic. In Figure 3.13 was evident that as the

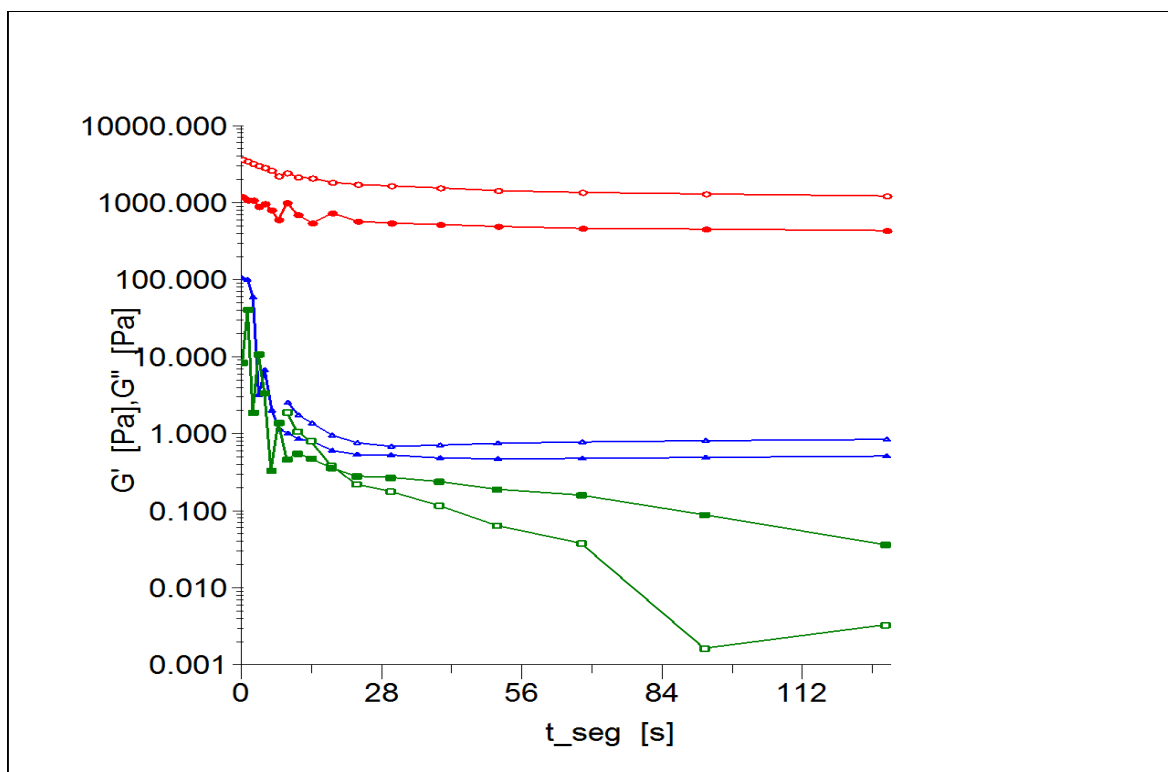
elastic modulus increased, deformation was reduced. The elastic moduli of the drug conjugated ovalbumin were higher than the native and modified ovalbumin. The addition of a bioactive such as captopril enforced the intermolecular forces between ovalbumin and captopril, also reinforcing the S-S bond between the two components. The increased breaking point of the drug conjugated ovalbumin may have been due to the interchange of S-H and S-S bonds between ovalbumin and captopril according to Erni *et al.*2006. The breaking point was marked by the saturation of the intermolecular bonds, including the S-S bonds, resulting in deformation.



**Fig.3.13.** Elastic modulus ( $G'$ ) as a function of temperature ramp ( $^{\circ}\text{C}$ ) for the native polymers. Povalbumin (native ovalbumin). Cp-ovalbumin (captopril bound ovalbumin). Movalbumin (thiol modified ovalbumin).

### 3.3.8.2. Frequency sweep

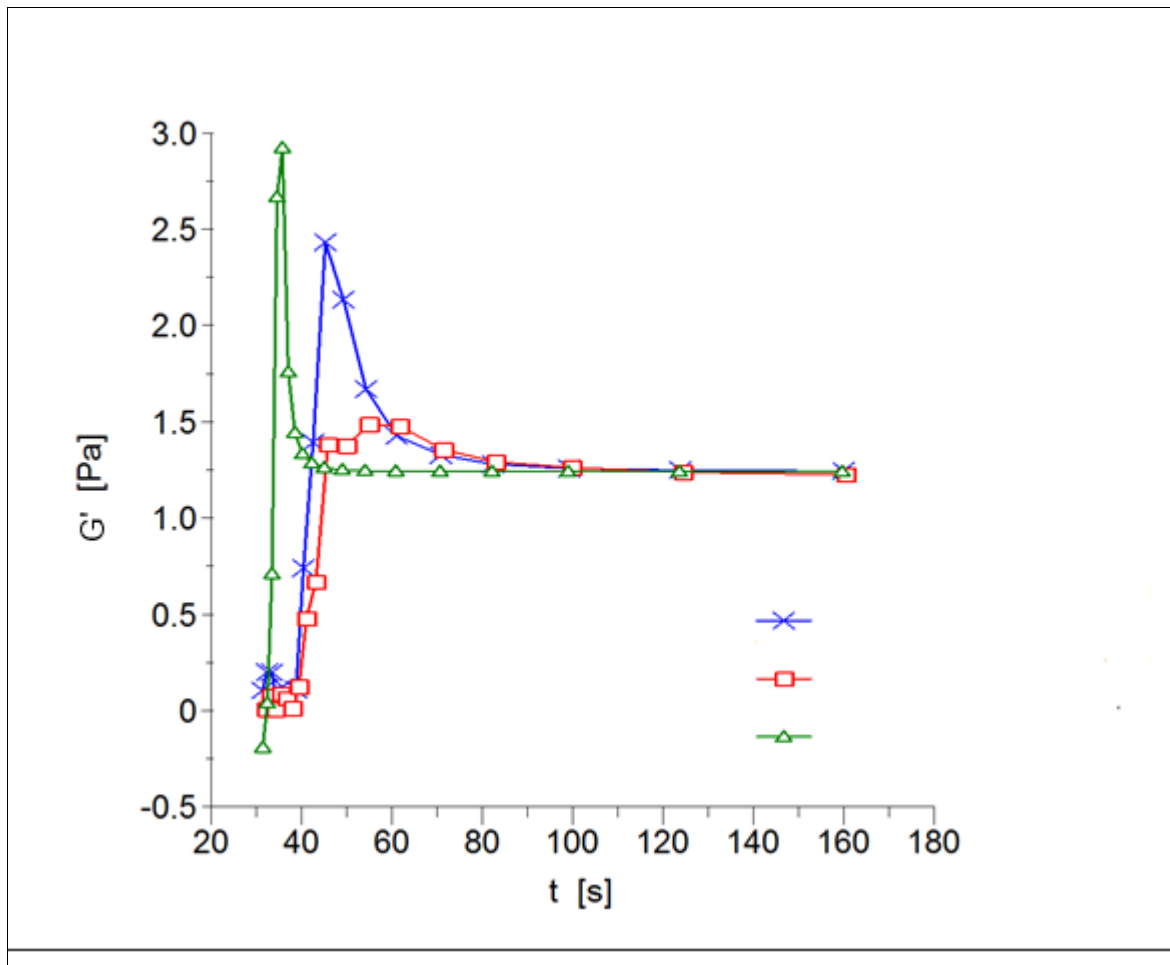
The elastic and viscous contributions to the interfacial shear modulus are shown by filled and hollow symbols respectively in Figure 3.14. At low frequencies the interface response was dominated by high viscous effects and  $G'$  was greater than  $G''$ . There was no crossover between  $G'$  and  $G''$  for the native polymer, G1 and G2. The crossover frequency  $\omega$  decreased and the corresponding modulus values also decreased with increasing time. The crossover of the frequency occurred at very low frequencies for the modified (G3 and G4) and for captopril bound ovalbumin (G5 and G6). The lower crossover frequency observed at higher bulk concentrations corresponds to a longer relaxation time period, implying that the interface had larger aggregates or was a more compactly packed protein [rheology]. Initially G3-G6 was more viscous before the crossover, and after the crossover was more elastic. This indicated that G3-G4 behaved in a solid-like manner instead of a gas or liquid manner. The native and modified ovalbumin behaved more elastic as the  $G'$  was greater than the  $G''$ , whereas the captopril conjugated ovalbumin was more viscous because  $G''$  was greater than  $G'$  for the remainder of the test. On the contrary, the G1 and G2 were parallel. The elastic moduli were greater than the loss moduli, signifying the undeformed state of the polymer, as the structure was uninterrupted.



**Fig.3.14.** Frequency sweep showing storage ( $G''$ ) and loss ( $G'$ ) modulus (Pa) versus time segment (s). G1 ( $\circ$ ), G2 ( $\bullet$ ), G3 ( $\Delta$ ), G4 ( $\blacktriangle$ ) G5 ( $\square$ ) and G6 ( $\blacksquare$ ).

### 3.3.8.3. Oscillation stress sweep

Interfacial shear rheology provides a sensitive tool to study aging kinetics, which can be affected by numerous parameters such as diffusion and adsorption behaviour, rearrangement, physical gelation, secondary adsorption and S-H to S-S exchange in protein molecules. To get comprehensive information on the rheological state of the formulation, oscillation measurements yielding information about viscous and elastic properties of the investigated system were performed. Oscillation tests are dynamic methods for determining the viscoelastic properties of the tested material in its rheological ground state. When determining the oscillation measurements of a solid formulation, the viscoelastic region must be measured first by a stress sweep at constant frequency. By definition, a stress sweep test is a test where the complex modulus  $G'$  is measured as a function of stress at a constant frequency. The range of stress over which  $G'$  is independent of the applied stress is called the linear viscoelastic region. Over the linear region, the complex structures of the macromolecules remain intact, despite them displaying different behavioural patterns. A value of 1Pa was chosen as the stress amplitude in the subsequent studies since it lies in the viscoelastic region for both tested systems. A decrease of the elastic modulus was indicative of the viscoelastic. In Figure 3.15 was evident that as the elastic modulus increased, deformation was reduced. The elastic modulus of the drug conjugated ovalbumin was higher than the native and modified ovalbumin. The addition of a bioactive such as captopril enforced the intermolecular forces between ovalbumin and captopril, also reinforcing the S-S bond between the two components. The increased breaking point of the drug conjugated ovalbumin may have been due to the interchange of S-H and S-S bonds between ovalbumin and captopril according to Erni et al., (2006). The breaking point was marked by the saturation of the intermolecular bonds, including the S-S bonds, resulting in deformation.



**Fig.3.15.** Elastic modulus ( $G'$ ) as a function of time (sec) for the polymers. Pure native ( $\square$ ) ovalbumin, ovalbumin-captopril ( $\Delta$ ), thiol modified ovalbumin ( $X$ ).

#### 3.3.8.4. Physicomechanical properties of ovalbumin

The viscosity of native ovalbumin was  $72.9 \pm 0.74 \text{ Pa}\cdot\text{s}$ . The increase in viscosity of the modified ovalbumin-SH was due to the intermolecular creation of disulphide bonds. It was also noticed that the viscosity of the modified ovalbumin was time dependant, with increased ovalbumin-SS bond formation. These results verify the existence of intermolecular sulphide bridges between ovalbumin thiols and the captopril thiols. To quantify the viscosity of ovalbumin-captopril and confirm the increase in viscosity rheology experiments were performed and confirmed the increase in viscosity of  $182.8 \pm 26.83 \text{ Pa}\cdot\text{s}$ .

A direct correlation existed between the decreases in the number of thiols against the increase in viscosity. Thiolated polymers are capable of providing comparatively more pronounced increase in viscosity, as extensive crosslinking occurs due to the formation of disulfide bonds between the polymer chains (Fleming et al., 1989). In the modified

ovalbumin as the number of thiol groups decreased there was an increase in the viscosity of the ovalbumin solution. This was caused by the increase in the formation of inter- disulphide bonds as previously stated. The reduction of disulphide bonds caused a reduction in the secondary structure of ovalbumin, which resulted in a reduction of the stabilizing bonds within ovalbumin (Bernkop-Schnurch et al., 2003).

### **3.4. Concluding Remarks**

Thiol functional groups play an important role in stabilising and solubilising proteins in aqueous solutions. The reaction of the thiol groups lead to physical and chemical conformational changes which directly affect the bond formed. The successful conjugation of free thiol groups provides a versatile tool for functionalizing proteins for protein and thiol-containing bioactives. This research demonstrates how the role of thiol and disulphide chemistry in proteins such as ovalbumin may lead to new methods being employed in formulating thiol based pharmaceuticals.



## CHAPTER 4

### Sustained Delivery of Captopril from Ovalbumin Particles

---

#### 4.1. Introduction

Captopril (Cp; 1-[(2S)-3-mercapto-2-methylpropionyl]-L-proline), is an orally administered active angiotensin-converting enzyme (ACE) inhibitor used worldwide as an effective treatment of hypertension and congestive heart failure (Seta et al., 1988; Boomsma et al., 1981; Volland et al., 1994). It is metabolised into the *n*-carboxyl derivative in the liver and excreted mainly in the urine (Duchin et al., 1988). It has been reported that a single dose of captopril can regulate hypertension for up to eight hours and the duration of the antihypertensive action of a single dose of 35-75 mg would be taken at 8 hour intervals for 24 hours (Khalil et al., 2001; Darren et al., 2009). Hence the necessities in developing controlled release formulations to maintain relatively constant blood pressure levels for longer periods of time. Captopril contains a reactive thiol group, which binds onto the zinc ion of the angiotensin converting enzyme thereby inhibiting activity of the enzyme (Singhvi et al., 1982).

The binding of  $Zn^{2+}$  onto the enzyme results in the formation of disulphide linkages with plasma proteins (Mandel et al., 2011) but also results in the formation of disulphide dimers of captopril, captopril-cysteines and relative endogenous thiol containing compounds (Miazaki et al., 1982). A number of drug delivery systems have been designed to sustain the release of captopril; these include microcapsules (Andreoli et al., 1993), floating tablets (Bagchi et al., 1989), bioadhesive polymers (Antonaccio et al., 1982), pulsatile delivery systems (Rezende et al., 2007), hydrophobic tablets (Singh et al., 1988), semisolid matrix systems (Matharu et al., 1992) and coated tablet (De Crosta et al., 1987).

Pharmaceutical research has been aimed at reducing the problems with not only conventional drug delivery systems but also with drug delivery systems that require biocompatible and stable drug delivery systems for molecules. The preparation of the hydrogels directly affects the bioavailability of the drug by protecting and supporting the process of site specific targeting of the drug delivery system. Hydrogels have been used widely in the development of biocompatible and bioavailable biomaterials due to their low interfacial tension and frictionless surface in the presence of an aqueous medium. Chemically hydrogels are cross-linked to each other by covalent bonds, and thus, the hydrogel is one molecule regardless of its size. Hydrogels have similar physical properties as that of living tissue, and this similarity is due to the high water content, soft and rubbery

consistency, and low interfacial tension with water or biological fluids. Factors like polymer composition, water content, crosslinking, density, and crystallinity, can be used to control the release rate and release mechanism of bioactives from hydrogels (Wong et al., 1981).

The ability of hydrogels to absorb water is due to the presence of hydrophilic functional groups such as the –OH, –CONH and the –COOH, which directly affect the swelling properties of hydrogels. Since hydrogels have high permeability for water soluble drugs and proteins, the most common drug release mechanism is through diffusion. Hydrogels affect properties such as the permeability, mechanical and surface properties as well as biocompatibility. Various factors can be used to control the release rate and drugs from the drug delivery systems but most important were factors such as the polymer composition, crosslinking, water content and crystallinity. Hydrogels are technically characterised in a number of ways, e.g. by SEM, XRD, *in vitro* diffraction, FTIR, swelling behaviour and rheology, to name a few. The challenge that has been associated with designing controlled drug release systems for captopril has been in the instability of the drug *in vivo* (Soares et al., 2004).

The success of an effective drug delivery system may be evaluated completely by stability studies. The sole purpose of stability testing is to obtain a stable product which maintains its efficacy to the maximum shelflife at specific storage conditions and maintain peak drug release profiles. The advantages of a stable formulation are:

- Prolonged residence time at the site of action
- Localization of dosage form at a specific site
- Increased drug concentration gradient across the intestine, increasing contact of the drug particles with the mucosa
- Direct contact with the intestinal cells, which precedes particle absorption (Rashid et al., 1990).

Captopril tends to have a burst phenomenon because of its high water solubility when formulated as a controlled or sustained release drug delivery system. In this chapter we utilise the openly vulnerable reactive thiol in captopril to bind to a protein that can act as a carrier thus stabilise captopril release *in vivo* and *in vitro*. Another important factor also contributing to the release of captopril is its solubility in an acidic environment. Due to its pKa of 3.7, captopril is highly soluble at pH 1.9 and has a half-life of 2 to 3 hour, it was necessary to develop a sustained drug delivery system. The prolonged captopril delivery system would have to increase the mucosal residence time, effectively control the release of the captopril

and improve its half-life of captopril, while providing better blood plasma stability concentration of captopril *in vivo* and *in vitro*. Only free captopril is pharmacologically active; hence the conjugation of the captopril to the ovalbumin vehicle carrier would have to be biocleavable. The disulfide derivative may act as a reservoir for free captopril and contribute to a longer duration of action than predicted by the blood concentrations of free captopril (Thakur et al., 1988). Captopril is rapidly and extensively metabolized in reactions involving its thiol group. The major metabolic pathway for captopril involves not only the formation of its disulfide dimer but also of mixed conjugates with endogenous thiol-containing compounds and plasma proteins (Wong et al., 1981).

Investigations into polymers with various molecular characteristics have led to a number of inferences regarding the molecular characteristics required for mucoadhesion. The properties exhibited by a good mucoadhesive may be summarized as, (i) strong hydrogen bonding groups specifically the hydroxyl and carboxyl groups [-OH, -COOH]; (ii) strong anionic charges; (iii) sufficient flexibility to penetrate the mucus membranes or tissue crevices; (iv) surface tension characteristics suitable for the wetting mucus/mucosal tissue surface and lastly (v) high molecular weight (Bernkop et al., 2005).

The interactions of different polymers such as natural or synthetic polymers play an important role in the release of a captopril. Cationic and anionic polymers bind more effectively than neutral polymers. Polyanions are better than polycations in terms of binding, and water soluble polymers give greater flexibility in the type of dosage forms compared with rapidly or slowly dissolving water-soluble polymers. Anionic polymers with sulphate groups bind more effectively than those with carboxylic groups. The degree of binding is proportional to the charge density on the polymer. The high binding hydrogels include sodium alginate, hydroxypropylmethylcellulose and polyvinyl alcohol. Table 1 includes a theoretical summary of the the three above mentioned hydrogels and their uses in pharmaceutical drug delivery systems.

The aim of the chapter is to examine the pharmacokinetics of three main hydrogel polymers known for their controlled release properties namely, sodium alginate, 2-hydroxy propyl methyl cellulose and poly vinyl alcohol. These above mentioned hydrogels also have bioadhesive properties that could potentially increase the release of the captopril from the ovalbumin vehicle carrier system across the intestinal mucosa. The aim would also provide a comparative of the three hydrogels and the formation of the most suitable nanoparticles for the release of captopril.

**Table 4.1:** Hydrogels and their intended application.

<b>Chemical Structure</b>	<b>Co-polymer</b>	<b>Application</b>
$(C_6H_7NaO_6)_n$	Sodium Alginate	Biodegradation, adhesiveness, Thermo and pH sensitivity  Gelling, thickening and stabilizing applications binding agents in tablets,  Targeting to mucosal tissues  Slow release applications
$[CH_2CH(OH)]_n$	Polyvinyl (alcohol)	Adhesiveness, Biodegradation Gelling, Controlled release systems Thermo sensitive
$C_{56}H_{108}O_{30}$	Hydroxypropylmethylcellulose	Gelling, Thickening Adhesiveness

## 4.2. Materials and Methods

### 4.2.1. Materials

Purified lyophilised ovalbumin (OVA), Dithiothreitol (DTT), 2-Mercaptoethanol (2-ME) and captopril were purchased from Sigma (Sigma Aldrich, Missouri, USA). Ethanol, Sodium Alginate, Polyvinyl (alcohol), Hydroxypropylmethylcellulose, Potassium phosphate monobasic and Disodium hydrogen phosphate were purchased from Merck (Merck KGaA, Darmstadt, Germany). All the chemical agents were analytic grade and used without further purification

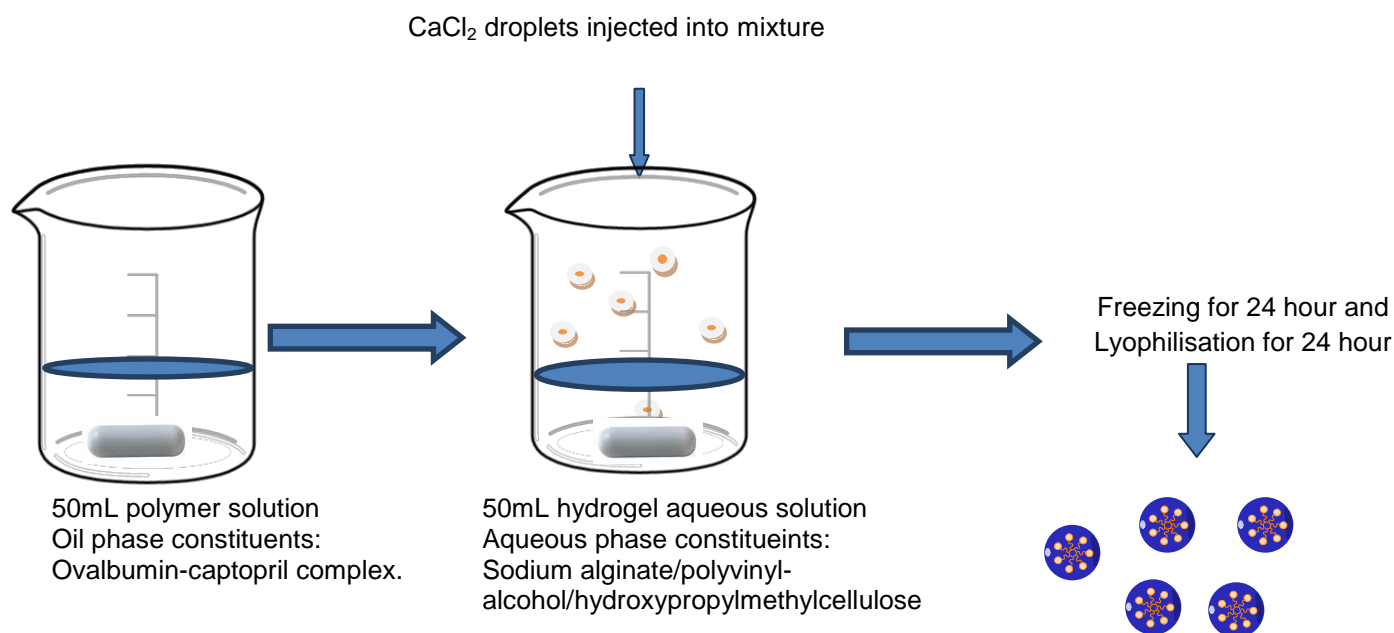
### 4.2.2. Preparation of the disulphide ovalbumin conjugates

As previously described in Section 3.2.2.4., predetermined 50mg of captopril was added to the 100mM reduced ovalbumin solution and incubated for 1 hour to ensure complete thiol-thiol binding saturation. The ovalbumin-captopril conjugate solution was then centrifuged and washed three times with deionised water, frozen at -70°C and lyophilised for 24 hours.

### 4.2.3. Preparation of nanoparticles

#### 4.2.3.1. Synthesis of ovalbumin-captopril nanoparticles

A concentration of 0.06<sup>w/v</sup> for the three hydrogels namely, sodium alginate, poly-vinyl alcohol and hydroxyl propylmethyl cellulose was kept constant for the comparable release of captopril from all formulations (Manjanna et al., 2013; Chitra et al., 2012). The ovalbumin-captopril conjugate were encapsulated with sodium alginate (NaAlg), poly-vinyl alcohol (PVA) or hydroxypropylmethylcellulose (HPMC) using calcium chloride. Preparation for the nanoparticles was as follows: Three sets of hydrogel coatings were prepared using cation-induced controlled gelification methods. In all hydrogel methods 5mL of 18mM CaCl<sub>2</sub> as a crosslinker was added dropwise to 50mL hydrogel solutions while stirring. OVA-captopril solution (20mL) was injected into the hydrogel solution dropwise using a 20mL syringe while stirring. The resultant biopolymeric OVA-captopril hydrogel solutions were then agitated overnight on a magnetic stirrer (CNW 21-2 Homothermal, China) at room temperature. The polymeric solution was then pre-frozen at -70°C for 24 hours and lyophilized at 1.35mtorr for 24 hours. The three sets of hydrogels were prepared in a similar way with certain modifications to each hydrogel. The parameters and compositions of the hydrogel formulations were summarised in Table 4.2 and 4.3. Figure 4.1 illustrates the formulation method for the three hydrogel ovalbumin carrier systems.



**Fig.4.1.** Summary of the formulation method of the ovalbumin captopril carrier hydrogel formulation.

**Table 4.2.** Parameters for the formulation preparation.

Parameter	Settings	Units
Polymer to cross linker ratio	1:5	w/v
Magnet speed	1000	rpm
Ambient Temperature	25	°C

#### 4.2.4. ATR-FTIR spectroscopy of NaAlg, PVA, and HPMC

FTIR spectra of dried samples were acquired on a Perkin Elmer Fourier Transform Infrared spectrophotometer (FTIR) (PerkinElmer 100, Beaconsfield, United Kingdom) at wavelengths of 400-4000  $\text{cm}^{-1}$ . The spectra were collected at a resolution of  $4\text{cm}^{-1}$  with 150 scans per spectrum. A background spectrum was acquired and assigned for use on subsequent spectral acquisitions for each sample.

#### 4.2.5. Thermal characterization of NaAlg, PVA, and HPMC

Differential Scanning Calorimetry (DSC) (1 STAR<sup>e</sup> system, Mettler Toledo, Schwerzenbenbach, Switzerland) was used to thermally characterize the three formulations. 50mg/mL of native ovalbumin, modified ovalbumin and drug-SS-ovalbumin were heated from 25 to 100°C at 1 k/min. The denaturation temperature (Td) was evaluated using STARe software. The total enthalpy change and the enthalpy changes of the individual components were determined by integration of the peak area upon deconvolution of the recorded thermogram of the three components.

#### 4.2.6. Drug encapsulation efficiency of NaAlg, PVA, and HPMC

The drug encapsulation efficiency (DEE) was calculated using the following equation.

$$\text{DEE} = \frac{M_i - M_d}{M_i} \times 100\% \quad (1)$$

Where  $M_i$  is the initial amount of ovalbumin-captopril dissolved in the hydrogel solution and  $M_d$  the amount of hydrogel mass measured in the gelling media ( $\text{CaCl}_2 \cdot 2\text{H}_2\text{O}$  solution).

#### **4.2.7. Morphological characterization of the each NaAlg, PVA, and HPMC formulations**

The size and morphology of the nanoparticles was analysed using the Scanning Electron Microscope (Perkin Elmer, USA). To determine the mean size of the nanoparticles dynamic light scattering was used for zeta size determination (Perkin Elmer, UK). To prepare the samples for zeta size: 10mg of sample was dissolved into 10mL of 4.1 pH borate buffer and immediately analysed to prevent swelling of the nanoparticles. The experiments were carried out in triplicate. For the zeta potential, to determine the stability of the nanoparticle, the same procedure as above was followed.

#### **4.2.8. Weight Variation of the NaAlg, PVA, and HPMC hydrogel matrices**

Three capsules were randomly selected from each batch and individually weighed. The average weight and standard deviation of the 3 capsules were calculated. The batch passes the test for weight variation if all three of the individual capsules were similar to the average weight measured.

#### **4.2.9. Size increase index of the NaAlg, PVA, and HPMC hydrogel matrices**

Swelling measurements were analysed directly using the zeta sizer (Perkin Elmer, UK) at 24 hours. The extent of swelling can be measured in terms of % size increase gained by the capsule. The capsule was soaked in 6.8 pH buffer solution for 24 hours and removed from the solution and weighted using the zeta sizer. The size increase ratio  $Q_s$  was calculated by the amount of absorb water and calculated using the following equation:

$$Q_s = \frac{S_s - S_d}{S_d} \times 100 \quad (2)$$

Where  $S_d$  is the weight of the capsule dry state and  $S_s$  the weight in the capsule's swollen state.

#### **4.2.10. Rheological analysis of the dry NaAlg, PVA, and HPMC hydrogel matrices**

The viscosity of the three sets of nanoparticles namely, sodium alginate, poly-vinyl alcohol (PVA) and hydroxypropylmethylcellulose (HPMC) hydrogel were measured using the Haake viscometer (USA). The specific viscosity of hydrogel solutions (100mg/ml 20mM phosphate buffer, pH 7.0, containing 0.1 M NaCl, filtered through a 0.45 $\mu$ m filter) was subject to 24 hour incubation at room temperature before viscosity measurements were implemented.

#### 4.2.11. *In vitro* Drug release from the NaAlg, PVA, and HPMC hydrogel matrices

The *in vitro* release experiments were performed in Simulated Intestinal Fluid (SIF) to compare the performance of the three ovalbumin-captopril hydrogel. Complete formulations of each set of the nanoparticles were accurately weighed and placed in 500mL of temperature 37°C glass, volumetric flasks containing 500mL of the Simulated Intestinal Fluid. 1mL samples were taken from the release medium at specific time intervals for a total of 24 hours and replaced by fresh 1ml SIF buffer solution. The separate drug release profiles were then analysed using the four pharmacokinetic equations. Sink conditions were maintained by replacing the withdrawn 2mL samples with freshly prepared simulated intestinal fluid at each sampling time. The concentration of the drug released was determined utilizing the Ultraviolet Spectrophotometer (Cecil CE 3021, 3000 Series, Cecil Instruments, Cambridge, England) at  $\lambda$ 271nm. From this concentration value the actual amount of drug was then calculated.

- **Zero-order model**

Drug dissolution from dosage forms that do not disaggregate and release the drug slowly can be represented by the equation:

$$Q_0 n.Qt = K_0t \quad (3)$$

Rearrangement of equation (3) yields equation (4):

$$Qt = Q_0 + K_0t \quad (4)$$

Where  $Q_t$  is the amount of drug dissolved in time  $t$ ,  $Q_0$  is the initial amount of drug in the solution (most times,  $Q_0 = 0$ ) and  $K_0$  is the zero order release constant expressed in units of concentration/time. Values of  $0.5 < n < 1$  indicate non-Fick I or anomalous mechanism due to both diffusion and polymer chain relaxation.

- **First order model**

This model has also been used to describe absorption and/or elimination of some drugs, although it is difficult to conceptualize this mechanism on a theoretical basis. The release of the drug which followed first order kinetics can be expressed by the equation:

$$\frac{dC}{dt} = -kc \quad (5)$$

Where  $K$  is first order rate constant expressed in units of  $\text{time}^{-1}$ . Equation (5) can be expressed as:  $\log C = \log C_0 - Kt / 2.303$  (6) where  $C_0$  is the initial concentration of drug,  $k$  is



the first order rate constant, and  $t$  is the time. The data obtained are plotted as log cumulative percentage of drug remaining vs. time which would yield a straight line with a slope of  $n^{K/2.303}$ .

- **Higuchi model**

This model is based on the hypotheses that (i) initial drug concentration in the matrix is much higher than drug solubility; (ii) drug diffusion takes place only in one dimension (edge effect must be negligible); (iii) drug particles are much smaller than system thickness; (iv) matrix swelling and dissolution are negligible; (v) drug diffusivity is constant; and (vi) perfect sink conditions are always attained in the release environment. Accordingly, model expression is given by the equation:

$$Ft = Q = A \sqrt{D} (2C_0 - C_s) C_s^{s.t} \quad (6)$$

Where  $Q$  is the amount of drug released in time  $t$  per unit area  $A$ ,  $C_0$  is the drug initial concentration,  $C_s$  is the drug solubility in the matrix media and  $D$  is the diffusivity of the drug molecules (diffusion coefficient) in the matrix substance.

- **Korsmeyer-Peppas model**

Korsmeyer et al., (1983) derived a simple relationship which described drug release from a polymeric system equation:

$$M_t / M_\infty = Kt^n \quad (7)$$

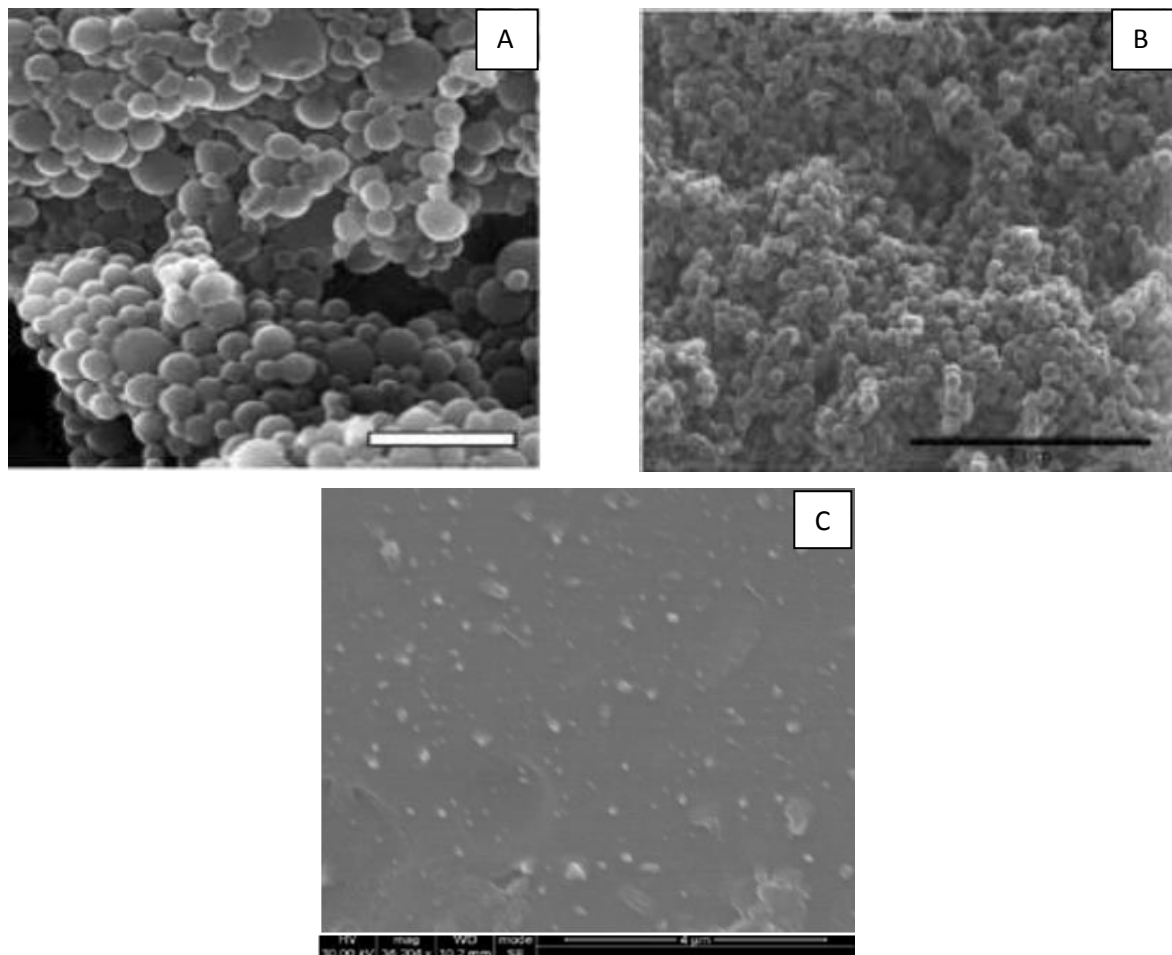
Where  $M_t / M_\infty$  are a fraction of drug released at time  $t$ ,  $k$  is the release rate constant and  $n$  is the release exponent. The  $n$  value is used to characterize different release for cylindrical shaped matrices.

### 4.3. Results and Discussion

#### 4.3.1. Morphological studies of the NaAlg, PVA, and HPMC nanoparticles

The surface morphology of sodium alginate, polyvinyl alcohol and hydroxymethylcellulose microgels containing the ovalbumin-captopril drug carrier system were analysed. The microgels for sodium alginate and hydroxypropylmethylcellulose were poly dispersed but the

polyvinyl alcohol microgels were embedded in the polyvinyl alcohol hydrogel. The microgels for sodium alginate were larger in size with an even surface whereas the surfaces polyvinyl alcohol and hydroxylmethylcellulose were smoother were the smallest in size, Figure 4.1.

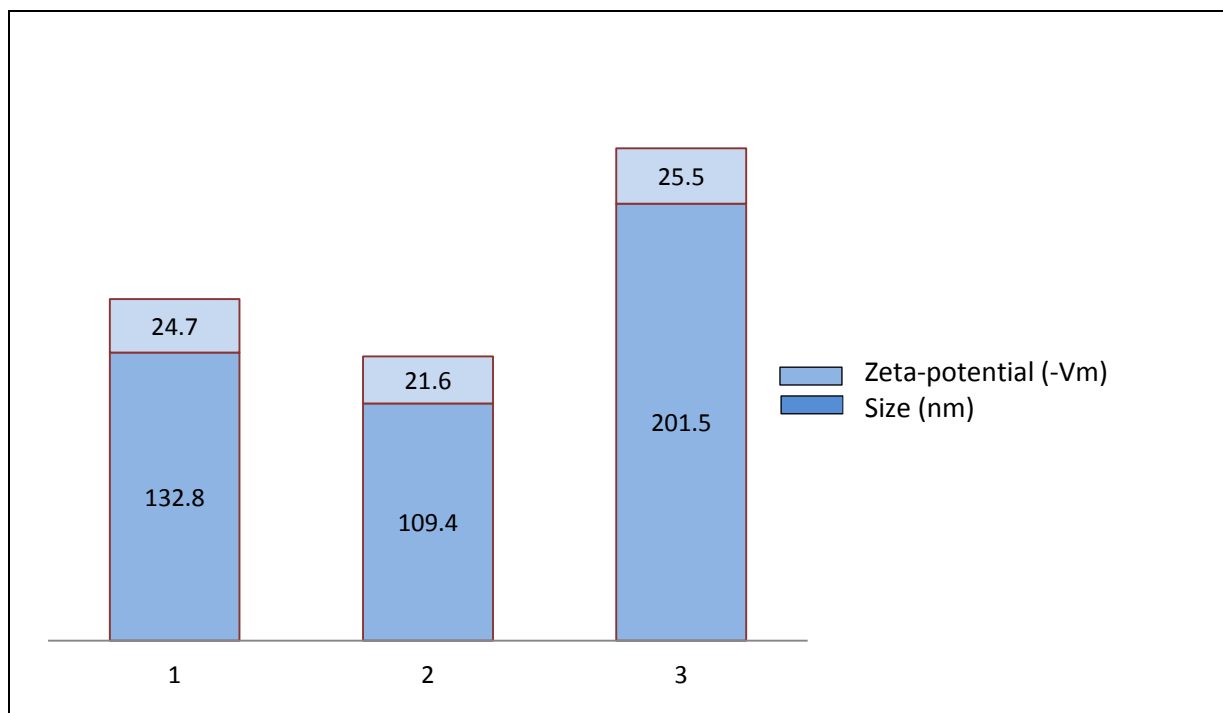


**Fig.4.1.** The SEM images for (A) sodium alginate, (B) polyvinyl alcohol and (C) hydroxyl methylcellulose micro gels containing the ovalbumin-captopril drug carrier system.

#### **4.3.2. Size and swelling of the NaAlg, PVA, and HPMC particles**

The zeta potentials of the sodium alginate hydrogel was -25.5mV, -21.6mV and -24.7mV (Figure 4.3) for the hydroxyl methylcellulose and polyvinyl alcohol hydrogel nanoparticles respectively. In all samples the stability of the hydrogel nanoparticle showed good stability ranging between -20 to -30mV in an aqueous solution. The size distribution graphs of the hydrogel formulations are provided in Figure 4.4. Polyvinyl alcohol resulted in two peaks showing that the aggregation and coagulation of the particles. Sodium alginate and hydroxyl methylcellulose showed single peaks of average stable particles. It was however noteworthy

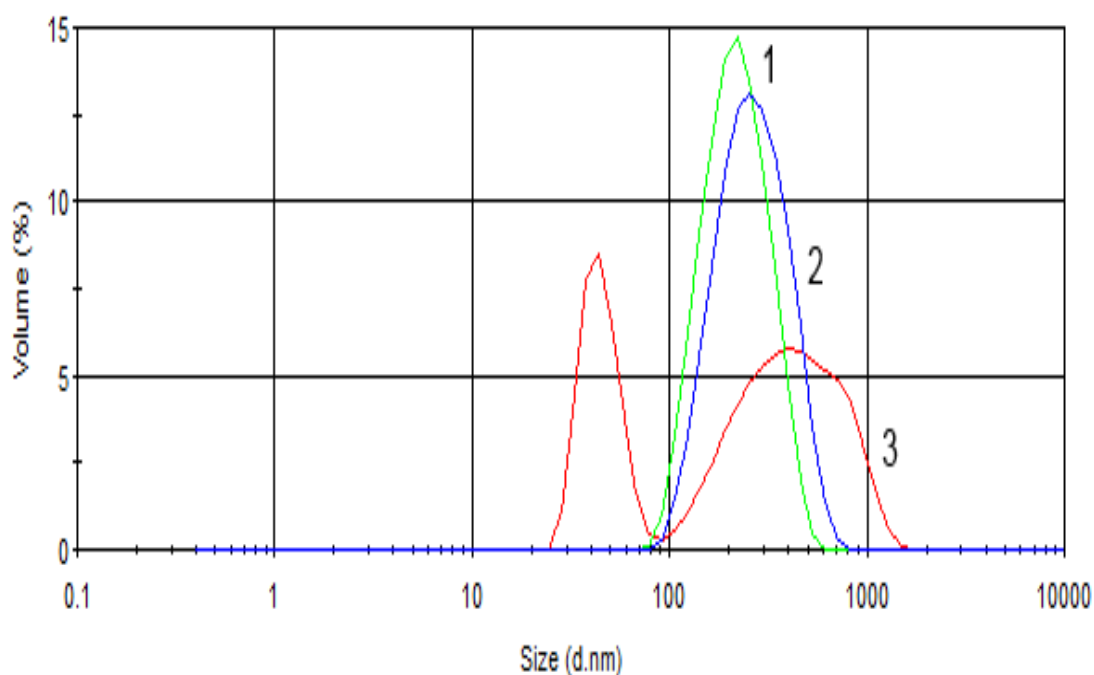
that the hydrogel nanoparticles would aggregate over time due to slow coagulation or flocculation of the nanoparticles when suspended in a flowing medium. The swelling results were summarised in (Table 4.4) with sodium alginate showing the highest swelling percentage, followed by polyvinyl alcohol and hydroxyl methylcellulose. These results show no statistical significance  $p < 0.05$ . The swelling percentage showed 83-85% increase in mass of the hydrogel formulations. There was no statistical significant difference between the formulations.



**Fig. 4.2.** The graphs represent the comparative size and zeta-potential values of the three particles. 1- Polyvinyl alcohol, 2- hydroxyl methylcellulose, and 3- sodium alginate.

**Table 4.4.** Average size distribution of the hydrogel nanoparticles before and after swelling of nanoparticles.

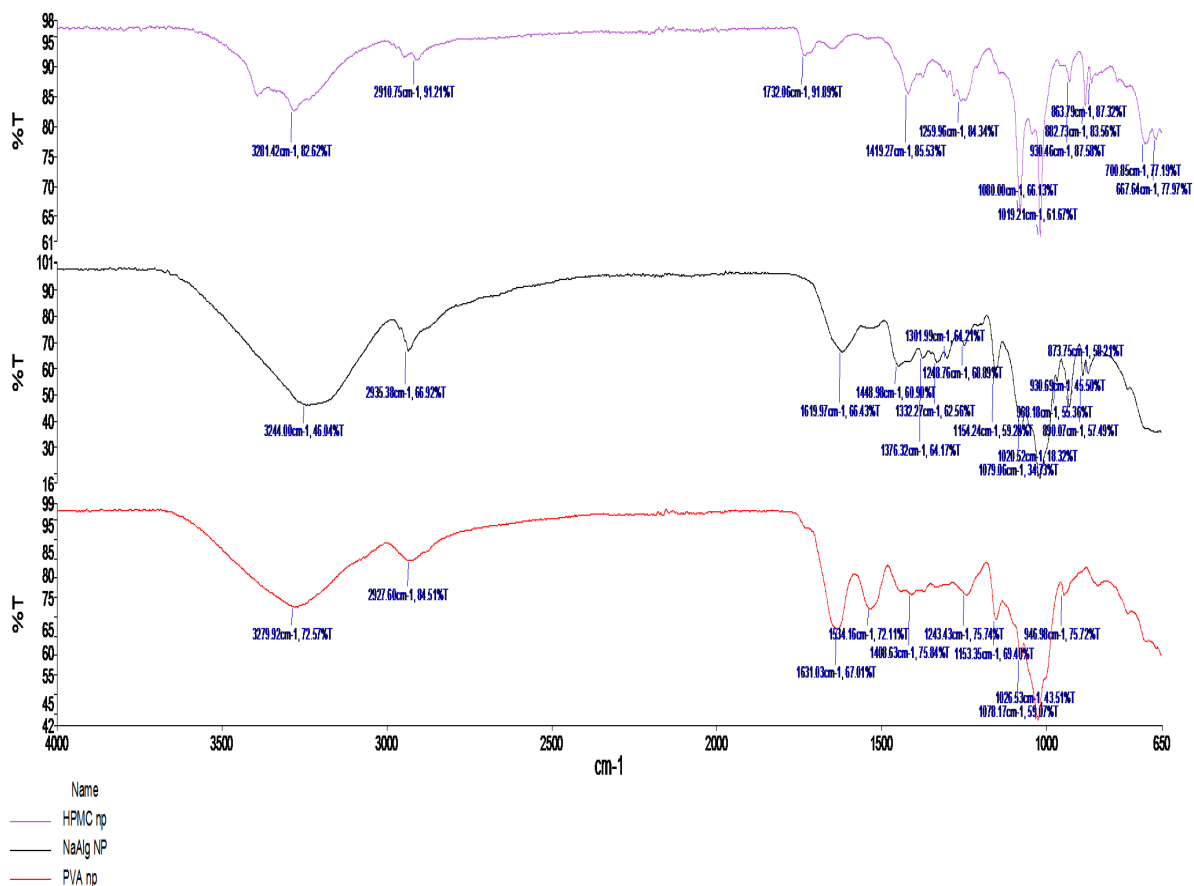
Sample	Initial Size (nm)	After swelling (nm)	Swelling (%)
PVA	132.8±5.8	817±23.3	83.83%
HPMC	109.4±6.9	649±28.9	83.17%
NaAlg	201.5±17.6	1363±33.7	85.22%



**Fig. 4.3.** Size distribution graphs of the three Nano gel systems formed, namely, 1- polyvinyl alcohol, 2- hydroxyl methylcellulose, and 3- sodium alginate.

#### 4.3.3. IR spectra for the NaAlg, PVA, and HPMC nanoparticles

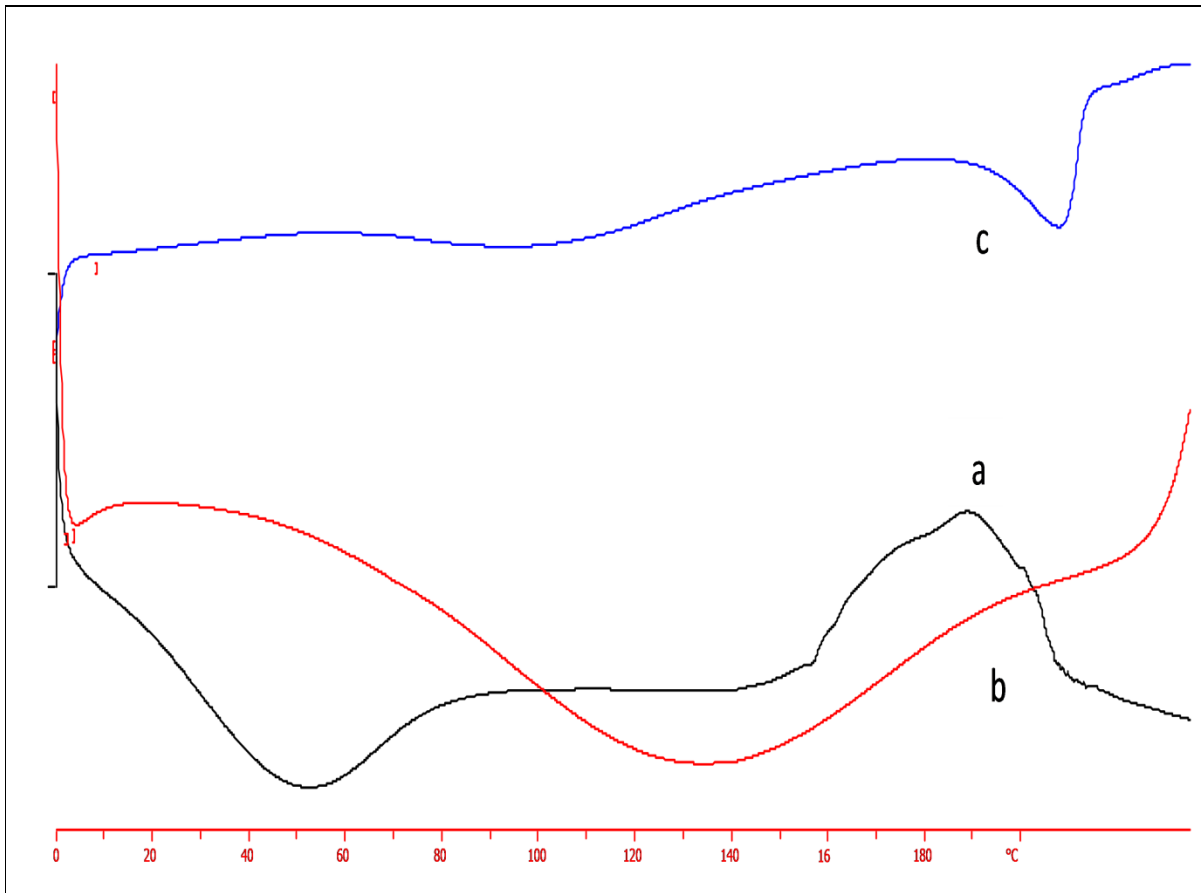
The IR spectra for the native ovalbumin polymer and captopril and the conjugate complex ovalbumin-captopril were shown in Chapter 3, Section 3.3.2. The spectra for the three hydrogel formulations were similar, with some noted differences. Figure 4 shows all three spectra highlighted stretching of the OH grouping at  $3281\text{-}3279\text{cm}^{-1}$ , CH stretching at  $2910\text{-}2927\text{cm}^{-1}$ , and COO stretching at  $1732\text{-}1631\text{cm}^{-1}$ . Amide I and II stretch at  $1534\text{cm}^{-1}$ . The ovalbumin drug carriers system was a multiple-component delivery system achieved by multi crosslinking processes. The spectrum was different from the individual components, (spectra not shown). Some peaks were diminished and some new peaks were visible. The system contained possible alkyl, carbonyl and aliphatic esters, which explain the peaks at  $3281\text{cm}^{-1}$  to  $667\text{cm}^{-1}$ . The alkyl groups may be found at  $3281\text{cm}^{-1}$ ,  $3244\text{cm}^{-1}$ ,  $1419\text{cm}^{-1}$ . The carbonyl groups were visible at  $1619\text{cm}^{-1}$ ,  $1631\text{cm}^{-1}$  and  $822\text{cm}^{-1}$ . The aliphatic groups were visible at  $770\text{cm}^{-1}$  and  $667\text{cm}^{-1}$ .



**Fig.4.5.** Spectra for sodium alginate captopril bound nanoparticles, polyvinyl alcohol bound nanoparticles and hydroxy propylmethyl cellulose bound nanoparticles.

#### 4.3.4. Thermal analysis of the NaAlg, PVA, and HPMC nanoparticles

As a powerful analytical tool, differential scanning calorimetry is capable of elucidating the factors that contribute to the folding and stability of biomolecules. The thermograms for the three hydrogel compositions are shown in Figure 4.6. The glass transition of hydroxy propylmethyl particles showed the thermal decomposition at a higher temperature of 183°C whereas the thermal decompositions of sodium alginate and polyvinyl alcohol were lower at 40 and midway 115°C respectively. The glass transition temperature for native sodium alginate was reported to be 220°C (Zhang et al., 2009), which affected the increased Tg of the nanoparticles. The combination of the sodium alginate with a lower Tg polymer such as ovalbumin resulted in a shift to a lower temperature. The Tg temperature for the polyvinyl alcohol polymer was reported to be 85-89°C and that of hydroxy propylmethyl as 210°C (Guiguis et al., 2012). Polyvinyl alcohol nanoparticles demonstrated the most decrease in the thermal decomposition of the particles. Table 4.5 provided a summary of the thermal changes of the three hydrogel formulations.



**Fig.4.6.** DSC Thermograms for the (a) sodium alginate, (b) polyvinyl alcohol, (c) hydroxyl methylcellulose hydrogel composites.

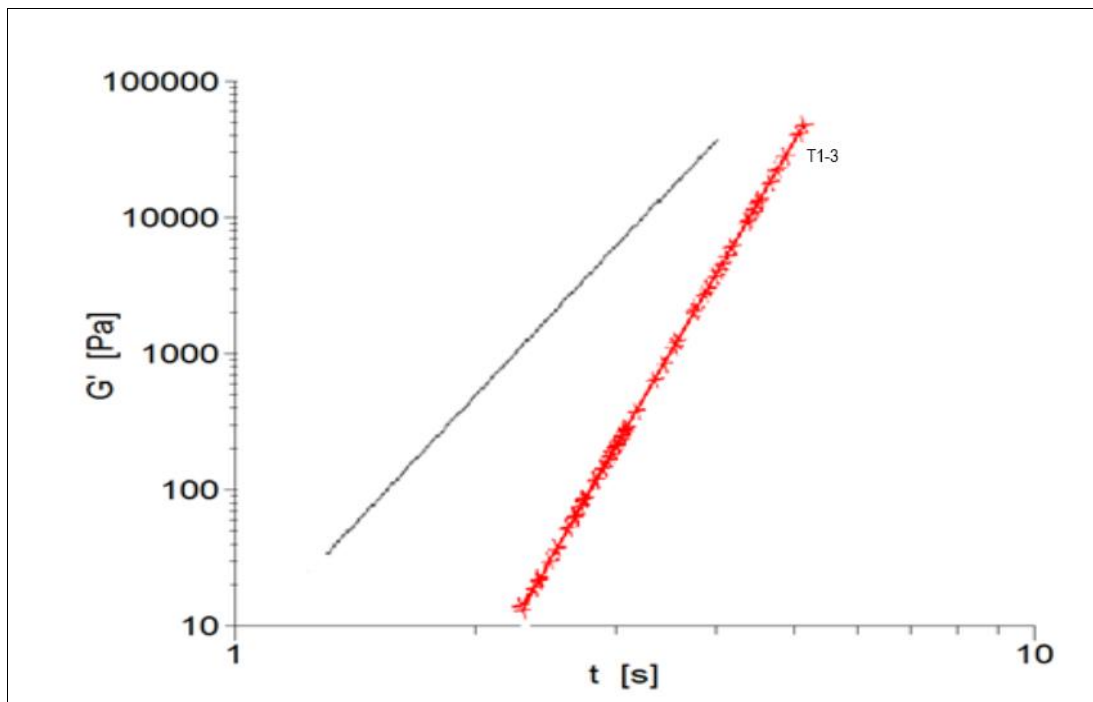
**Table 4.5.** Summary table for the thermal characterization of the three hydrogel composites.

<b>At glass phase transition (%)</b>		
<b>Hydrogel composites</b>	<b>Tg (°C)</b>	<b>H (J/g)</b>
sodium alginate/ovalbumin	43	16557.15
polyvinyl alcohol /ovalbumin	115	1753.56
Hydroxypropylmethyl/ovalbumin	182	1895.20

#### **4.3.5. Newtonian Flow model for the NaAlg, PVA, and HPMC nanoparticles**

The Newtonian Flow model of fluids demonstrates a linear relationship that exists between shear stress and shear rate, where the coefficient of viscosity is the constant of proportionality. The laminar flow that is not characterized by a linear relationship between shear stress and shear rate is called non-Newtonian. Figure 4.7 demonstrated a linear flow

graph of the three hydrogel formulations. The yield flow analysis showed that the intermolecular forces within the structures caused conformational deformation within the strands, resulting in the hyper entanglements in the hydrogel structure. The entanglements in the hydrogel structures were enforced and caused shear thickening (T1-3), where T1, 2 and 3 lay in a straight line.

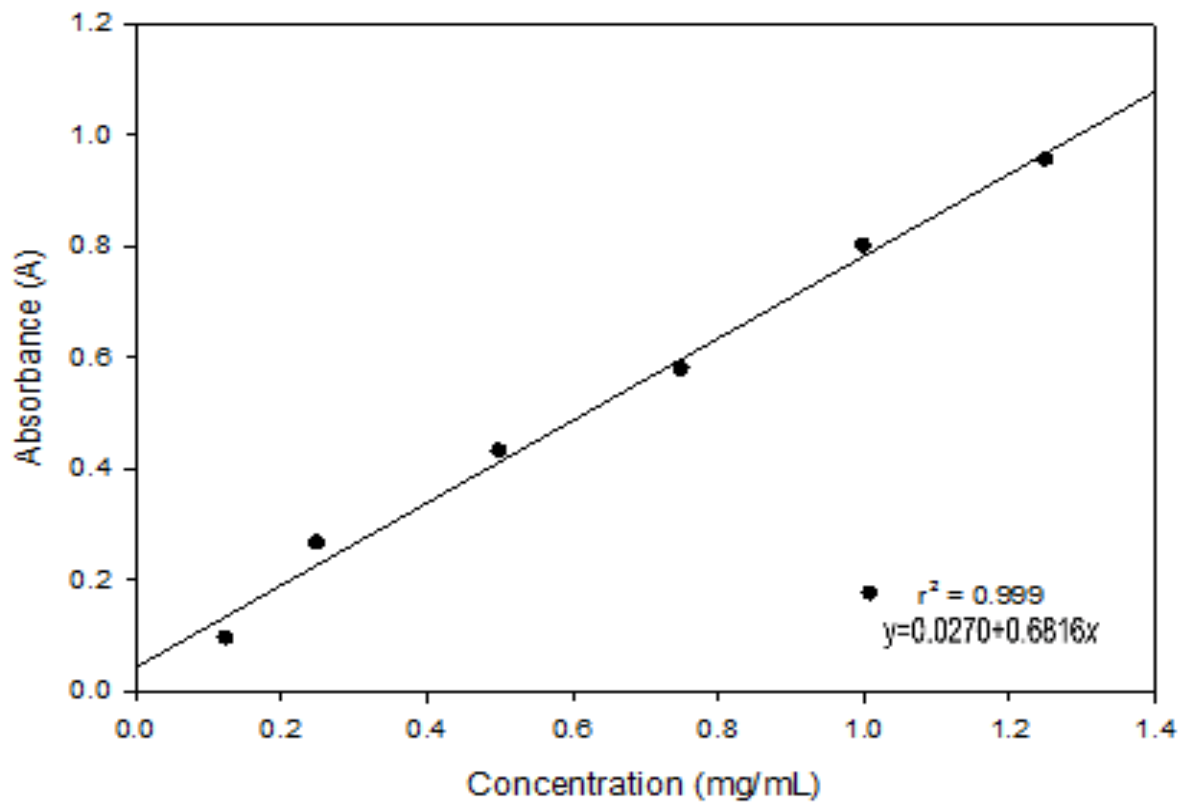


**Fig.4.7.** Characterisation of viscoelastic particles flow based on the Newtonian and non-Newtonian flow. T1-3 (x).

#### 4.3.6. Captopril release of the NaAlg, PVA, and HPMC nanoparticles

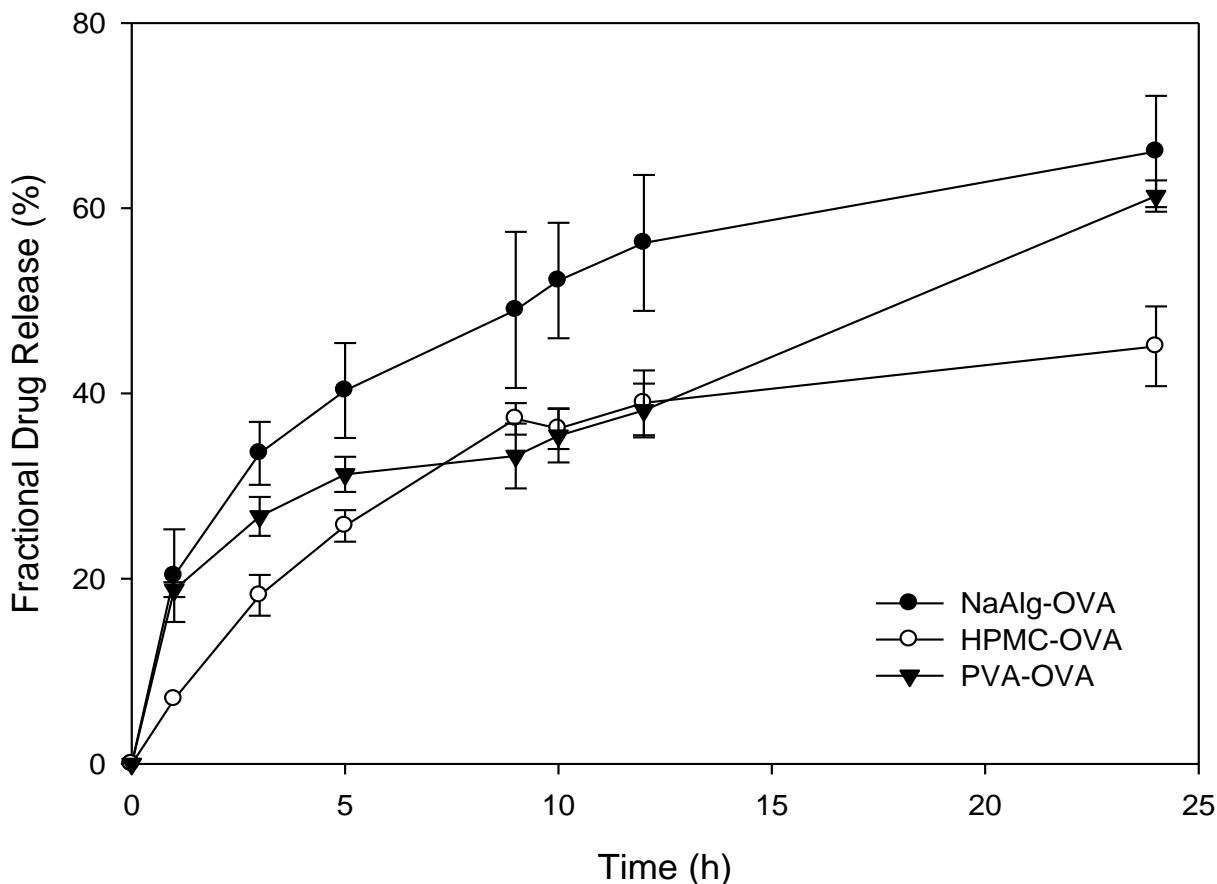
Figure 4.9 depicts the difference in the cumulative drug release profiles of the three comparative formulations. The highest fractional drug release percentage at 24 hours was achieved by sodium alginate 78%, and then followed by polyvinyl alcohol at 61%, and last by hydroxy propylmethyl cellulose 40%. These results could be because of the influence of kosmotropic anions, according to Hofmeister series (Wang et al., 1999; Xing et al., 2003) which directly influence hydrogen bonding within the hydrogel matrix. Due to the small radius and the large charge density of the chloride ion, it had the strongest ability to compete for water molecules and form hydrogen bonds with other water molecules, which minimized or weakened the water-polymer hydrogen bonding. This in turn could have minimized the hydroxypropylmethyl and polyvinyl alcohol hydrogen bonding with water which ultimately led to a reduced amount of captopril being released (Leuner et al., 2000). Amidon provided an

alternative explanation that the ions disrupt the hydration process at the water-solute interface (Amidon et al., 1995). The concentrations were extrapolated from the calibration curve from Figure 4.8.



**Fig.4.8.** Calibration curve of captopril in simulated intestinal fluid.





**Fig.4.9.** Comparative drug release profiles of the three hydrogel composites.

#### 4.3.7. Release order analysis of the NaAlg, PVA, and HPMC nanoparticles

The drug-release data were fitted to various kinetic equations to evaluate the drug release mechanism and kinetics. Regression coefficients ( $R^2$ ) were obtained from zero-order, first order, Higuchi model and the Korsmeyers coefficient-Peppas equations. The best fit with the highest correlation was shown in the first-order and the Korsmeyer-Peppas model, followed by the Higuchi model and lastly the zero-order as shown in Table 4.6. The Korsmeyer-Peppas model was used to determine the n-value, which described the drug release mechanism. According to this model, the n-value was less than the 0.45 for the hydroxypropylmethyl cellulose and polyvinyl alcohol particles, which was indicative of Fickian diffusion. Fickian diffusion release occurred by molecular diffusion due to the chemical potential gradients in pH 6.8 media. The Fickian diffusion was higher than 0.45 for sodium alginate which was indicative of non-Fickian diffusion, so showing less diffusion in the media. In addition, the release rate constant (k) was higher for the sodium alginate than the hydroxypropylmethyl composite particles.

**Table 4.6.** Kinetics Parameters of Hydrogel Loaded with ovalbumin particles and captopril.

Gel Formulae	Zero-order		First-order	Higuchi- model	Korsemeyer-model	
	R <sup>2</sup>	K (% h <sup>-1</sup> )	R <sup>2</sup>	R <sup>2</sup>	R <sup>2</sup>	n
HPMC	0.8387	2.541	0.8904	0.4657	0.6887	0.242
PVA	0.8133	3.042	0.8193	0.7172	0.7939	0.277
NaAlg	0.9415	4.529	0.9867	0.7800	0.9567	0.426

r<sup>2</sup> coefficient of determination. *K* rate constant according to zero-order analysis. *n* diffusional exponent Korsemeyer model indicative of the mechanism of drug release.

<sup>a</sup> Analysed by the regression coefficient method.

#### 4.4. Concluding Remarks

Various hydrogels were used, which influence to the drug entrapment efficiency, size distribution, mean particle size, surface morphology, swelling behaviour and *in-vitro* drug release. Sodium alginate, hydroxypropylmethyl cellulose and polyvinyl alcohol particles were prepared and from the data and analysis it was clear that sodium alginate provided the best combination of hydrogel properties of the three formulations. Sodium alginate particles resulted in the highest drug release of 78% as compared to hydroxypropylmethyl cellulose and polyvinyl alcohol particles which released 40% and 61% of captopril. The sodium alginate particles also provided the best drug entrapment efficiency, size distribution, mean particle size, surface morphology and swelling behaviour. The combination of the ovalbumin polymer with that of sodium alginate has shown good interaction for the prolonged release of a thiol-containing captopril, by providing a pharmaceutical dosage form for sustained captopril release.

## Chapter 5

### Limiting Factors Affecting the Release of Captopril from the Ovalbumin-Captopril Carrier System

---

#### 5.1. Introduction

Solubility is one of the most important physicochemical properties studied during the pharmaceutical preformulation. For solid or powder dosage form development, accurate solubility data are required for the robustness of the finished product. Furthermore there is a need to assess that the adequate amount of drug is released from the drug delivery system for absorption *in vivo*. If presumably a solid dosage form has a low aqueous solubility it may be subject to dissolution rate-limited or solubility-limited absorption in the gastrointestinal within the residence time (Soares et al., 2004; Wong et al., 1981). The importance of solubility in biopharmaceutical system is its use by the Biopharmaceutical Classification System (BCS) described by Amidon. This system describes low solubility compounds as those whose solubility is less than that of the total dose tested in 250mL of 1-7.5 pH aqueous solution (Zhang et al., 2009). Solubility values are used to estimate the Maximum Absorbable Dose (MAD), which is influenced by many variables including temperature, pH, solvents used in the solubility test, the state of solid, polymer concentrations, common ions in the medium and so on (Guirguis et al., 2012).

Within the field of controlled drug release and timed release systems, it is vital to understand the dissolution behaviour of polymers. In most of these systems the bioactive is usually dispersed in the matrix of the polymer, and when introduced into a suitable solvent for the polymer, swelling usually results (Wang et al., 2011). The swelling allows the solvent to permeate the polymer matrix, resulting in increased mobility of the bioactive which allows the bioactive to diffuse out the matrix into the surrounding medium. Normally these systems produce programmable concentration-time profiles that produce optimum therapeutic responses (Millard et al., 2002; Luener et al., 2000). The design of the controlled drug delivery system provides stability both *in vivo* and *in vitro* for unstable bioactives, while also providing an increased residence time at the site of action. Bioactives that would otherwise be discarded for being unstable or have reduced bioavailability may now be rendered useful due to a selection of novel polymeric drug delivery system (Amidon et al., 1995; Wang et al., 1999).

In order to achieve a successful oral drug delivery system for gastric sensitive bioactives, there is a need to protect them from the harsh gastric environment. pH-sensitive hydrogels

are employed as alternative choices against the biodegradation of the bioactive in the lower pH (~1.2) found in the stomach. Swelling of these hydrogels should be minimal at lower pH thus reducing the amount of bioactive lost by the drug delivery system. At higher pH as those found in the intestine, swelling of the hydrogels should be increased gradually.

Alginate is one such polymer that is known for its swelling abilities at higher pH. Alginate is a water soluble linear polysaccharide extracted from brown seaweed and is composed of alternating blocks of 1-4 linked  $\alpha$ -L-gluronic and  $\beta$ -D-mannuronic acid residues (Shargel et al., 1999; Xing et al., 2003). The crosslinking ability of alginate to ions such as  $\text{Ca}^{2+}$ ,  $\text{Ba}^{2+}$  or  $\text{Sr}^{+}$  retains the biological activity of the bioactive by encapsulating in the bioactive during the process of crosslinking. The covalent binding ability of the alginate polymer to thiol surfaces also makes it a novel choice in a hydrogel. Thiolated polymers such as alginate attach to mucoadhesive surfaces forming disulphide bonds with the mucus surface increasing contact between the hydrogel matrix and intestinal wall thus resulting in an increased retention time allowing increased drug absorption across the intestinal wall [Gum et al., 1992; Schnurch et al., 2001; Kuashlik et al., 2011). In addition to the improved adhesive properties, swelling behaviour and cohesive properties are also improved which makes alginate a useful excipient for the prolonged controlled drug delivery system (Karuppaiya et al., 2009). For the formulation of a prolonged release drug delivery system in the form of a capsule, specific polymer factors are required. Figure 5.1 demonstrates the simulated 3D conjugation process of sodium alginate and ovalbumin.

Enteric coated capsules also directly contribute to the delay onset of action of the encapsulated excipients. To a certain extent, enteric coated formulations postpone onset of action via targeted release in the intestine (Bingol et al., 2010; Bingol, 2010; Das et al., 2011; Fakri et al., 2013). The active substance content in a core with an enteric coating can be released about two to three hours later than the initial dosage coated thereon. Delaying the onset of action achieved to improve the biological availability of medicaments. Targeted release in the small intestine may be used to achieve higher local active substance concentrations (Cojocaru et al., 2007).

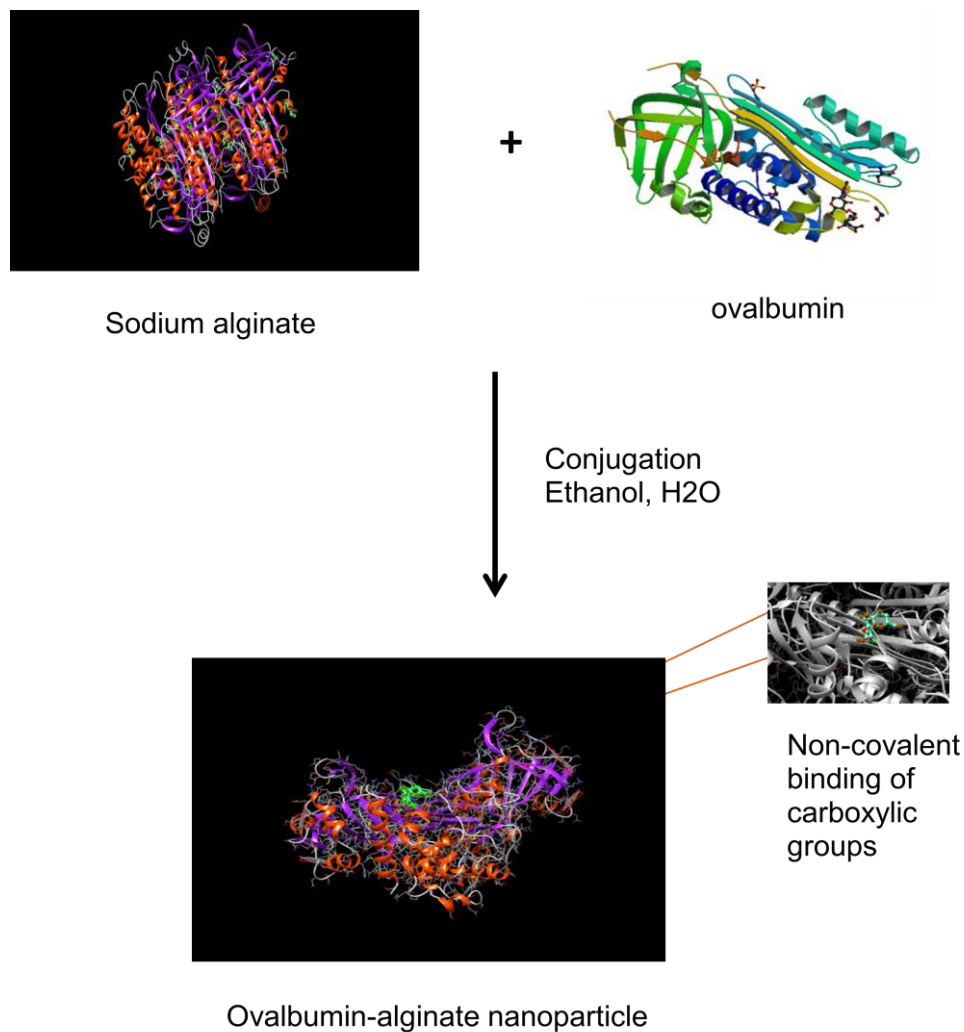
Enteric coatings are in particular used to:

- protect active substances destroyed by the acidic gastric juice,
- improve tolerability of medicaments irritating the stomach by only releasing them in the small intestine,
- making active substances available after a time delay (sustained release),

- achieve targeted release and concentration in the small intestine (Thoma et al., 1992) .

Hard gelatin capsules of provided they display adequate resistance and disintegration properties, are pharmacokinetically appropriate and meet stability requirements. Coatings on capsules this type display important potential applications in: (1) ensuring biological availability, (2) controlling the effects of medicaments and, (3) avoiding side effects (El-Malah et al., 2006; Shargel et al., 1999; Arai et al., 2009).

The aim of this chapter was to analyse the responses of the components that make up the ovalbumin drug carrier system for optimization in the chapter to follow. The aim was to further determine the parameters of each excipient and the effect each component has on the performance of the ovalbumin captopril carrier system.



**Fig.5.1.** Simulated 3D conjugation of sodium alginate and ovalbumin using Hyperchem software.

## **5.2. Analysis of the thermal effects on the sodium alginate nanoparticles**

### **5.2.1. Materials and Methods**

#### **5.2.2. Materials**

Purified lyophilised ovalbumin (OVA), Dithiothreitol (DTT), and captopril were purchased from Sigma (Sigma Aldrich, Missouri, USA). Ethanol, Sodium Alginate, Potassium phosphate monobasic and Disodium hydrogen phosphate were purchased from Merck (Merck KGaA, Darmstadt, Germany). All the chemical agents were analytic grade and used without further purification. It should be noted that no differences were found between the Sigma obtained ovalbumin and the self purified native ovalbumin.

#### **5.2.3. Methods**

##### **5.2.3.1. Effects of the pH and salt concentrations of the ovalbumin native polymer**

Native ovalbumin solutions were prepared by Differential Scanning Calorimetry (DSC) was performed on the DSC (1 STAR<sup>®</sup> system, Mettler Toledo, Schwerzenbenbach, Switzerland). Two sets of chemically treated ovalbumin solutions were prepared. Firstly 20mg of ovalbumin solutions were prepared and treated with 0, 0.5 and 1.0M of sodium chloride solutions. Secondly, a separate 20mg of native ovalbumin were dissolved in pH buffer solutions of 1.2, 4.0, 6.8 and 10 and both were heated from 25 to 100°C at 1 °C/min, individually. The samples were placed in silver sealed containers (70µL) and weighed on average 30mg. The denaturation temperature (Td) was evaluated using STAR<sup>®</sup> software. The total enthalpy change and the enthalpy changes of the individual components were determined by integration of the peak area upon deconvolution of the recorded thermogram.

##### **5.2.3.2. Limiting factors affecting captopril release from the ovalbumin carrier system**

###### **5.2.3.2.1. Preparation of the sodium alginate ovalbumin captopril particles**

The ovalbumin-captopril conjugate were encapsulated with sodium alginate (NaAlg) using calcium chloride. Preparation for the nanoparticles was as follows: Sets of hydrogel coatings were prepared using cation-induced controlled gelification methods. In the various polymeric solutions 5mL of CaCl<sub>2</sub> with varying concentrations were added dropwise to 50mL of the above sodium alginate polymer solutions while stirring. Ovalbumin-captopril solution (20mL) was injected into the hydrogel solution dropwise using a 10mL syringe while stirring. The resultant biopolymeric solution was then agitated overnight on a magnetic stirrer (CNW 21-2 Homothermal, China) at room temperature. The polymeric solution was then pre-frozen at -70°C for 24 hour and lyophilized at 1.35mmTorr for 24 hour. The combinations of the variables used are tabulated below, Table 5.1.

**Table 5.1.** Limit determinations of the upper and lower variables.

<b>Variables</b>	<b>Lower</b>	<b>Upper</b>
Ovalbumin	100mg	250mg
Sodium alginate	0.04 ( <sup>w</sup> / <sub>v</sub> %)	0.08 ( <sup>v</sup> / <sub>v</sub> %)
CaCl <sub>2</sub>	12mM	24mM

#### **5.2.3.2.2. Drug Release Analysis**

The *in vitro* release experiments were performed in simulated intestinal fluid (SIF) pH 6.8 in USP Apparatus 2. Each set of the nanoparticles, equivalent to 100mg of captopril, were accurately weighed and placed in 500mL glass volumetric flasks containing 500mL of the simulated intestinal fluid at 37°C. Samples (1mL) were taken from the release medium at specific time intervals for a total of 24hour and replaced by fresh 1ml SIF buffer solution. pH 1.2 and 7.4 drug release profiles were also assessed to measure the different gastric and intestinal drug release percentages. Sink conditions were maintained by replacing the withdrawn 1mL samples with simulated intestinal fluid at each sampling time. The concentration of the drug released was determined utilizing the Ultraviolet Spectrophotometer (Cecil CE 3021, 3000 Series, Cecil Instruments, Cambridge, England) at  $\lambda$ 271nm. From this concentration value the actual amount of drug was then calculated.

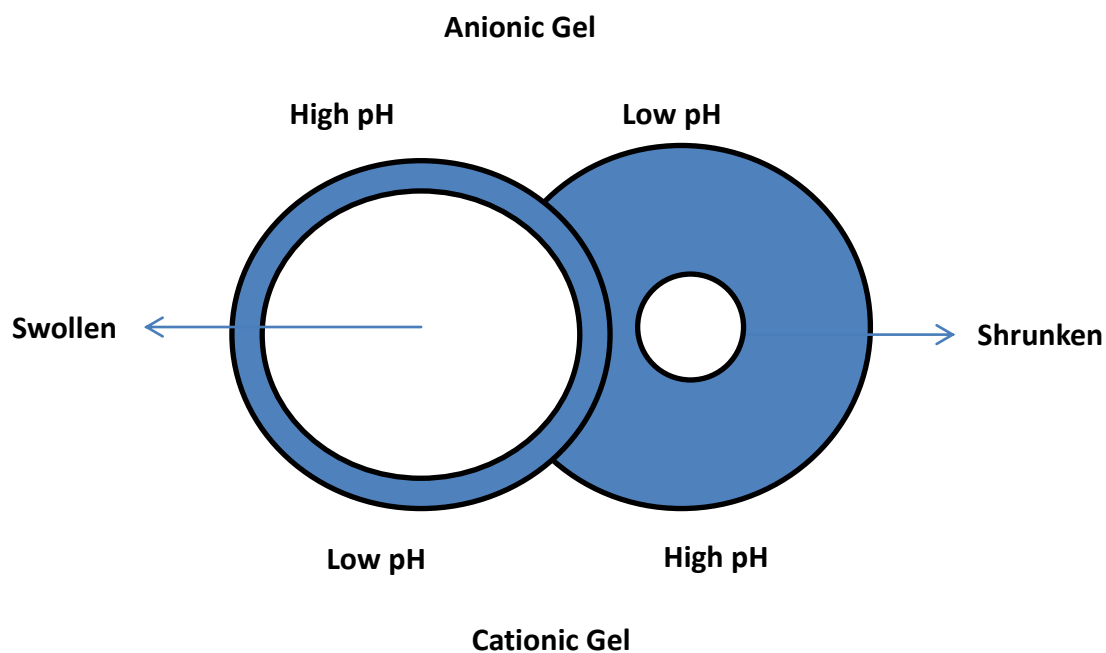
### **5.3. Results and Discussion**

#### **5.3.1. Results**

##### **5.3.1.1. Effects of pH and salt on the denaturation of the ovalbumin protein**

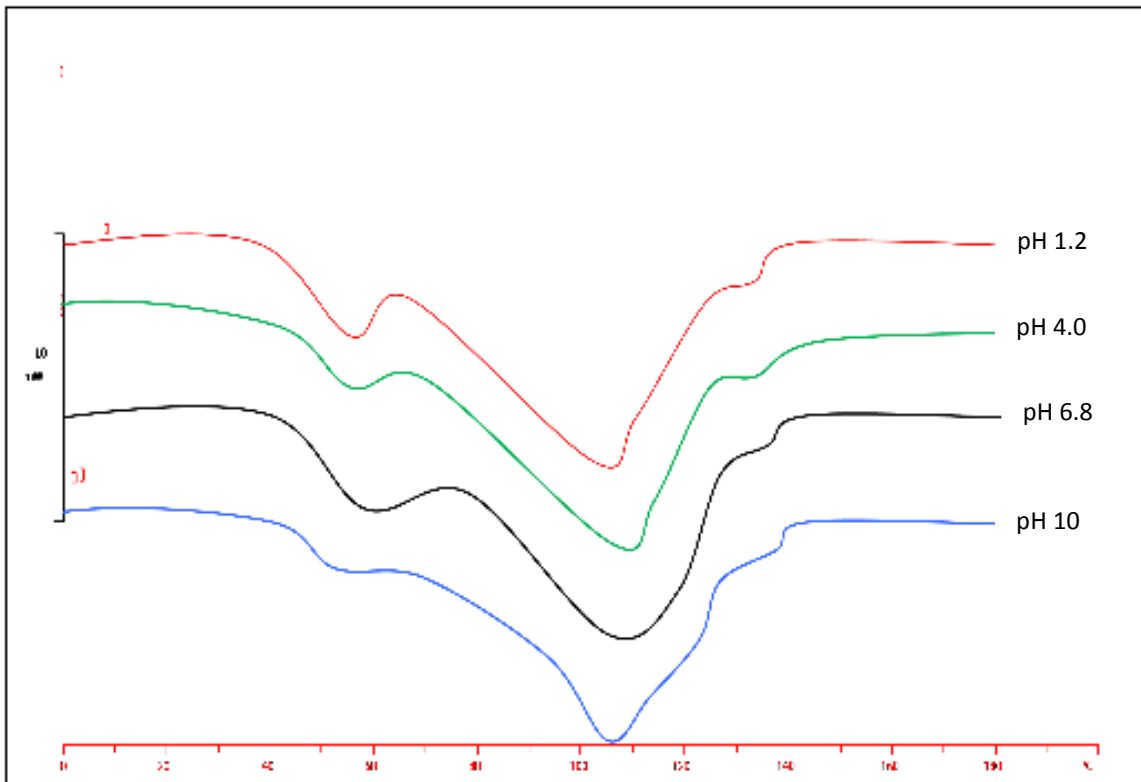
Thermal characterisation of food and pharmaceutical consumables is important especially if the contents thereof contain proteins (Behnken et al., 1999). It is well known that the thermal characterisations of proteins are affected by pH, temperature, ion intensity and protein concentration. By treating natural polymers such as ovalbumin with salts, sugars, acidity and alkaline chemicals, the resultant effect is a shift or change in the stability of the protein (Govender et al., 2005). These conformational changes vary in the effect they have on the structure of the protein. At isoelectric point, the protein is uncharged and charge repulsions of similar functional groups are generally minimal, which allows for aggregation to take place. Many proteins precipitate under these conditions, and even for proteins that remain in solution at their isoelectric point this is the pH of minimum solubility (Ferriera et al., 2007).

Figure 5.2 demonstrated the effect cationic or anionic ovalbumin would display when placed in an acidic or alkaline pH, and its effect on drug release. The shrunken state would ultimately decrease the total amount of captopril released and the swollen state would be vice versa. In Figure 5.2 the thermal effect of different pHs on ovalbumin was assessed at pH 1.6, 4.0, 6.8 and 10 using DSC. It showed that as the pH increased, the denaturation curve increased, resulting in a shift to lower temperatures of 60°C. Contrastingly in Figure 5.3, as the CaCl<sub>2</sub> concentration was increased there was a decrease in the denaturation of ovalbumin and a shift to higher temperatures of 80°C. Consequently, a significant captopril increment would be noticed (Rothgang et al., 1975). Schematic 5.2 showed that the increase in ionic strength of CaCl<sub>2</sub> could have caused instability, reduced polymer solubility, and polymer precipitation which results in reduced viscosity. It also showed that changing pH to higher values increases the stability of proteins and the heat effect of unfolding.

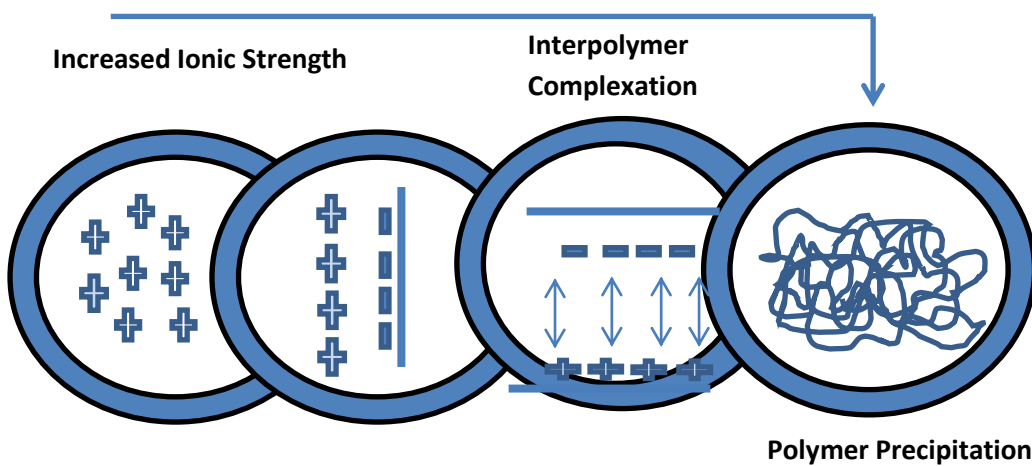


**Fig. 5.2.** The response of cationic or anionic ovalbumin to pH values of acidity and alkalinity. Adapted from Mastropietro et al.,(2013).

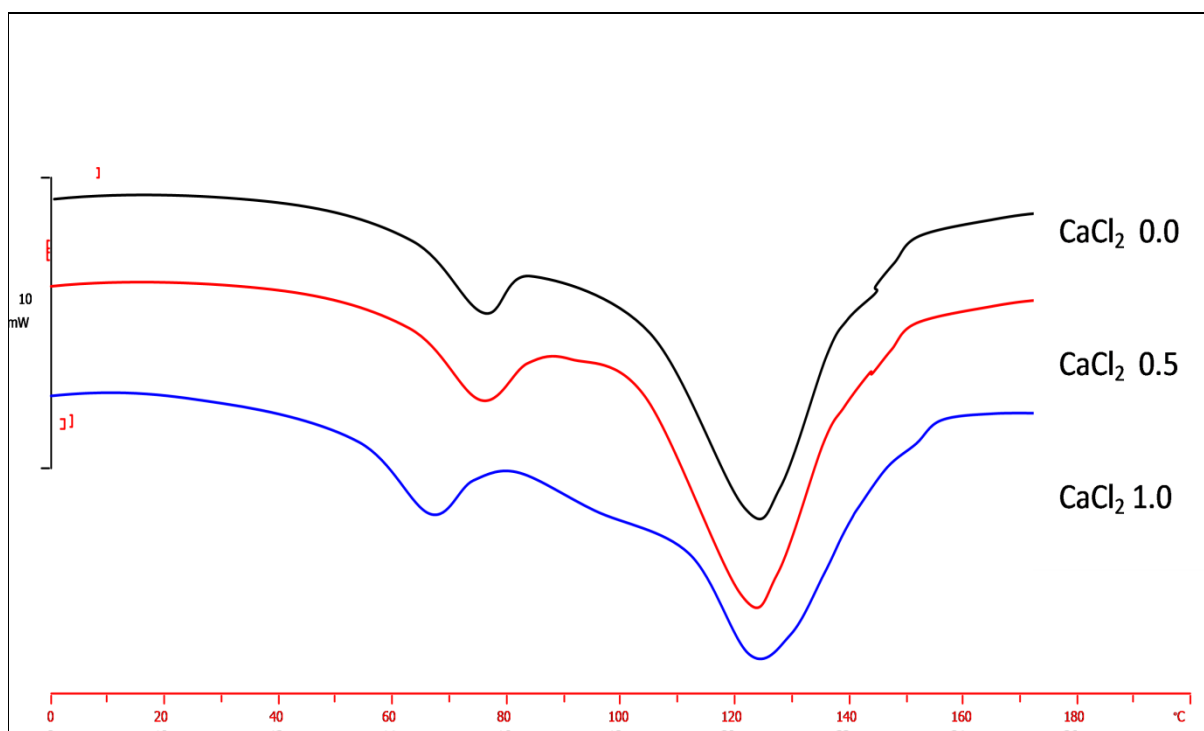




**Fig.5.2.** The DSC curves for the analysis of comparing the thermal effect of different pHs on the ovalbumin.



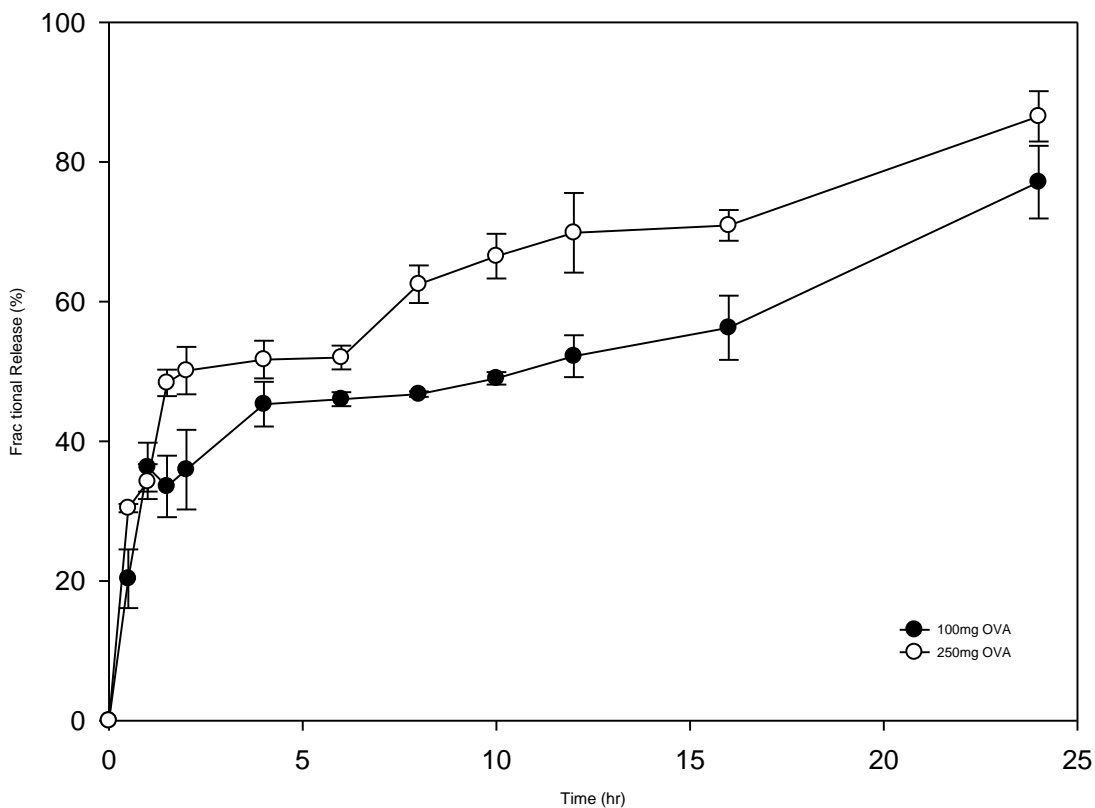
**Fig.5.3.** The effect of ions on the ovalbumin polymer solubility and viscosity. Adapted from Mastropietro et al.,2013.



**Fig.5.3.** DSC curves comparing the thermal effect of different CaCl<sub>2</sub> salt concentrations on ovalbumin.

#### 5.4.2. Drug Release Analysis

Figure 5.4 showed very little if no significant difference in the fractional release of captopril. This could be due to the dissolution of the disulphide bond formed between the ovalbumin polymer and captopril being broken due to the abundant hydrogen molecules found in the 7.2 medium. The drug entrapment was measured on average at  $79.1 \pm 6.5\%$ .

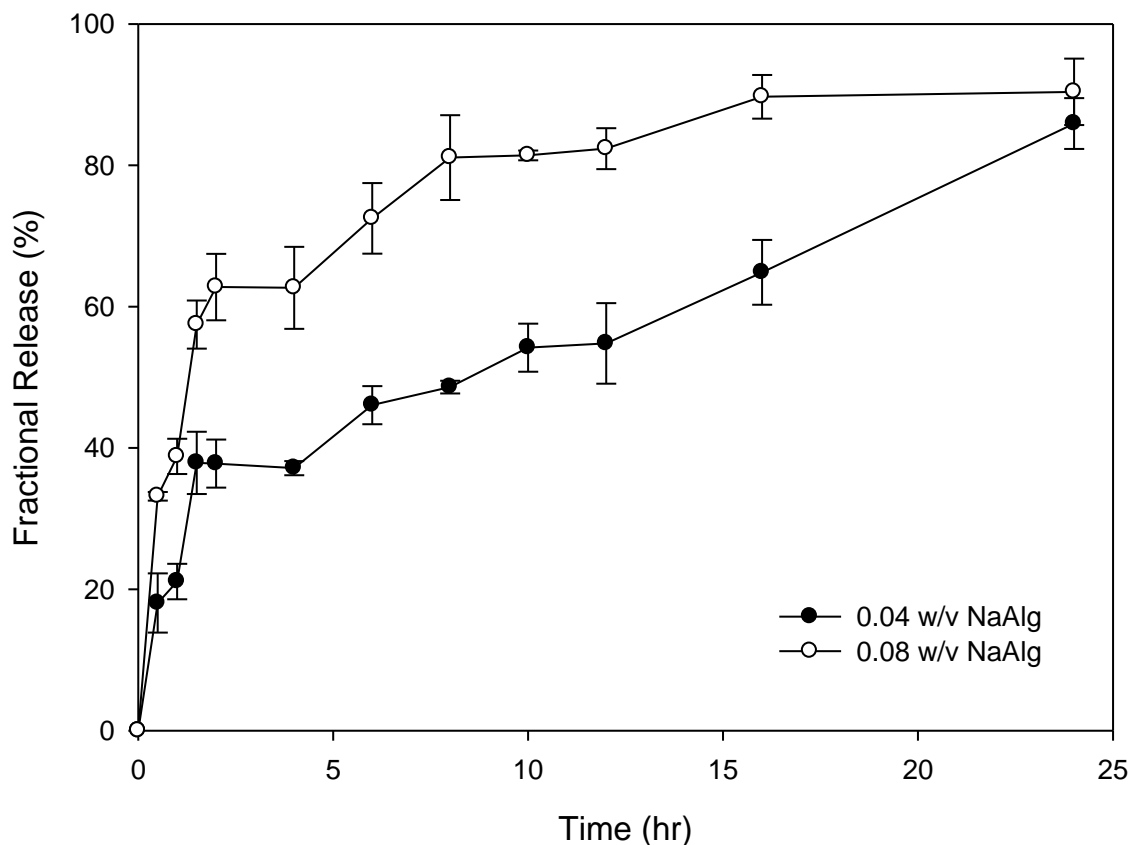


**Fig.5.4.** Comparison of the effect of different masses the ovalbumin polymer has on the release of captopril.

The effect of different concentrations of hydrogel in this case sodium alginate, showed similarity in the shape of the drug release profile. Both drug release profiles demonstrated first-order drug release profile, with the only difference being the fractional percentage of drug released with 0.08 w/v sodium alginate at 98% and 0.04 w/v at 88%, (Figure 5.5). This could be because of the increased availability of hydrogen moieties on the more concentrated sodium alginate than the less concentrated, but as mentioned previously the total fractional release was generally similar with little statistical difference. p-Value of <0.005.

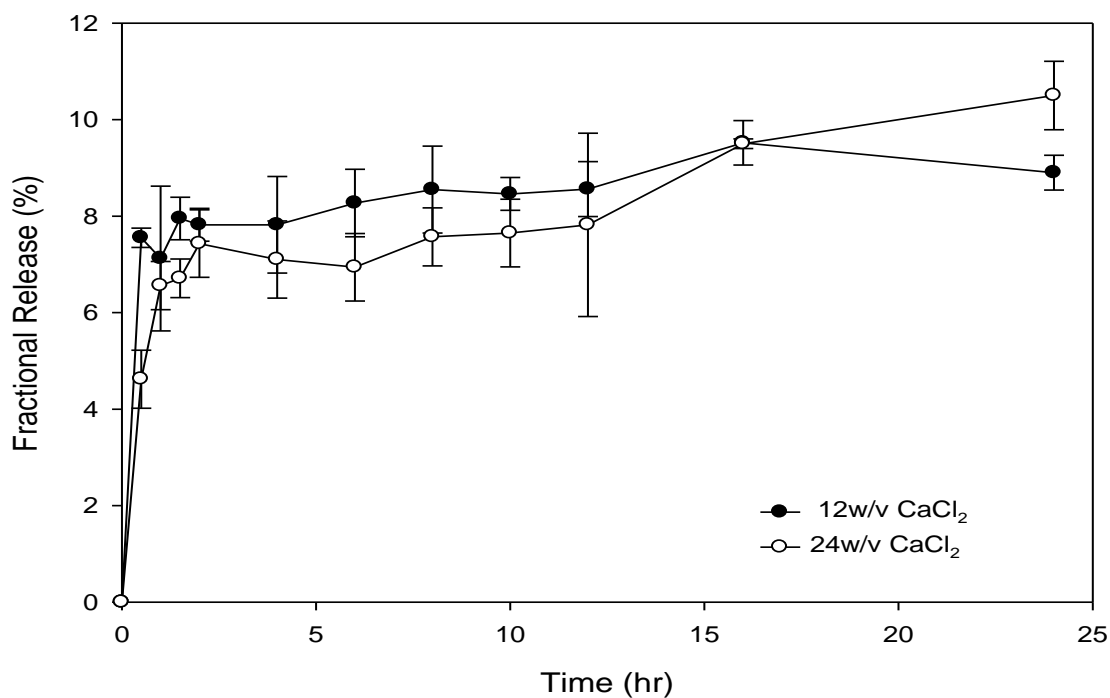
The effect of the concentration of  $\text{CaCl}_2$  on the release rate of captopril showed no significant difference between the chosen lower and upper level concentrations. This signifies the important role  $\text{CaCl}_2$  played in the crosslinking of the hydrogel to the ovalbumin polymer, but the concentration did however affect the drug release profile obtained. From Figure 5.6 it was evident that the lower concentration of 12w/v  $\text{CaCl}_2$  displayed a first-order drug release profile with a 1hour burst effect while the higher concentration displayed a zero order drug

release profile. The lower concentrations of  $\text{CaCl}_2$  showed an initial drug burst release effect, which could be due to rapid swelling of the hydrogel. This type of drug release would be suited for an immediate response drug delivery system, with prolonged drug effects maintained in the blood stream.

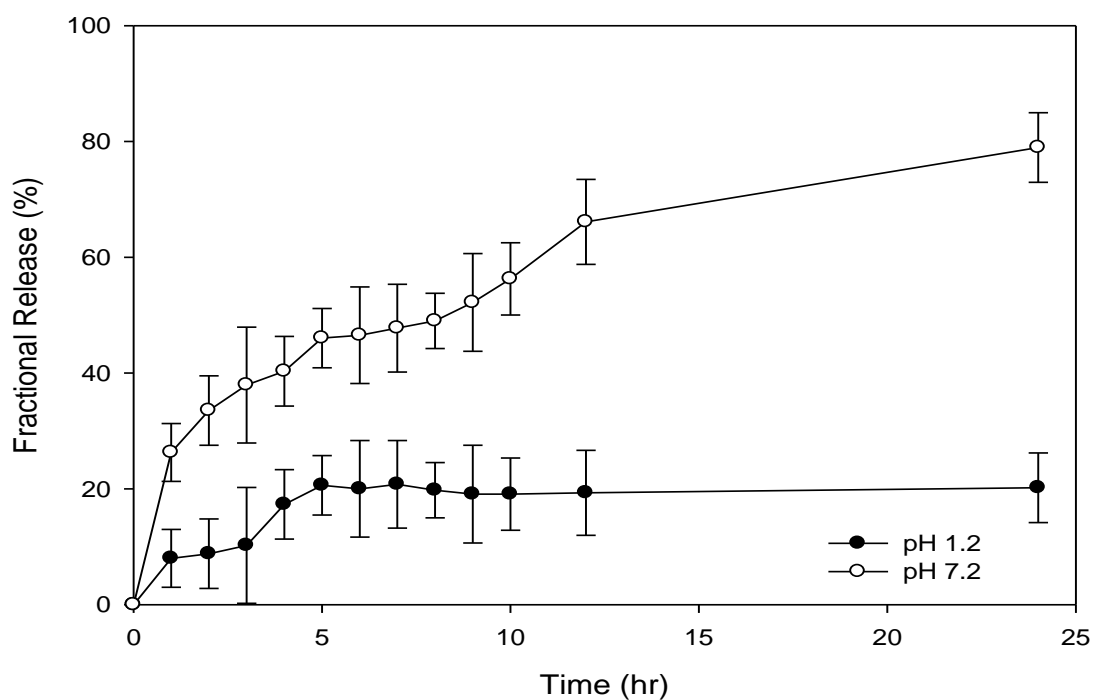


**Fig.5.5.** Comparative drug release profile of showing the effect of sodium alginate (NaAlg) variable.

At a lower pH the release rate and total amount of the drug released was reduced, because of the reduction in the swelling ability of sodium alginate at pH 1.2 (Figure 5.7). The rate of diffusion into the hydrogel was reduced due to the decreased ionic interaction between the hydrogel and water molecules.



**Fig. 5.6.** Comparative drug release profile of the effect of calcium chloride (CaCl<sub>2</sub>) on the release of captopril.



**Fig.5.7.** Comparative drug release profile of the different effects pH has on the release of the captopril.

#### **5.4. Concluding Remarks**

The importance of drug release in pharmaceutical preparations is very important. If a drug is not getting dissolved or miscible in vehicle then it becomes very difficult to administer it and hence forth it shows poor bioavailability. The release of captopril from the ovalbumin carrier system was determined by many factors, including the amount of the polymer excipients, the polymer interactions with other excipients such as the calcium chloride cross-linker and the concentrations of the hydrogel. The functionality of the ovalbumin vehicle system was dependent on the quantities of the individual excipients, their concentrations and the optimal pH at which the release of the drug was optimal. The drug release from the particles was affected by the pH of the dissolution medium results more sustained effect in alkaline medium. The release of the captopril from the ovalbumin carrier system was also dependent on the pH, calcium chloride effects on the native ovalbumin itself. It can be concluded that the selected excipients have enhanced the release of captopril from the ovalbumin vehicle system.

## CHAPTER 6

### Optimisation of the ovalbumin drug carrier system

---

#### 6.1. Introduction

Drug delivery systems require a detailed understanding of the relationship between process parameters and quality attributes. It is necessary to develop a science based design system to identify multidimensional combinations of the many casual factors that determine target quality (Gohel et al., 1971). It is however difficult to obtain an optimised formulation with rapid and complete dissolution using the old formulation screening and optimisation process, one-factor-at-a-time. The single factor optimisation process does not consider the interactions between factors and may require a large number of experiments (Nazzal et al., 1981).

Various experimental designs have been designed to reduce the experimentation process and provide estimates of the relative significance of different variables of a formulation (Chang et al., 2007; Yasir et al., 2013; Hao et al., 2011). In recent years, the application of statistical experimental designs to formulations have shown a high level of success in understanding the relationship between independent and dependent variables in a formulation. The response surface methodology (RSM) was useful in the simultaneous analysis of variables and their interactions when the interactions are complicated. The success in many studies demonstrated the value of response surface methodology for obtaining optimal formulation in various drug delivery systems (Gazori et al., 2009; Fakri et al., 2013).

RSM is a statistical technique that uses quantitative data obtained from appropriately designed experiments to determine regression model and operating conditions (Jabasingh et al., 2010). It was developed to build mathematical models which allow one to assess the effects of several factors onto a desired response. It is suitable for multi-factor experiments and investigates the common relationship between various factors for the most favourable conditions of the processes (Laurent et al., 2008).

The Box-Behnken design is an independent, rotatable quadratic design, i.e. contains no embedded factorial or fractional factorial design, in which the treatment combinations are at the midpoints of the edges of the process space and at the centre (Nguyen et al., 2008; Biro et al., 2009). Experimental designs have been used frequently for nanoparticle optimisation considering the advantages such as, (1) reduction in the number of experiments that need to

be performed, (2) development of mathematical models to assess the relevance and (3) statistical significance of the factor effects, and evaluation of interaction effect between studied factors (Jarrott et al., 1981; Medvedovici et al., 2009; El-Kamel et al., 2006; Hayashi et al., 1985). Box-Behnken designs are based on a 3-level incomplete factorial design and are useful tools for optimisation following response surface methodology because it permits estimation of the parameters of the quadratic model, building of sequential designs and detection of lack of model fit (Darren et al., 2009). A Box-Behnken design does not contain combinations for which all factors are simultaneously at highest and lowest levels, avoiding experiments performed under extreme conditions for which unsatisfactory results might occur (Woitiski et al., 2010). The purpose of this study was to optimize nanoparticle formulation for orally dosed captopril, investigating the relationship between design factors and experimental responses via a response surface methodology specifically a with Box–Behnken experimental design.

## **6.2. Materials and Methods**

### **6.2.1. Materials**

Purified lyophilised ovalbumin (OVA), Dithiothreitol (DTT), and captopril were purchased from Sigma (Sigma Aldrich, Missouri, USA). Ethanol, Sodium Alginate, Potassium phosphate monobasic and Disodium hydrogen phosphate were purchased from Merck (Merck KGaA, Darmstadt, Germany). All the chemical agents were analytic grade and used without further purification. It should be noted that no differences were found between the Sigma obtained ovalbumin and the self purified native ovalbumin.

### **6.2.2. Methods**

#### **6.2.2.1. Preparation of the ovalbumin drug delivery hydrogel matrices in accordance with the Box-Behnken experimental design template**

Fifteen formulations were prepared using various combinations of the processes of interphase, co-particulate, co-solvent, pre-freezing and lyophilisation guided through a two-level, three factor and three centre points Box-Behnken quadratic design using Minitab Statistical Software, Version 14 (Minitab Inc., State College, PA, USA). Three categories of independent variables composed of the two primary polymer concentrations and the linker were employed in formulating the ovalbumin drug delivery systems. As previously stated the analysis was based on a statistically and mathematically generated Box-Behnken design template.



Each compound employed in formulation of the fifteen formulations and their rationales for their selections are outlined in Table 6.1. Combinations of both the polymeric and non-polymeric additives were employed in the fabrication of the drug delivery systems in order to facilitate the development of an effective formulation with the optimum physicochemical and performance qualities suitable for the intended application as an oral drug delivery system.

Table 6.1 and 6.2 present the variables selected, the two levels of the independent variables employed and the experimental design template for the 3 factors, 3 centre points and the 15 experimental runs respectively. The lower and upper limits for the factors were set based on their ability to form stable, sustained release drug loaded systems, using minimal quantities of the individual components.

**Table 6.1.** Rationale for the selection of the variables employed in the experimental design.

<b>Component</b>	<b>Rational for selection and Function</b>
Ovalbumin	Thiol conjugate, drug carrier/vehicle
Sodium Alginate	Permeation enhancer, control release polymer properties
Calcium Chloride	Polymer cross-linker

**Table 6.2.** Levels of independent variables employed in the Box-Behnken design template.

<b>Independant Variable</b>	<b>Levels</b>		<b>Units</b>
	<b>Low</b>	<b>High</b>	
Ovalbumin <sup>a</sup>	100	250	mg
Sodium Alginate <sup>b</sup>	0.04	0.08	mM
Calcium Chloride <sup>c</sup>	12	24	mM

<sup>a</sup> Ovalbumin, <sup>b</sup> Sodium Alginate, <sup>c</sup> Calcium Chloride.

**Table 6.3.** Box-Behnken Template for the preparation of each of the 15 formulations.

Formulation	Composition		
	NaAlg (mg/ml)	Ovalbumin (mg)	CaCl <sub>2</sub> (mg/ml)
1	0.08	100	18
2	0.04	100	18
3	0.04	250	18
4	0.04	175	12
5	0.06	100	24
6	0.04	175	24
7	0.06	100	12
8	0.06	250	24
9	0.08	250	18
10*	0.06	175	18
11	0.06	250	12
12	0.08	175	12
13*	0.06	175	18
14*	0.06	175	18
15	0.08	175	24

\*Centre points of the Box-Behnken Design template

Fifteen ovalbumin captopril carrier formulations were prepared using predetermined quantities of ovalbumin, sodium alginate and CaCl<sub>2</sub> according to Table 6.3. The combinations of the polymeric and non-polymeric solutes, ovalbumin and sodium alginate were dispersed separately in deionised water and ethanol respectively.

Briefly, each formulation contained 50mg of captopril which was dispersed in the aqueous sodium alginate. The two dispersions (ovalbumin and sodium alginate) were homogenised together and the respective quantities of were used to increase the crosslinking of both the polymeric dispersions. The crosslinking process was used to enhance homogenization to form stable particles with a single continuous phase. The resulting blends of the 15 ovalbumin captopril carrier formulations formulations were pre-frozen at -72°C for 24 hours to aid the formulation of the homogenous blend and then subjected to lyophilization by placing them into a freeze dryer (Bench Top 2K, Virtis, New York, USA) set at -48 ± 5°C, at a pressure of 0.42mBar for 24 hours.

Post lyophilisation produced white powdered batches of the 15 formulations and the samples were stored at room temperature ( $25 \pm 5^\circ\text{C}$ ) until further use. To prevent atmospheric water absorption by the individual formulations, active silica-containing desiccant bags were packaged with the formulations.

To determine the actual amount of captopril loaded, each of the fifteen formulations were individually dissolved in 100mL of simulated intestinal fluid (pH 6.8). The release medium (2mL) was manually withdrawn after 24 hours and filtered through with a  $0.22\mu\text{m}$  pore sized filter (Millipore Corporation, Bedford, MA, USA). The sample was diluted accordially and the absorbance was measured to determine the concentration of the captopril released, utilizing the Ultraviolet Spectrophotometer (Cecil CE 3021, 3000 Series, Cecil Instruments, Cambridge, England) at  $\lambda 271\text{nm}$ . From this concentration value the actual amount of drug was then calculated. All experiments were carried out in triplicate.

#### **6.2.2.2. Evaluating the *in vitro* drug release behaviour of the sodium alginate ovalbumin optimisation formulae**

Drug release studies were conducted by immersing each of the previously mentioned 15 formulations into 500mL of simulated intestinal fluid pH 6.8. The experiments were performed in similar conditions as mentioned above, and three replicate samples of each individual formulation were analyzed. For experimental compliance, the temperature was maintained at  $37^\circ\text{C} \pm 0.5^\circ\text{C}$  and 90 rpm using the USP II dissolution system (Erweka DT 700, Erweka GmbH, and Huesenstamm, Germany). 1mL dissolution samples were manually withdrawn at the following predetermined time intervals 30 minutes, 1, 2, 4, 6, 8, 10, 12, 16, 20, 24 hours and filtered thorough a  $0.22\mu\text{m}$  pore sized filter (Millipore Corporation, Bedford, MA, USA). Sink conditions were maintained by replacing the withdrawn 1mL samples with freshly prepared simulated intestinal fluid at each sampling time. The concentration of captopril released was determined utilizing the Ultraviolet Spectrophotometer (Cecil CE 3021, 3000 Series, Cecil Instruments, Cambridge, England) at  $\lambda 271\text{nm}$ . From this concentration value the actual amount of drug was then calculated.

The varied dissolotion patterns were analysed and substantiated by the time-point approach referred to as the mean dissolution time (MDT). The mean dissolution time provides an accurate view of the drug release behaviour as it was determined as a sum of the individual periods of which a specific fraction of the total drug was released.

$$\text{MDT} = \int_0^\infty \frac{(M - M(t))}{M} dt \quad (6.1)$$

Where  $M_t$  is the fraction of dose released at time  $t_i$ ,  $t_i = (t_i + t_{i-1})/2$  and  $M_\infty$  corresponds to the loading dose.

### 6.3. Results and Discussion

#### 6.3.1. Cumulative drug release profiles of the Box-Behnken experimental design formulations

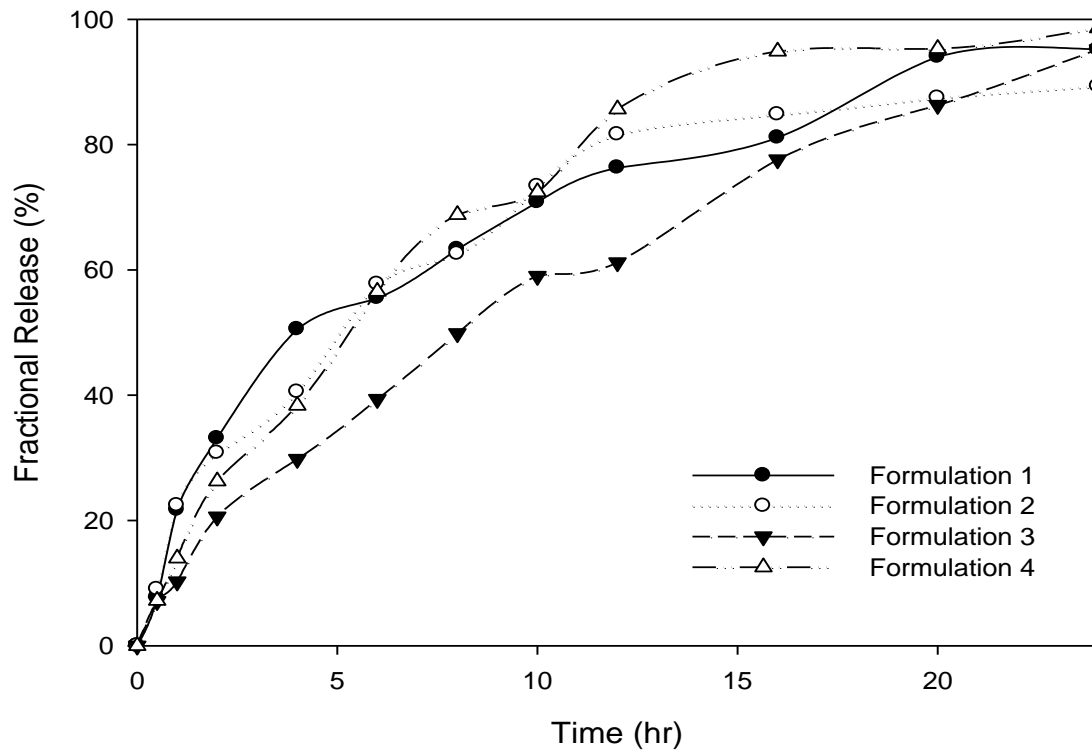
All the 15 ovalbumin captopril carrier formulations elicited variable levels of captopril release for the 24 hours time period. The drug carrier system demonstrated the potential for application as a controlled release system over the 24 hour period. The levels of both natural polymers to cross-linker contained in each formulation appeared to have noticeable effects on the drug release pattern. A summary of the responses of each the ovalbumin captopril carrier formulations were tabulated in Table 6.4.

Generally, the ovalbumin captopril carrier formulations comprised of higher levels of ovalbumin displayed a more controlled release pattern while the reverse was observed for those containing higher levels of the hydrogel, sodium alginate. Figure 6.1 (a-d) demonstrated the observed trend of captopril release may be advantageous to the intended application of the drug delivery system as a controlled prolong release drug delivery system. Overall, the differences in the quantities of the formulation constituents could have influenced the water influx and hydration, particle size which influenced the captopril release behaviour of each formulation. Based on the limiting response variables tabulated in Table 6.4, the responses targets were determined by the Box-Behnken design. Table 6.5 summarises the response results for the 15 ovalbumin captopril carrier formulations, which include the size and zeta-potentials of the particles, the mean dissolution time and cumulative captopril release of 24 hours.

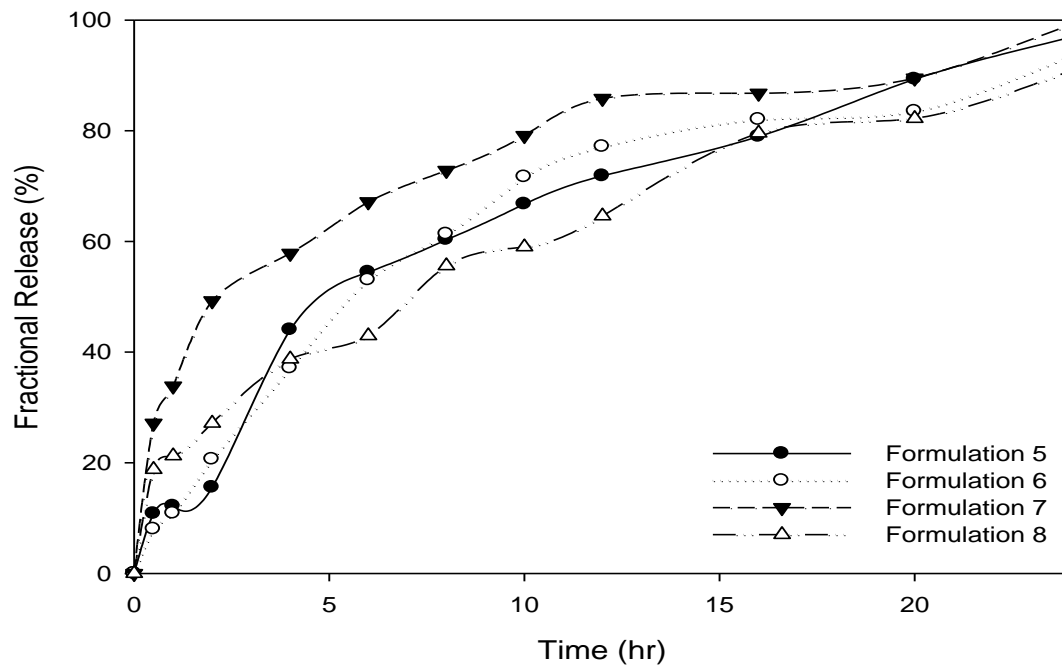
**Table 6.4.** Targets for the selected response parameters.

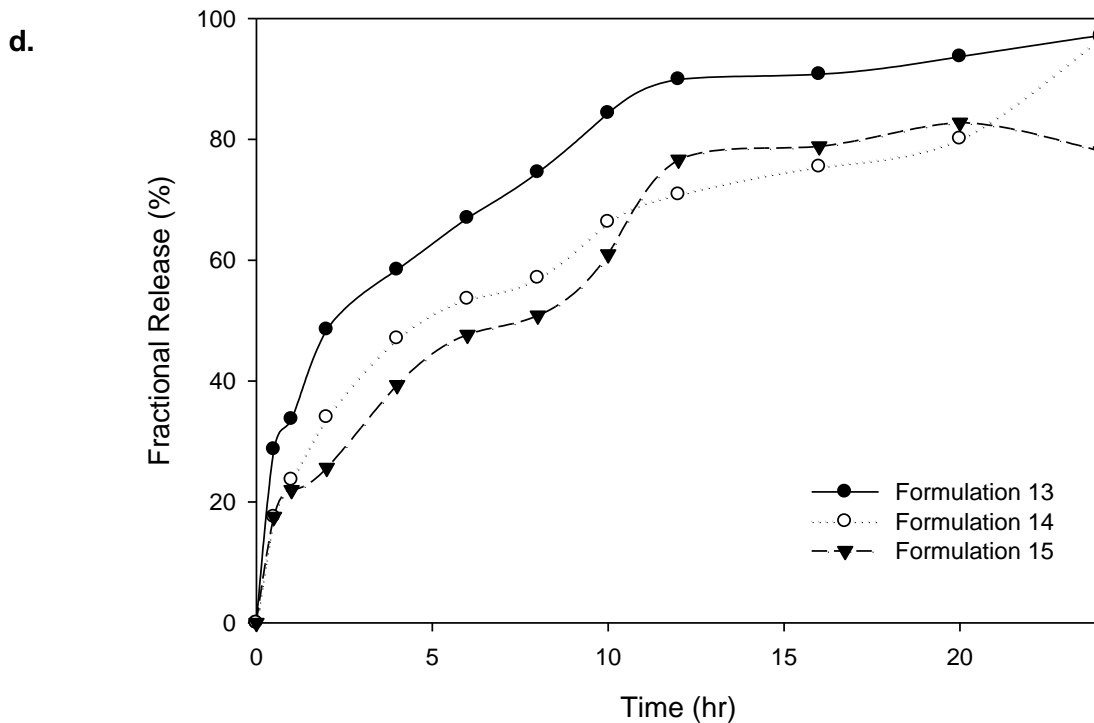
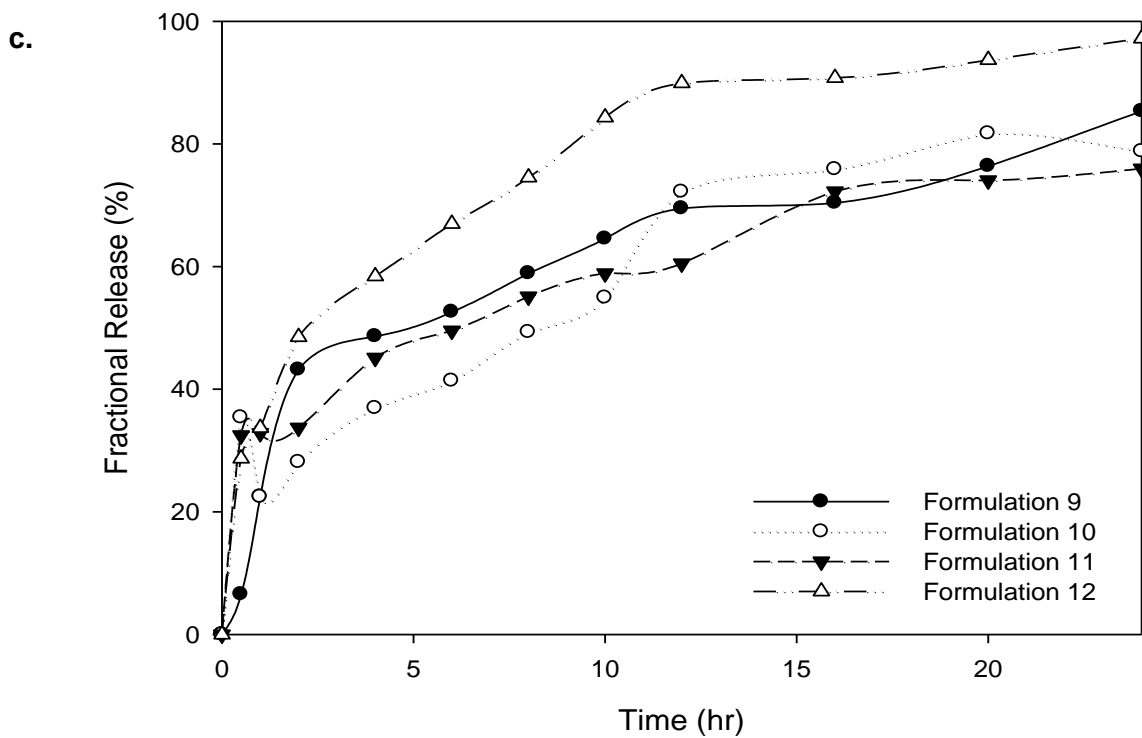
Responses	Lower	Target	Upper	
Zeta-potential (mV)	-27.7	-27.7	-29.4	Maximize
Mean dissolution time	0.0149	7.0	7.056	Minimize
Drug entrapment efficiency(%)	38.88	45.1	45.1	Maximize
Accumulated drug Release	55.2	96	98.6	Minimize
Size (nm)	99.78	220	283.9	Minimize

a.



b.





**Fig. 6.1.a.** Drug release profiles for F 1-4. **b.** Drug release profiles for F 5-8. **c.** Drug release profiles for F 9-12. **d.** Drug release profiles for F 13-15. Average  $SD \pm 0.67$ .

**Table 6.5.** Cumulative Results of the independent variables of the Box-Behnken Experimental Template.

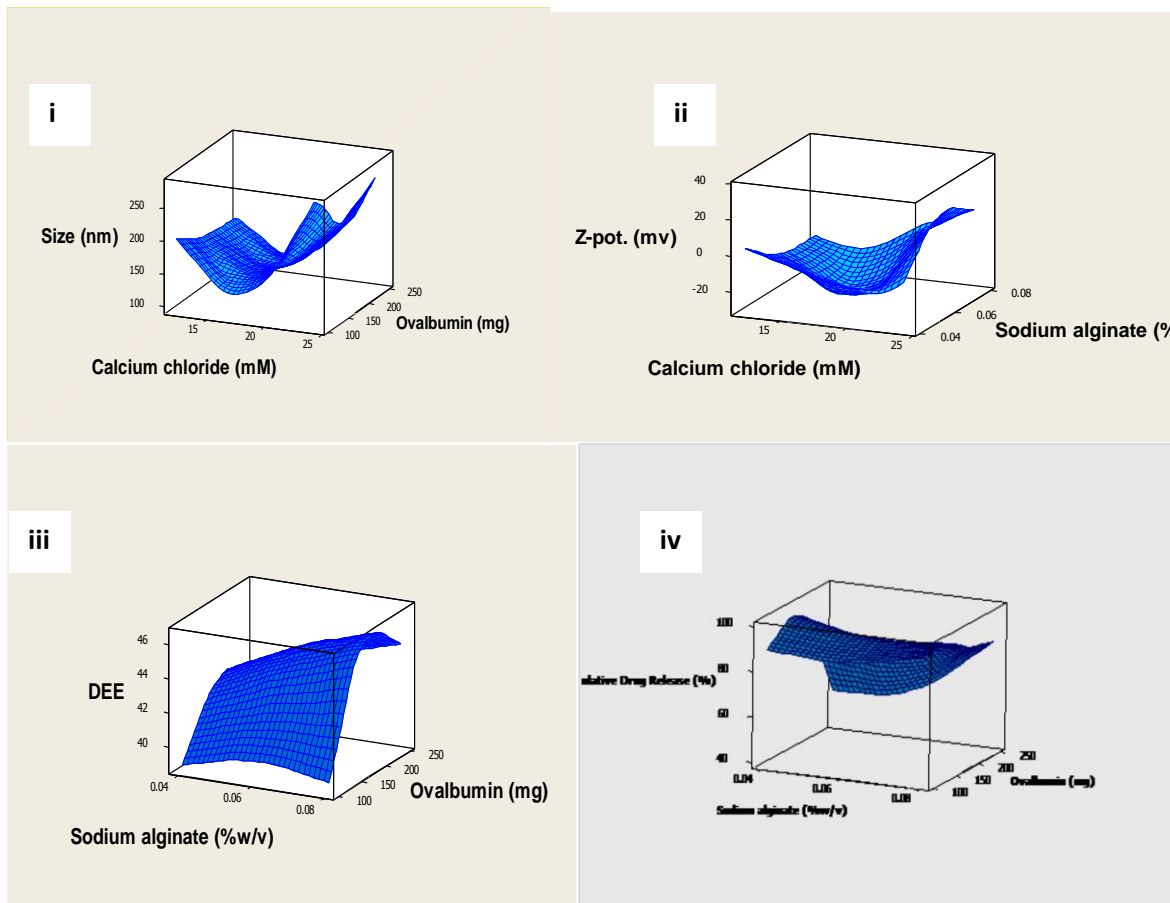
<b>Formulation</b>	<b>Size (nm)</b>	<b>Z-pot. (mV)</b>	<b>Cum. Release (%)</b>	<b>MDT (hr)</b>	<b>DEE (%)</b>
1	166.8	-24.4	70.65	6.920	39.17
2	99.78	-26.2	89.30	3.772	38.88
3	110.4	-29.4	55.20	6.551	40.11
4	226.8	-23.6	78.60	6.076	40.73
5	283.9	-25.4	76.90	3.603	39.46
6	240.0	-25.4	73.50	4.476	44.39
7	201.2	-22.3	79.20	0.015	40.03
8	255.6	-22.4	40.83	4.471	42.76
9	142.1	-26.1	85.34	2.758	44.60
10	138.7	-26.5	76.78	7.456	44.96
11	166.5	-20.4	78.98	4.885	43.40
12	121.5	-23.0	77.28	3.679	45.50
13	138.8	-26.7	76.83	7.322	44.14
14	138.7	-26.8	76.77	7.475	44.55
15	201.4	-20.7	87.03	0.999	46.50

### 6.3.2. Elucidation of the variable responses using the Box-Behnken Design Template

#### 6.3.2.1. Surface Plots

The surface plots of the response functions are useful in understanding both the main and interaction effects of the factors (Arai et al., 2009). The 3D surface plots of the response (Y) indicated the same results as observed in the interaction plot. The surface plots for size and zeta-potential are indicated in Figure 6.2. i and ii. The surface plot of size versus calcium

chloride and ovalbumin (Figure 6.5.a) indicate that size was highest when ovalbumin and calcium chloride were 250mg and 25mM respectively. The zeta-potential was highest when calcium chloride was 25mM and the sodium alginate was 0.06w/v, Figure 6.2.ii. The zeta-potential increased with increased calcium chloride concentrations, whereas the size of the particle increased with increased ovalbumin and sodium alginate concentrations. The concentration of calcium chloride also increases zeta potential to values lower than -20 mV, affecting the stability of nanoparticles in suspension.

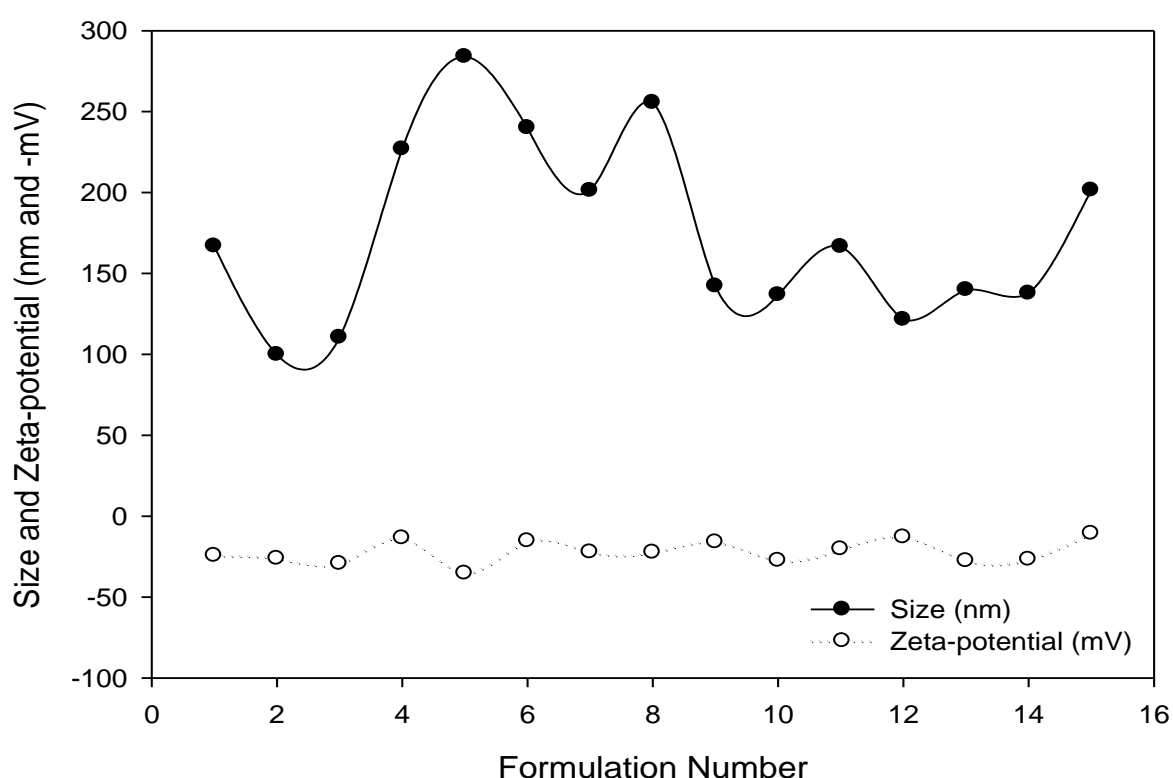


**Fig. 6.2.i.** 3-D Response surface showing the influence of the concentration of calcium chloride and ovalbumin on the average particle size of the nanoparticles. **ii.** surface showing the influence of the concentration of calcium chloride and ovalbumin on the average zeta-potential of the nanoparticles. **iii.** surface showing the influence of the concentrations of sodium alginate and ovalbumin on the percentage drug entrapment efficiency of the nanoparticles. **iv.** surface showing the influence of the concentration of sodium alginate and ovalbumin on the cumulative drug release.



### 6.3.2.2. Comparative of the Box-Behnken formulations for size and zeta-potential

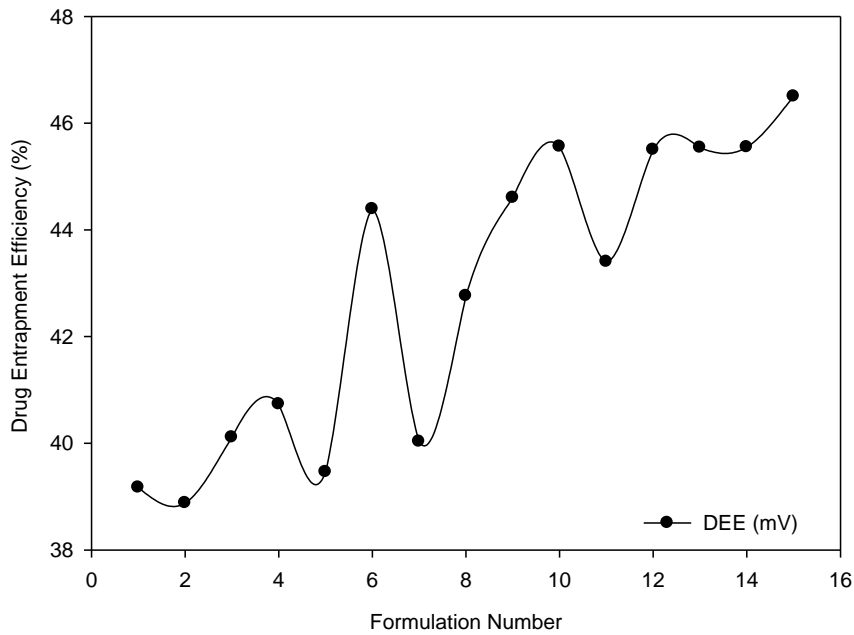
All formulations yielded a zeta potential below -20mV, which was indicative of good stability of the particles. The size of the particles varied with Formulation 2 yielding the smallest particles, 99nm and Formulation 5 the largest particle sizes, 283.9nm. Particles with small size are highly desirable in order to increase contact with the intestinal mucosa due to higher surface area per volume and mucoadhesive strength (Darren et al., 2009) also increasing nanoparticle uptake through the intestinal mucosa. Figure 6.3 showed a summary of the size and zeta-potential 15 ovalbumin captopril carrier formulations



**Fig.6.3.** Summary of the size and zetapotential for the 15 Box-Behnken Design formulations.

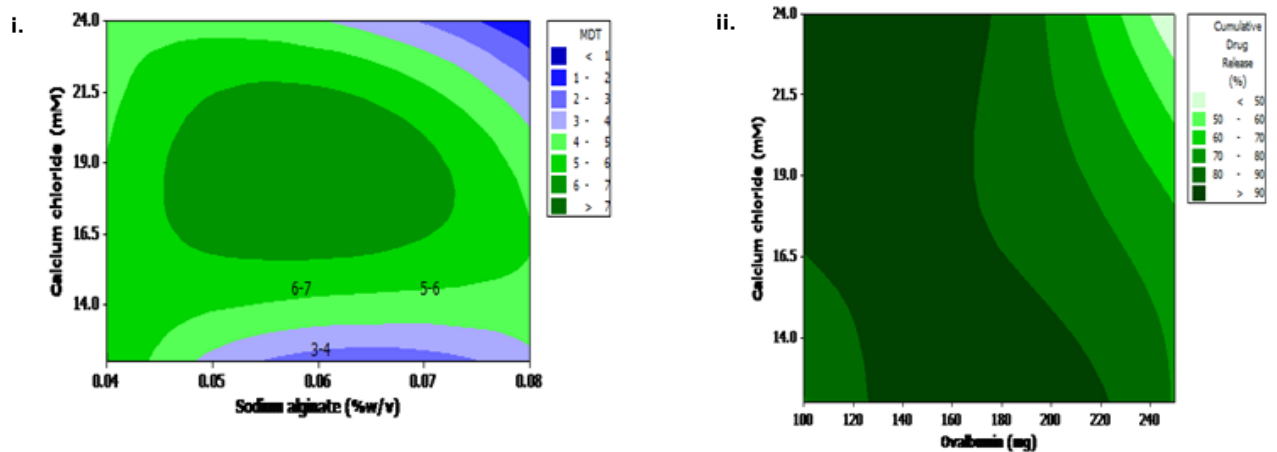
### 6.3.2.3. Response surface analysis of the mean dissolution time and drug entrapment efficiency

Response surface analyses were plotted in three-dimensional model graphs for optimization of nanoparticles with physicochemical properties for the ovalbumin drug carrier system. The three-dimensional response surface plots for drug entrapment efficiency and accumulated drug release percentage were analysed. Entrapment efficiency is influenced by ovalbumin concentration as seen in Figure 6.2.iii., when calcium chloride was kept constant. In Figure 6.4 a summary of the comparison across all the 15 formulations was shown.



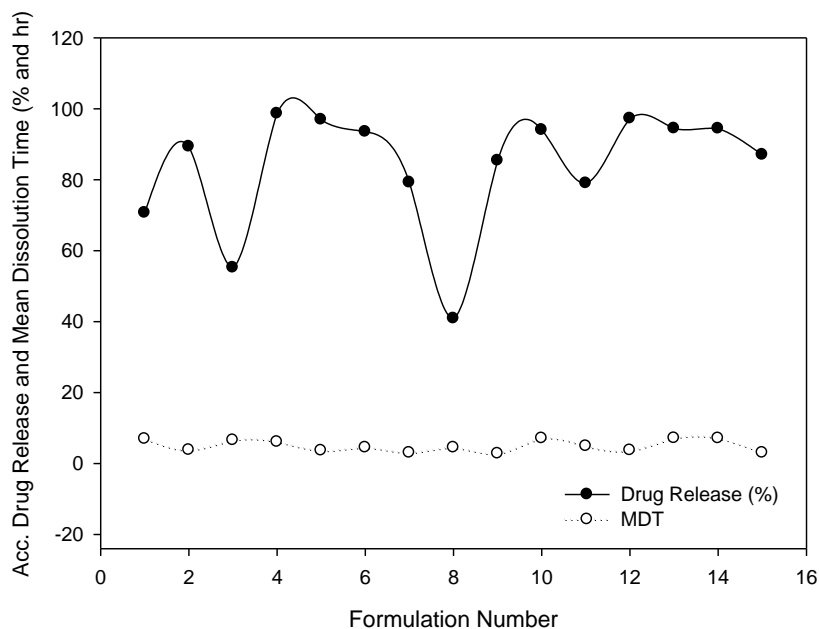
**Fig.6.4.** Summary of the the drug entrapment efficiency for the 15 Box-Behnken Design formulations.

It can be concluded that from Figure 6.5. (i and ii) the mean dissolution time was directly increased by ovalbumin, sodium alginate and calcium chloride.



**Fig.6.5.i.** Contour plot showing the influence of the concentration of sodium alginate and calcium chloride on the mean dissolution time. **ii.** Contour plot showing the influence of the concentration of ovalbumin and calcium chloride on the cumulative drug release percentage.

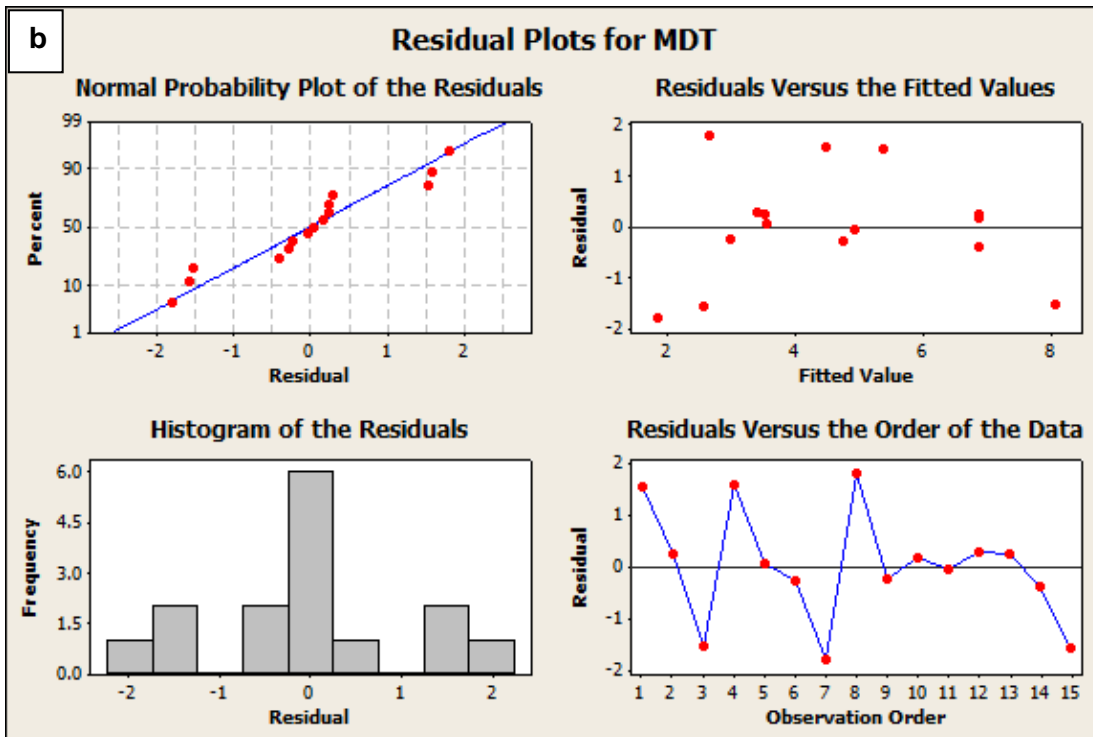
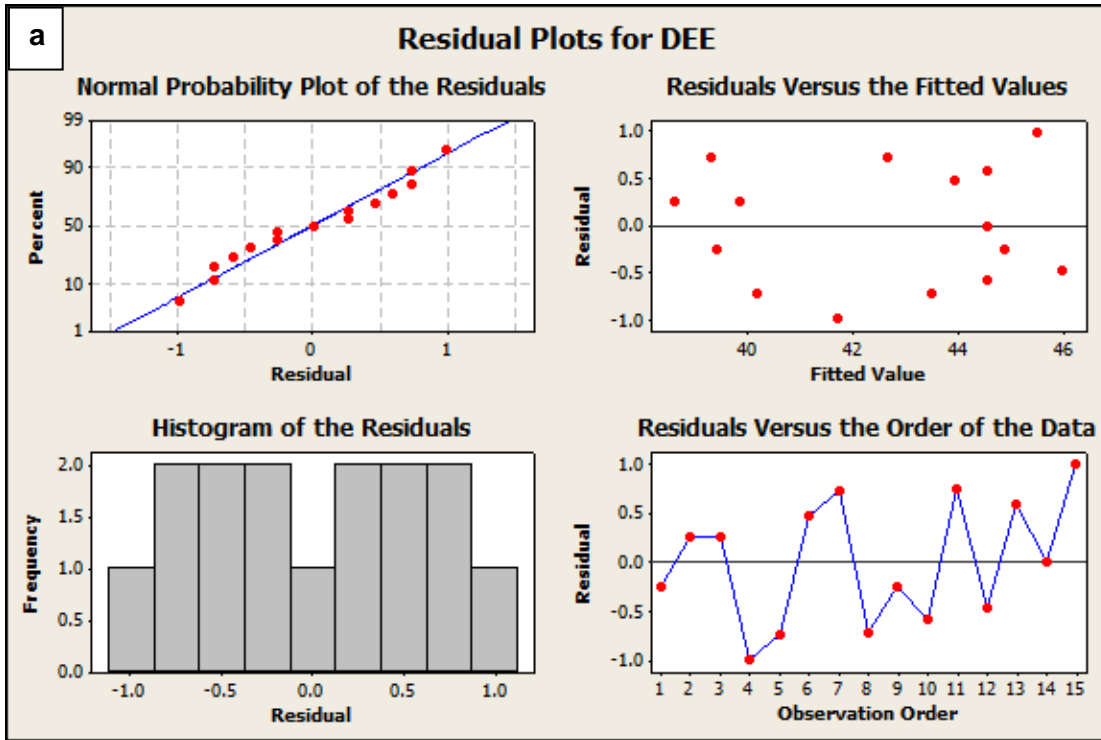
A summary of the mean dissolution time and accumulated release of the ovalbumin captopril carrier formulations were provided in Figure 6.6. It should be noted that the higher the concentration of ovalbumin the lower the MDT.

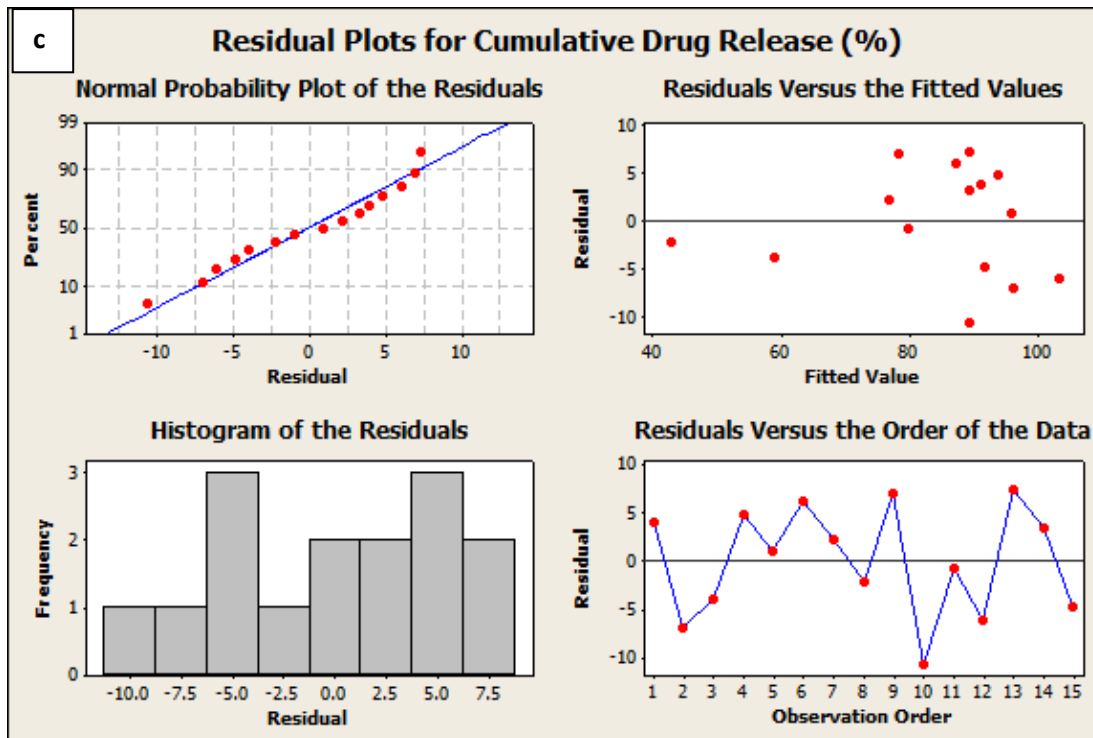


**Fig.6.6.** Summary of the the drug mean dissolution time and cumulative drug release for the 15 Box-Behnken Design formulations.

#### 6.3.2.4. Residual Plots of the optimised ovalbumin-captopril formulations

Residuals plots may be employed to analyze the fit of regression models in a Box-Behnken Design. These plots can be defined as measuring the variation between the actual observed responses and the predicted responses. On analysis of  $k$  and the  $R^2$  values for the drug release from the predetermined variables, it was found that there was an indiscriminate distribution of data. The scatter of data observed in the residual versus fitted value plots showed a random arrangement of data indicating that the fit of the data linear regression model was of a satisfactory nature. The residual histogram exhibited nearly bell-shaped curves with the exception of a few, namely the cumulative drug release and the drug entrapment efficiency. The bell-shaped histogram curves were indicative of normal data distribution. The non bell-shaped histograms as mentioned previously were indicative of an aspect of the data that was not accounted for in the model which suggested that the error terms did not correlate amongst one another. The observed residual were linear for the entrapment efficiency, mean dissolution time and accumulated drug release (Figure 6.7. a-c).





**Fig.6.7.a.** Residual plot for the drug entrapment. **b** for the mean dissolution time, and **c.** for the cumulative drug release.

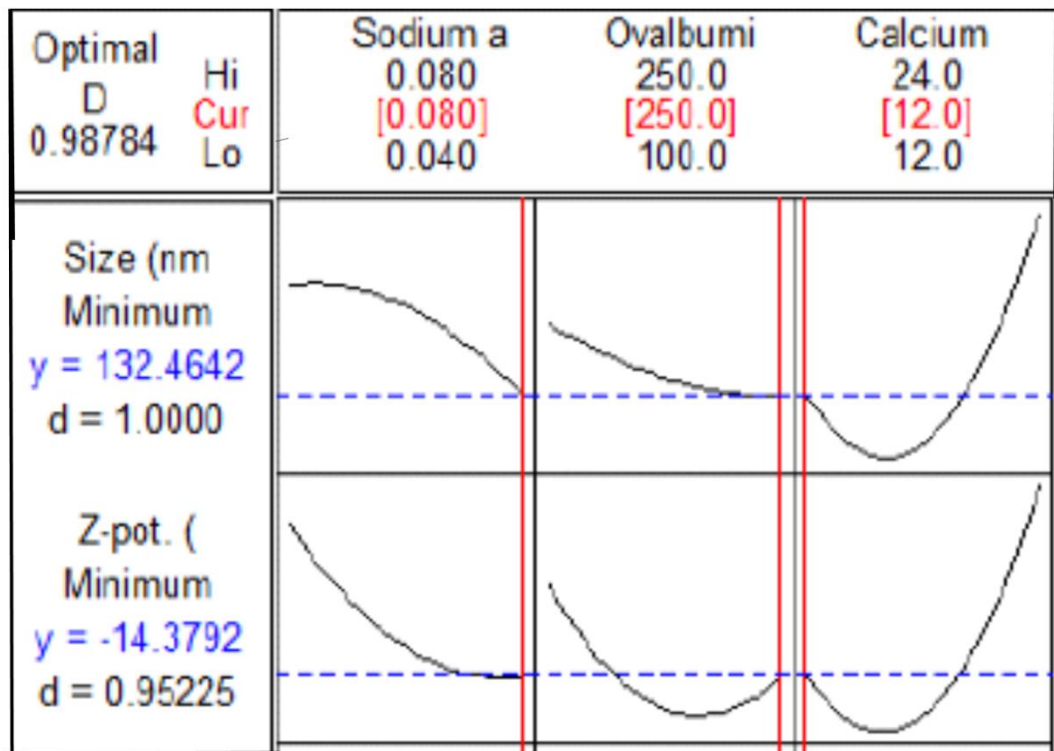
## 6.4. Response Optimised

### 6.4.1. Fabrication of the optimised formulation

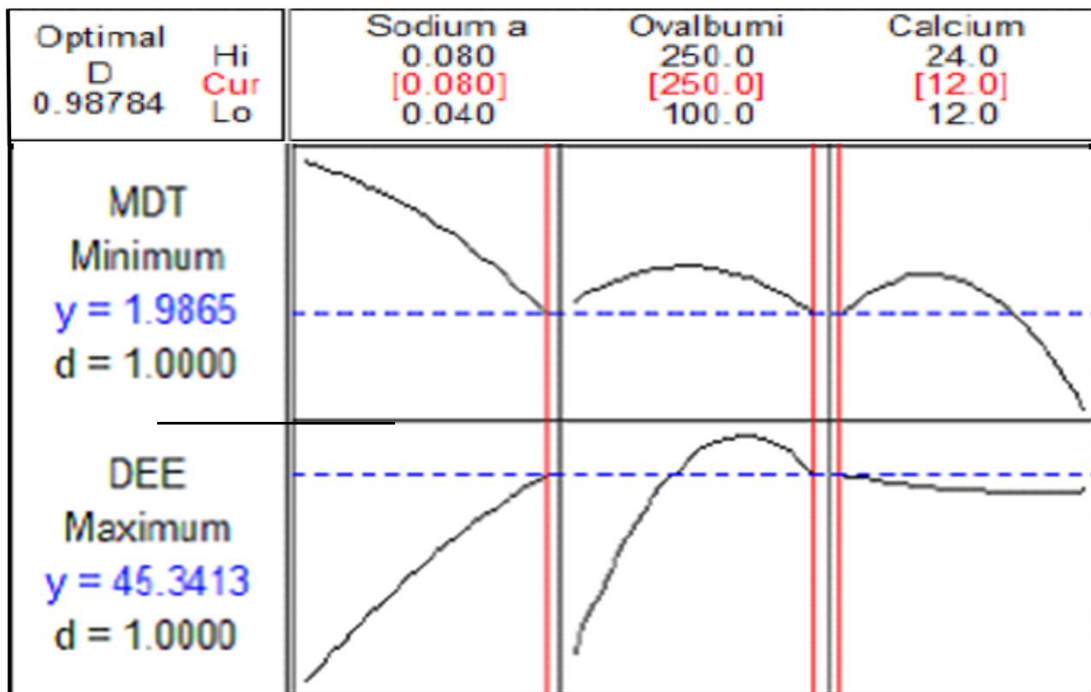
The optimised formulation was obtained from Minitab®, V14 (Minitab® Inc, Pennsylvania, USA). The optimised formulation was in accordance with the independent variables and the responses obtained.

### 6.4.2. Application of the desirability functions for size and zeta-potential

The desirability function was employed to obtain an optimal formulation of the four responses from the chosen independent variables. The responses were transformed to achieve a desirability target of 1. The responses were set into a lower, middle and upper response values for the independent values ovalbumin, calcium chloride and sodium alginate. The optimal formulation comprised of low levels of ovalbumin and sodium alginate were minimised and high levels calcium chloride. Figure 6.8 illustrated the set desirability functions in red and the responses in blue of the size and zeta-potential of the ovalbumin captopril carrier formulations.



**Fig.6.8.** Optimised plots and desirability functions for the size and zeta-potential of the drug carrier system.



**Fig.6.9.** Desirability functions for the drug entrapment and mean dissolution time of the drug carrier system.

For the desirability function, calcium chloride was minimised, sodium alginate and ovalbumin were maximised, (Figure 6.9) in red. The responses in blue for the captopril entrapment and mean dissolution time of the ovalbumin captopril carrier formulations were calculated as  $y=1.99$  and  $y=45.34$  for mean dissolution time and drug entrapment efficiency respectively.

**Table 6.6. Levels for the fabrication of the optimised drug delivery system.**

<b>Composition</b>	<b>Optimised Level</b>
Ovalbumin <sup>a</sup>	250 mg
NaAlg <sup>b</sup>	0.080 mg/mL
CaCl <sub>2</sub> <sup>c</sup>	12 mg/mL

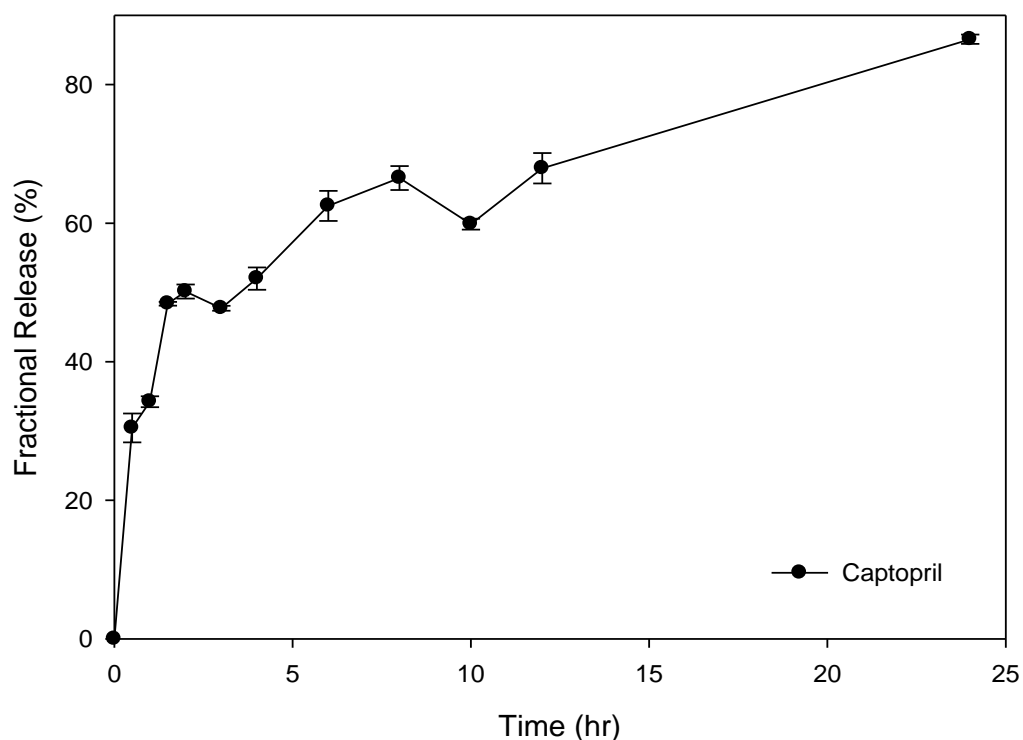
<sup>a</sup> Ovalbumin – ethanol based co-particulate dispersion.

<sup>b</sup> Sodium Alginate – aqua based dispersion.

<sup>c</sup> Calcium Chloride - crosslinker

Based on the optimization results, a formulation was developed for the synthesis of the optimized formulation (Table 6.6). The synthesised optimized formulation was assessed to ascertain the existence of a correlation between the experimentally and fitted data as well as confirming the suitability of the experimental design employed. The formulation was assessed based on its drug entrapment, particle size, zeta-potential, accumulated drug release and mean dissolution time. The drug release was designed as a 24 hour prolonged release system to aid patient compliance.

The optimised formulation had a drug entrapment efficiency mass of 44.5mg, a drug release percentage of 89% and an average mean dissolution time of 2.05 hours. The average sizes of the particles were 200nm and the zeta-potential was slightly higher than the predicted at -25mV. The optimized ovalbumin drug release carrier system retained its structure, of spherical particles. The representative drug release profile for the optimised formulation is shown in Figure 6.10. The optimised formulation displayed consistency in its drug release to those reported in the experimental design. The drug release of captopril was stable over the 24 hour period.



**Fig.6.10.** The drug release profile of the optimised ovalbumin drug delivery carrier system.

### 5.5. Concluding Remarks

The experimental design allowed the systematic optimization of the ovalbumin drug carrier system formulation to be examined. The optimization process determined the physicochemical parameters important for the oral dose of captopril, evaluating the most important factors and their observed responses. It investigated the relationship between factors affecting the performance of the ovalbumin drug carrier system using the response surface methodology. Box–Behnken design was successfully used to statistically optimize the formulation parameters and to evaluate the main interaction and quadratic effects of the independent variables on the particle size, zeta potential, entrapment efficiency and captopril release in simulated digestive fluids. A 3-factor, 3-level design was used to explore the quadratic and linear response surfaces and for constructing a zero order polynomial model.



## CHAPTER 7

### ***In vivo* Investigation and Analysis of the Optimised Ovalbumin Prolonged Drug Delivery System.**

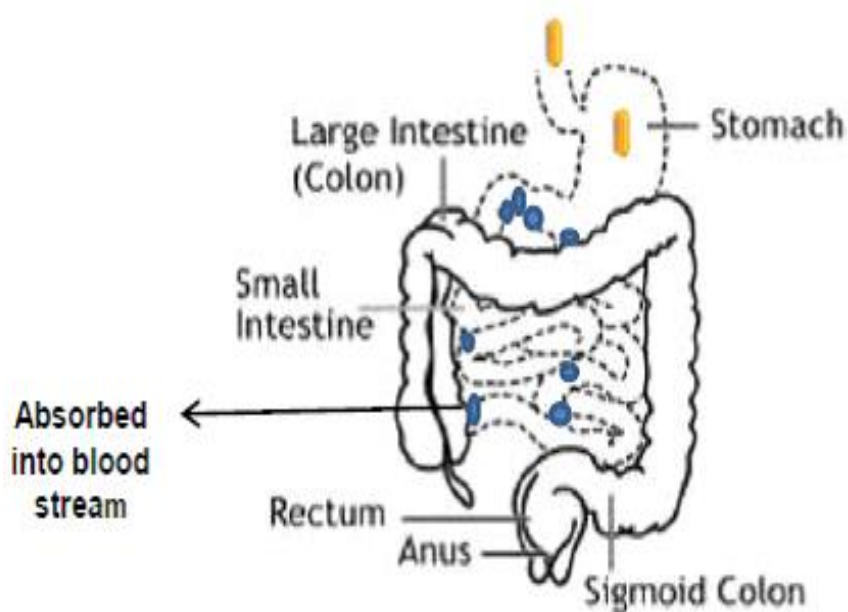
---

#### **7.1. Introduction**

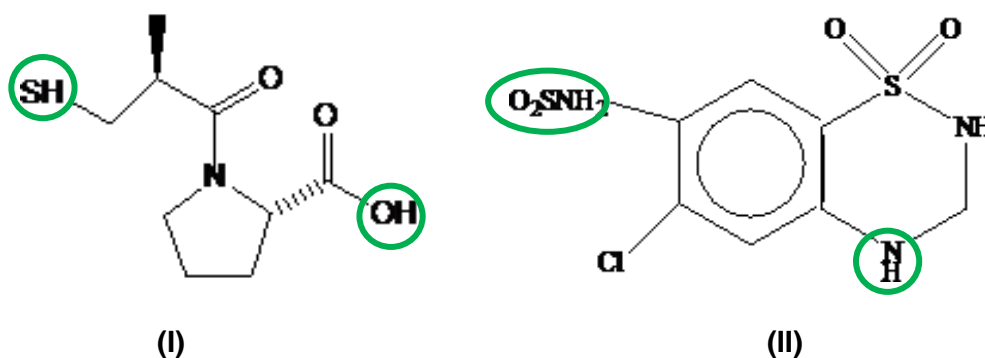
Captopril as previously stated, is a known antihypertensive, which works by inhibiting the angiotensin-converting enzyme (ACE). It has proven to be an effective and an outstanding clinical treatment for hypertension and congenital heart failure (Kripalani et al., 1980; Uslu et al., 2013). In most cases it is widely used as a first choice of drug for the treatment of hypertension. Despite its effectiveness as a an antihypertensive, captopril can at most regulate hypertension for a period of up to 8hour, which would require the a daily dose of 37-75 mg clinically thourice a day (Earl et al., 1964). It has a known short half-life of about 2hour and is metabolised to a *n*-carboxyl derivative in the liver and excreted mainly unchanged in the urine (Kok et al., 1997; Tache et al., 2002). It has been reported that captopril has a bioavailability of 70-75% (Rezende et al., 2007).

Hydrochlorothiazide is a thiazide diuretic, which acts moderately as a potent diuretic by reducing the reabsorption of electrolytes from the renal tubules in the kidneys (; Klein et al., 1990; Pereira et al., 1988). Hydrochlorothiazide is generally well absorbed in the gastrointestinal tract and has a half-life of 5-15 h (Salem et al., 2005). It has a bioavailability of 65-75% and excreted unchanged mainly in urine (Lees et al., 1989; Foroutan et al., 2003). Both captopril and hydrochlorothiazide are used in treatment of hypertension either individually or in combination with other antihypertensives such as ACE inhibitors and beta blockers. They are specifically used to treat peripheral oedema associated with heart failure and renal as well as hepatic disorders. The combination of these drugs, captopril and hydrothiazide, are there indicated for the treatment and management of hypertension. Figure 7.1. showed the structure of both captopril and hydrothiazide.

Based on the halflife duration of both drugs *in vivo*, there was a necessity to develop a controlled captopril release delivery system that would ultimately maintain relatively constant blood levels of captopril for a longer period of time *in vivo*. Scheme 7.1. demonstrated the oral administration of the ovalbumin drug carrier system.



**Fig 7.1.** Oral administration and absorption of the ovalbumin drug carrier system in a capsule also showing the absorption of the ovalbumin vehicle carriers.



**Schematic 7.1.** The structural formulae of captopril (I) and the internal standard hydrochlorothiazide (II), with circled reactive groups.

Due to the thiol reactive nature of captopril, it tends to form disulphide bonds easily with endogenous thiol-containing compounds/proteins. The easily accessible thiol groups tend to form random disulphide bonds with other thiol containing compounds, pose a pharmaceutical challenge due to the reactive nature of the thiols. Therefore the determination of free or unchanged captopril concentrations have to be preceded by the addition of a chemical stabilizer in order to prevent captopril disulphide formation.

Several methods of determining the free or total captopril in human plasma have been reported. LC- based methods have been employed for the determination of captopril (Kamel et al., 2008; Synniewski et al., 1997). In most cases liquid-liquid or solid-phase extraction is necessary in order to concentrate or to perform sample clean-ups in both cases. LC/MS has been used widely as a main tool in the identification, characterization and quantitative analysis of drugs and their metabolites because of its superior sensitivity, specificity and efficient technique (Bald et al., 1997).

There are unique advantages for the use of swines in this setting was that they share humans' similar anatomic and physiologic characteristics involving the cardiovascular, urinary, integumentary, and digestive systems. The similarity of diseases between humans and pigs, such as e.g. arteriosclerosis, metabolic syndrome, gastric ulcer, and wound healing (Synniewski et al., 1996) make the pig model a suitable alternative. Therefore, pigs are commonly used in research as preferred models for identification of new cardioalbuminscular agents (especially in the field of arteriosclerosis and myocardial infarction), agents for treatment of metabolic syndrome (such as diabetes), dermatology drugs, and diagnostic agents. However, the researchers need to be familiar with important anatomic, histopathologic, and clinicopathologic features of the laboratory pig and minipig in order to put background lesions or xenobiotically induced toxicologic changes in their proper perspective and also needs to consider specific anatomic differences (Cavrini et al., 1996).

In 1959, the report by Russell and Burch was published as 'The Principles of Humane Experimental Techniques', the basic tenet of their report being that "the humanest possible treatment of experimental animals, far from being an obstacle, is actually a prerequisite for a successful animal experiment."

The authors proposed the principles of Replacement, Reduction and Refinement (most often referred to as the 3R's) as the key strategies to provide a systematic framework to achieve the goal of humane experimental techniques. In addition animal experimentations had principles that were meant to be followed by the researcher which are integrity, respect for persons or animals beneficence, and justice.

The aim of the chapter was to assess the drug release of captopril from the ovalbumin drug carrier system *in vivo*. The objective was also to characterise and compare the release of captopril from the ovalbumin captopril carrier system *in vitro* and *in vivo* and ascertain the effectiveness of the delivery system.

## 7.2. Materials and Methods

### 7.2.1. Materials

Acetonitrile and formic acid were purchased from Aldrich® (Sigma–Aldrich Inc., St. Louis, USA). Other materials and excipients employed were of analytical grade and were utilized as purchased. Mobile phase used was acetonitrile (Merck, Wadeville, Gauteng, South Africa), orthophosphoric acid (Merck, Wadeville, Gauteng, South Africa) and double deionised water obtained from the Milli-Q System. The drugs used were captopril and hydrochlorothiazide (Sigma Aldrich, Steinheim, Germany. Blood samples were analyzed with the Ultra Performance Liquid Chromatography model Waters Acquity Ultra Performance Liquid Chromatography System (Waters, Milford, MA, USA). The column used in the UPLC was a C<sub>18</sub> column (2.1-50mm, 1.7µm particle size, Waters).

### 7.2.2. *In vivo* ethics clearance

The animal ethics clearance number for the research project was (2011/33/03) granted by the University of the Witwatersrand, Animal Ethic Committee (AEC), Johannesburg South Africa.

**Table 7.1.** The amount of drugs to be used for the animal study.

<b>Drug/Substance</b>	<b>Route</b>	<b>Dose</b>	<b>Frequency</b>
Captopril	Oral	50mg	Administration of the drug will be done during testing
Hydrochlorothiazide	Oral	50mg	Administration of the drug will be done during testing
Ketamine	Intramuscular injection	100mg/kg	Administered before Oral dosing and prior to euthanasia.
Xylazine	Intramuscular injection	5mg/kg	Administered before Oral dosing and prior to euthanasia.
Procaine	Topical	5mL	Administered before Oral dosing

### **7.2.3. Habituation and housing**

A total of twenty large Yorkshire gilts were used for the *in vivo* analysis investigation. The pigs day and night cycles were controlled similar to their natural habitat, with 12 hour days and nights. The pigs were placed individually in separate cages, with a controlled environmental temperature of  $25^{\circ}\text{C} \pm 3^{\circ}\text{C}$  and fed at preset times. The habituation was a period of 4 weeks, with regular twice a day visits to the pigs by the researchers. This period allowed the pigs to acclimatize to their new environment and to reduce any kind of social stress to the pigs.

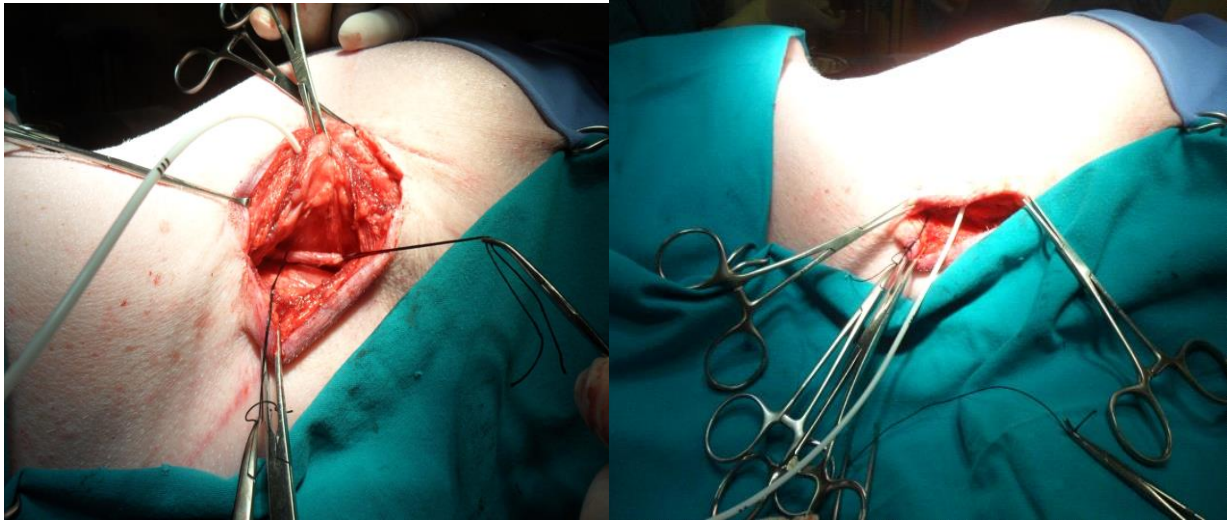
### **7.3. Jugular venous catheterisation for blood sampling**

The average weight the pigs weighed was between 30-35±2kg before catheterisation. During the habituation process, after two weeks, the pigs were weighed and prepared for catheterisation. Briefly, the catheter insertion into the jugular vein was as follows: The pigs were anaesthetised with ketamine (I.M.), xylazine (I.M.), and topical procaine (to reduce prick pain) was applied. The pigs were maintained under an oxygen atmosphere during the insertion of the catheter into the jugular vein. The duration of the surgery for each pig was 3 hours.

Briefly, an incision was made on the left side of the neck, directly above the jugular vein. The two lumen central venous catheter was then inserted into the lumen of the jugular vein. The length of the remaining catheter was then tunnelled subcutaneously dorsal to the scapula and out through the back of the neck (figure 7.2.). The catheter was used for the withdrawal of blood samples at predetermined time intervals without causing undue distress to the pig.

Post-operative care included monitoring of the pigs for the duration of the study to ensure that the catheter (1) had been inserted properly, (2) no complications had occurred during the surgery and (3) during the insertion process. Heparine saline was used to wash out the catheter twice daily, to prevent blood clots from forming which allowed for easy withdrawal of blood.

Blood samples were withdrawn using one of the ports (white or brown). Firstly the ports were flushed with 5mL of heparinised saline to ensure there were no blood clots that had formed in each of the ports. Blood (5mL) was then withdrawn and the port was further flushed with another 5mL of heparinised saline after sample withdrawal.



**Fig.7.2.** Surgical incision of 2cm to access the jugular vein. The catheter was then inserted into the jugular vein on the right side of the neck.



**Fig.7.3.** Catherter insertion surgery and post surgery. Once the catheters were inserted the pigs were then returned to their cages for full recovery.

### 7.3.1. Captopril gastric dosing and formulation testing

The pigs weight had increased to 45-54±3kg on dosing. The pigs were allowed an overnight 12 hour fasting period prior to testing. Baseline blood samples were withdrawn before the pigs were dosed, representing the zero time point.



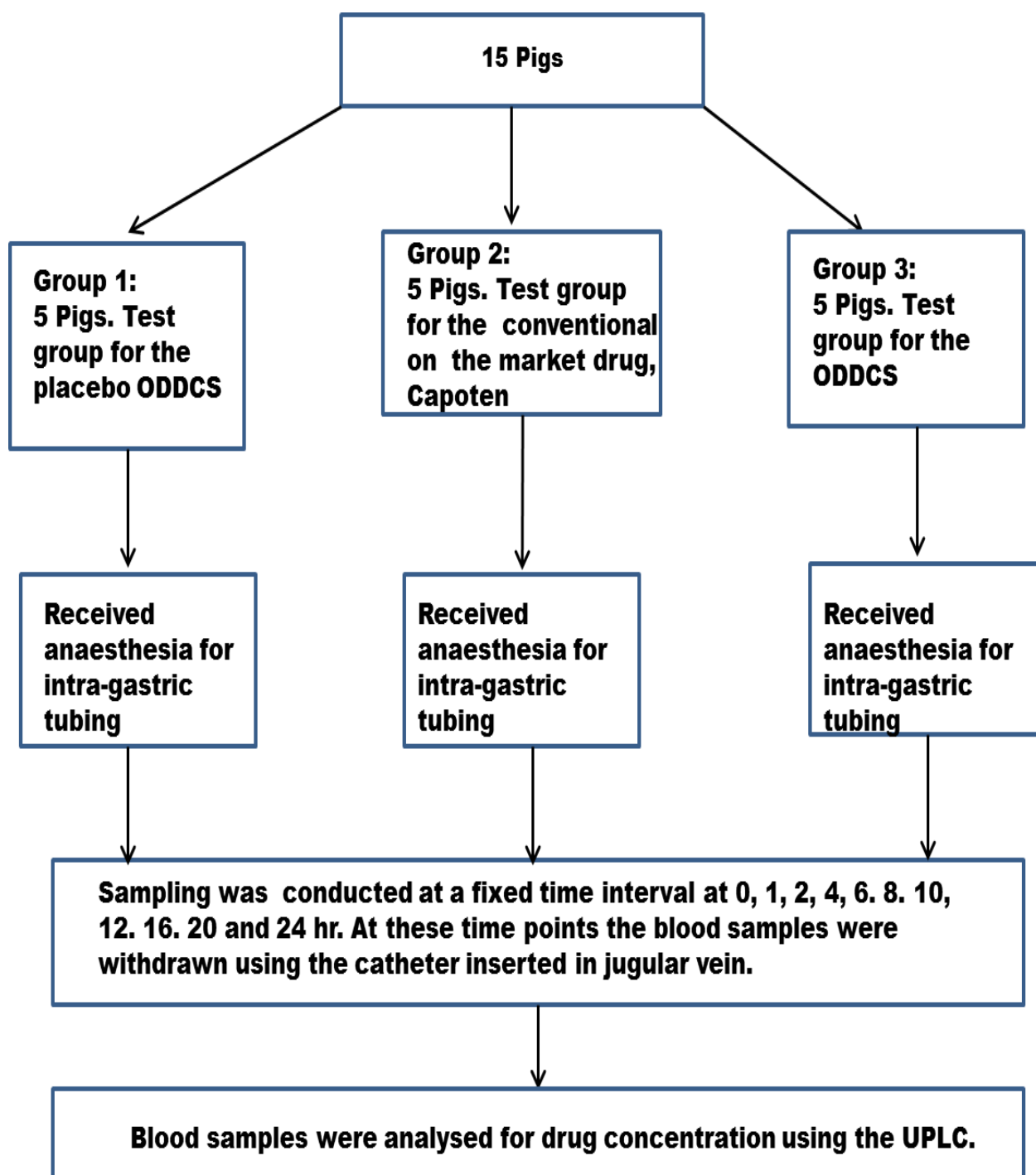
**Fig.7.4.** Oxygen was given and the pulse was monitored during the dosing of the pigs.



**Fig.7.5.** Preparation for the oral administration of the drug delivery system.

The pigs were anaesthetized (as described previously in Section 7.3) and oxygen was given to the pigs. The blood pressure was monitored continuously throughout the oral administration of the capsule procedure. Briefly, the pigs were held in an upright position while their mouths were kept open. Then an intragastric tube was inserted into the pigs' mouths, until it reached the opening of the rumen. Once the tube was positioned the capsule was administered through the tube and water was used to flush the capsule down the tube to ensure that the capsule reached the rumen. The intragastric tube was then pulled out and the pigs were returned to the cages. Blood withdrawals were taken over a period of 24 hour,

at 1, 2, 4, 6, 8, 10, 12, 16, 20, 24 hours respectively, with catheter maintenance procedures being followed between each withdrawal. 5mL of the blood was collected into EDTA vacutainers (BD Vacutainers, Franklin Lakes, NJ, USA) to prevent blood coagulation (Figure 7.3.). An overall flow diagram of the *in vivo* animal study experimentation procedure was illustrated in Scheme 7.2.



**Scheme 7.2.** Summary of the *in vivo* animal studies experimentation procedure.



#### **7.4. Ultra Performance Liquid Chromatography for blood analysis**

Quantitative Analysis of the blood samples were tested using the Waters Acquity™ UPLC/MS/MS MS system (Waters Corporation, Milford, MA, USA).

##### **7.4.1. Chromatographic method for detecting captopril and hydrochlorothiazide in blood plasma**

The liquid chromatography separations were achieved using the Acquity UPLC® BEH shield RP18 1.7µm, 2.1 x 150mm column. The mobile phase contained acetonitrile and the aqueous component (0.1% formic acid) in volumetric proportions 10:90. The separation was achieved isocratically in a maximum time of 2.5 minutes. The step gradient method to 90% ACN in 0.01 minutes, followed by another isocratic plateau of 1.2 minutes, was used for a run to run washout (for elimination of residual endogenous matrix having an increased apolar character). The initial mobile phase composition was obtained after another stepwise modification of the mobile phase composition in 0.01 minutes and column equilibration took 0.5 minutes. The complete separation cycle took 3.5 minutes. The temperature of the column was set at 40°C with a flow rate of 0.25mL/min and an injection volume of 5µL was used. The internal standard chosen for the study was hydrochlorothiazide, a potent antihypertensive drug.

##### **7.4.2. Preparation of the hydrochlorothiazide and captopril calibration curves in plasma**

Individual stock solutions of 0.1mg/mL of the hydrochlorothiazide and captopril were prepared separately. Stock solutions (50µL) were then used to spike 500µL of blank blood plasma for calibration.

##### **7.4.3. Extraction of bioactives in blood plasma**

There are two phases to the sample preparation procedure:

- 1) Derivation which includes the separation of the blood plasma and the red blood cells
- 2) The protein precipitation in which all the protein in the plasma is precipitated out.

In the first phase 40mL of whole blood were collected into the anticoagulant and were centrifuged. On completion the plasma was separated using a micropipette. 1mL of the aliquot was mixed with the internal standard solution (0.1mL, 500ng/mL in aqueous 0.1%

formic acid), followed by the addition of the derivatisation reagent solution (0.05mL, 4mg/mL in acetonitrile). After vortexing (15 seconds at 2500 rpm), the solution was rested for 30 min for the completion of the derivatization. The samples were then frozen at -70°C and stored until further analysis was required.

The second phase consisted of the unassisted thawing of the samples in phase 1, at room temperature. After thawing the 0.2 mL of plasma was aliquoted in 0.4 mL of acetonitrile for protein precipitation. The mixture was then vortexed for 5 min at 2500 rpm and centrifuged at 3000 rpm for 10 min. The supernatant was injected into 2.5 mL vials after a further dilution with 0.4 mL of deionised water. Five microliters were then injected onto the chromatographic column.

The derivatization was performed immediately after the blood samples were withdrawn and the plasma preparation procedure was performed. This was done to increase the stability of the drug over the storage period under the freezing conditions. It should be noted that without the derivatization process, captopril would quantitatively oxidise to disulphide bonds over a period of three months at a storage temperature of -70°C. The internal standard was added prior to the addition of reagents, as well as the target compound due to its thiol functional group. It was expected that the internal standard would behave similarly to captopril, throughout the analytical method. To eliminate the focussing effects, water was added as a dilution solvent, especially when using a 90% acetonitrile aqueous phase during the chromatographic run.

### **7.5. Pharmacokinetic modelling and analysis of captopril and hydrochlorothiazide *in vivo***

The pharmacodynamics and pharmacokinetics were analysed using the PKSolver excel spreadsheet addition. The obtained data was used to model the trends in the pharmacodynamic and pharmacokinetic parameters. The evaluation of bioequivalence was made by the pharmacokinetic parameters  $AUC_{total}$  (area under plasma concentration-time plot until the last quantifiable value) and  $C_{max}$  observed (maximum plasma concentration) for captopril. Secondary ( $T_{max}$  sampling time of the maximum plasma concentration) and auxiliary ( $T_{half}$  terminal elimination half-life; percentage of  $AUC_{extra}$  with respect to  $AUC_{total}$ ; MRT, mean residence time) parameters were also determined.

## **7.6. Results and Discussion**

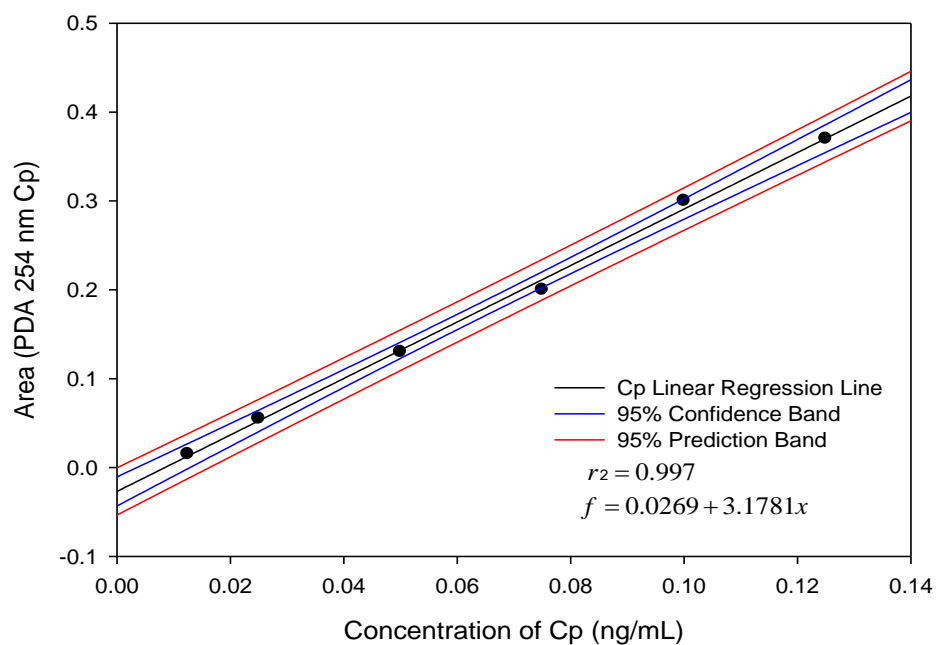
### **7.6.1. Method validation for captopril and hydrochlorothiazide in blood plasma**

The detector response function was evaluated over the concentration interval 2.5ng-1mg/mL, for blood plasma spiked with free captopril and prepared at six concentrations as described above in section 7.4.2. Three replicates were prepared for each concentration level. Relative standard deviations calculated at each of the concentration levels ranged from 0.1- 1.0%. The response function was found to be non-linear over the studied interval, also found (Georgita et al.,2008 and Medvedovici et al.,2009). To achieve linearization, the logarithm (10 base) of the peak ratio of captopril and internal standard derivation was represented against the logarithm of concentration. The log-log function was linear, being characterized by a correlation coefficient of 0.997, as seen in Figure 7.6, i and ii. The relative standard deviations found in each concentration of spiked plasma ranged between 3.2-7.6% interval for both captopril and hydrochlorothiazide.

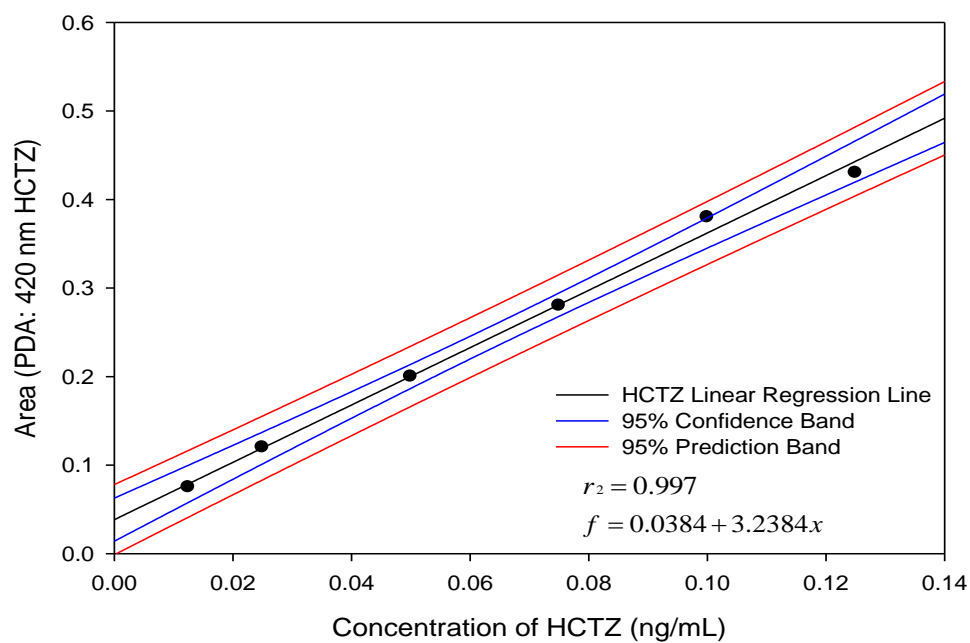
### **7.6.2. Recovery efficiency of captopril and hydrochlorothiazide**

Recovery of free captopril was evaluated by comparing the spike of captopril made in deionised water and blank plasma at 100ng/mL. Three replicates were made for the specified concentration level. Recovery was calculated as the percentage peak area in the chromatograph of the spiked captopril plasma from the peak area in the chromatogram of the corresponding spiked water sample. The internal standard was also considered for evaluation of the recovery at a single concentration level of 100ng/mL. The mean percentage recovery of captopril was 88% with a normal variation of  $\pm 4$ , ranging between 84 and 92%. For the internal standard mean recovery was calculated as 92%, with variation between 89 and 95%. These results demonstrate that the plasma matrix did not affect the derivation, isolation of the derivatives, their separation or ionization.

(i)



(ii)



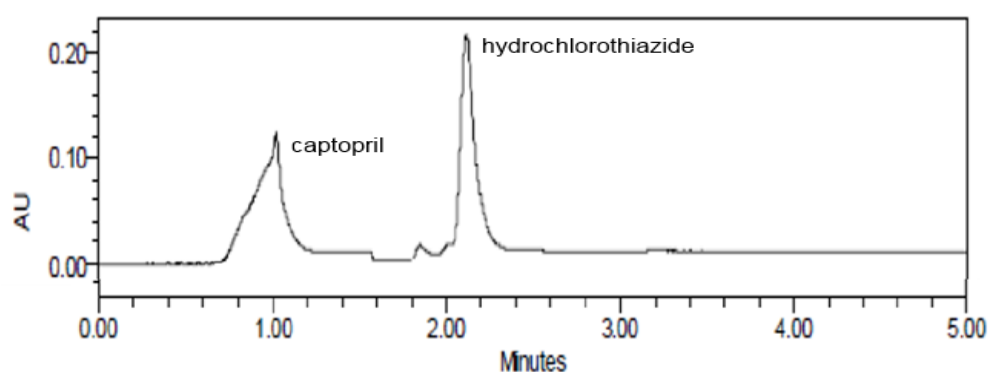
**Fig.7.6.** (i) Construction of the captopril calibration curve, (ii) hydrochlorothiazide abstracted from pig blood plasma.

### 7.6.3. *In vivo* blood analysis of captopril and hydrochlorothiazide

#### 7.6.3.1. Captopril and hydrochlorothiazide analysis using Ultra Performance Liquid Chromatography (UPLC)

The blank plasma samples did not yield any peak at the retention times of the analytes, when compared to the spiked drug samples, which indicated there was no interference and selectivity of the developed chromatograph method.

Figure 7.7 demonstrates the successful separation of captopril and hydrochlorothiazide from the spiked pig blood plasma. The UPLC assay method continued to perform in terms of accuracy in each analytical run. The method was successfully applied to accurately measure free captopril concentration on a large number of pig plasma from the bioequivalence study. A peak plasma concentration was observed generally about one hour after drug administration (Ohman et al., 1985). It was readily converted to its disulphide dimers and forms disulfide conjugates with endogenous thiol compounds. The major metabolic pathway for captopril involves not only the formation of its disulfide dimer but also of mixed conjugates with endogenous thiol-containing compounds and plasma proteins (Srinivas et al., 2003). The disulfide metabolites of captopril are inactive and there was evidence for their conversion back to the active form *in vivo* (Hadjmohammadi et al., 2008). This observation could explain the lack of concentration effect relationship for captopril metabolites. Figure 7.8 represents the concentration of blood plasma captopril from the ovalbumin captopril carrier system. It was evident that the concentrations of captopril *in vivo* were maintained constant, demonstrating the sustained release of captopril over the 24 hour period.



**Fig.7.7.** Separation of captopril and internal standard derivatives with hydrochlorothiazide from spiked plasma samples. Captopril was measured at a retention time of 1 minute and 2.2 minutes for hydrochlorothiazide.

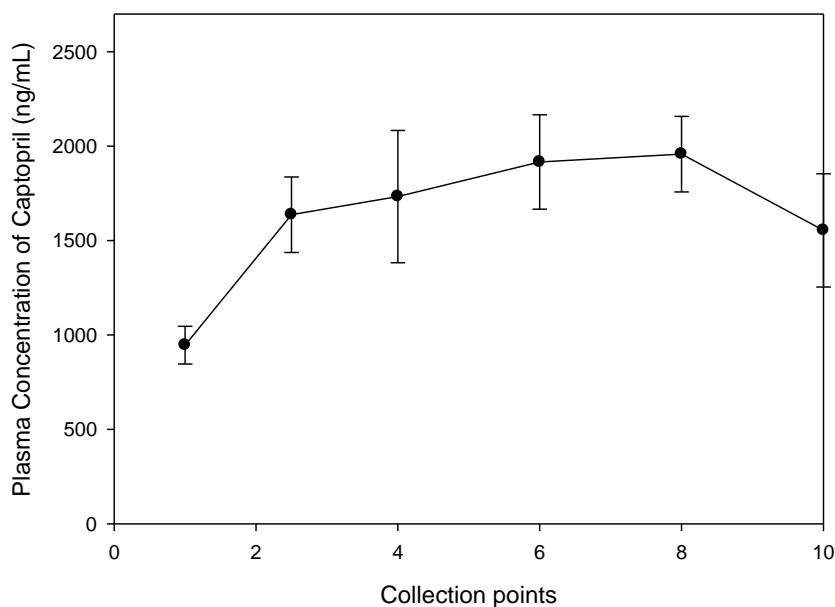


Fig.7.8. *in vivo* plasma concentration of captopril collected for 24 hours. The collection points represent times 2=4hr, 4=8hr, 6=12hr, 8=16hr, 10=24hr.

#### 7.6.3.1.2. Comparison of the pharmacokinetics parameters of the ovalbumin captopril carrier system against the conventional

The maximum reached concentration time curve ( $C_{max}$ ), area under the plasma concentration–time curve from 0 hour to the last measurable ( $AUC_0 - 24$  hour) and area under the plasma concentration–time curve from 0h to infinity ( $AUC_0 - \infty$ ) were compared and pharmacokinetic parameters were computed using WinNonlin Professional Software Version 4.0.1. Statistical calculations were defined at the level of  $P \leq 0.05$ . Bioequivalence for Capoten<sup>®</sup> and the ovalbumin drug carrier system formulations was concluded as the 95.0% confidence interval for  $C_{max}$ ,  $AUC_0 - t$  and  $AUC_0 - \infty$  fell within the range of 80.0–95.0% defined by both the Food and Drug Administration (FDA). According to literature the half-time of captopril was reported as 1-2 hour (Ohman et al., 1985), but in the ovalbumin drug carrier delivery system it was 5.6 hours. Pharmacokinetic parameters calculated for free captopril are represented in Table 7.2. From the experimental data, the bioequivalence between the two tested pharmaceutical formulations was determined with respect to the rate and extent of captopril absorption. The concentrations of captopril *in vivo* were within the therapeutic range.

**Table 7.2.** Statistic interpretation of pharmacokinetic parameters corresponding to captopril in tested pharmaceutical formulations against the reference (conventional) product.

Pharmacokinetic parameters	O		Conventional		Geometric mean ratio
	Mean	SD	Mean	SD	
AUC <sub>tot</sub> (ng/mL h)	625	37.2	526	26.7	1.188
AUC <sub>last</sub> (ng/mL h)	625	25.9	526	24.5	1.188
C <sub>max</sub> (ng/mL)	33.8	5.9	33.2	6.2	1.018
T <sub>max</sub> (h)	12	2.0	16	3.6	1.333
%AUC <sub>extra</sub>	0	-	0	-	0
T <sub>half</sub> (h)	5.65	3.9	1.42	0.29	1.275
MRT	7.83	34.7	2.44	8.7	3.558
E <sub>max</sub> (%)	0.046	-	0.022	-	-
EC50 (ng/mL)	4.074	-	0.499	-	-
R	0.929	-	0.753	-	-

T<sub>max</sub>, time to maximum concentration; C<sub>max</sub>, maximum concentration; AUC<sub>0–t</sub>, area under the curve of plasma concentration until the last concentration observed; AUC<sub>0–∞</sub>, area under the curve between the first sample and infinitive; T<sub>1/2</sub>, elimination half life.

### 7.7. Concluding Remarks

The ovalbumin drug carrier system demonstrated improved, drug release profiles *in vivo*, in addition increased the mean residence time, the half life and produced maintained relatively constant captopril concentration. There was correlation between the *in vivo* and *in vitro* drug release profiles of the ovalbumin drug carrier system, which proves that the system provided a better drug delivery system. The pharmacokinetic parameters determined *in vivo* also provide substantial evidence of a better drug delivery system in comparison to the conventional.

### Conclusions and Recommendations

#### 8.1. Conclusions

The synthesis of a multifunctional drug carrier system was to enable the bioconjugation of any thiol containing bioactive while remaining stable *in vitro* and *in vivo*. The novel ovalbumin polymer was used as the carrier because of its natural internally buried disulphide bonds that would provide an excellent potential site for bioconjugation. The FTIR was used to firstly monitor the reduction of the disulphide bonds buried in the interior of the ovalbumin polymer, resulting in the exposure of the resultant functional thiols. This process provided insight into the chemical behaviour of these functional thiols groups, in terms of their chemical properties. The thiols were successfully conjugated with the anti-hypertensive, captopril, resulting secondary conjugation of the ovalbumin thiols to an external source of thiols, forming disulphide bonds. The thiol redox responsive mechanism makes this system a novel innovative system for creating thiol functionalised drug delivery systems.

In order to create a drug delivery system, sodium alginate was used. Sodium alginate contains thiols that helped enable additional conjugation to ovalbumin and captopril thus allowing for the formation of a prolonged controlled drug delivery system. The successful Ovalbumin Drug Carrier Drug Delivery System was formulated.

Characterisation techniques were used to assess the, which include rheology, FTIR and the differential scanning calorimetry. These characteristics were determinable and employable for the characterisation of the drug delivery system. The extensive *in vitro* preliminary testing of each formulation was accomplished to produce an optimized design. Preliminary evaluation of dissolution and drug entrapment testing of the ovalbumin captopril carrier system established upper and lower limits for variant formulation parameters of ovalbumin polymer concentration, calcium chloride crosslinker and sodium alginate concentration. Similarly, the variables were deduced through dissolution.

A total of 15 formulations of the ovalbumin captopril carrier system were analysed by the Box-Behnken factorial design after individual formulation. The responses that were tested were fractional drug release, DEE and MDT. The average particle sizes and zeta-potentials were determined.

The optimised formulation produced improved drug release percentage, retention time and a prolonged controlled drug release system. The fabrications of the ovalbumin captopril carrier system particles were found to be spherically layered, with high drug entrapment.



Furthermore the mechanical strength and thermal of properties of the particles were found to be improved with the conjugation of the hydrogel and the crosslinker.

There was correlation between the *in vivo* and *in vitro* drug release of the ovalbumin captopril carrier system, which proves that the ovalbumin captopril carrier system provides a better drug delivery system because of the higher levels of captopril at 24 hour. The pharmacokinetic parameters determined *in vivo* also provide substantial evidence of a better drug delivery sytem in comparison to the conventional.

This study provides valuable information that can be employed in developing novel drug carriers for application in the oral delivery of thiol reactive drugs. The Box-Behnken quadratic design employed for the synthesis of the ovalbumin carrier system revealed the impact of thiol reactions on the physicochemical properties due to the variations in the levels of independent variables employed during the process of fabrication. The conjugation of the thiols to form disulphides, and the addition of a hydrogel proved to be efficient methods for the construction of the system. This indicates the efficiency of these methods as particles retained the contributing effects of individual chemical compounds characteristics that comprised each formulation. The physicochemical characteristics observed with the formulation imply that the carrier system explored in this investigation can be described as versatile which can make them attractive for the adaptive invention and construction of novel drug delivery systems. The statistical analysis data also confirmed the dependency of the measured physicochemical response parameters on the independent level. Physicochemical parameters which were selected, related to the application of the system, included particle size, zeta-potential, drug release and the mean dissolution time. The response and fitted values were closely related, indicating adequacy and reliability of the statistical design employed. Conclusively an optimised formulation was successfully design and the physicochemical properties revealed the potential of this matrix to be applied prolonged drug release systems.

## 8.2. Recommendations

The recommendations that could be made on the system would be to improve the bioconjugation of captopril to ovalbumin, using a more rigorous method such as photopolymerization. This would better ensure disulphide bond formation between polymers.

The *in vivo* analysis in the pig model posed a good choice for the analysis of the drug release, but the system would have to be tested in a human model to better improve and understand the mechanism of release. The ODCDS was found to be limited to thiol based bioactives, such as peptides and proteins. Maybe a broader ability of thiols to bind to a range of other chemical functional groups, such as halogens, epoxy and isocyanates would make this system a more approachable and user friendly site specific bioconjugation system.

**APPENDIX: A.1.**

**Animal Ethics Clearance Certificate**

AESC3



**STRICTLY CONFIDENTIAL**

**ANIMAL ETHICS SCREENING COMMITTEE (AESC)**

**CLEARANCE CERTIFICATE NO.** 2011/33/03

**APPLICANT:** Mr A Hibbins

**DEPARTMENT:** Pharmacy and Pharmacology

**PROJECT TITLE:** *In vivo* evaluation of polymeric oral drug delivery systems in Large White Pigs

**Number and Species**

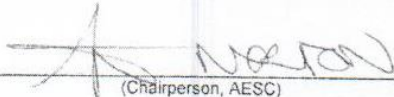
25 White pigs

Approval was given for to the use of animals for the project described above at an AESC meeting held on **06 September 2011**. This approval remains valid until **06 September 2013**.

The use of these animals is subject to AESC guidelines for the use and care of animals, is limited to the procedures described in the application form and to the following additional conditions:

Condition 1 - The PI to discuss appropriate anaesthetic combination with CAS Director and provide details of any known side effects.

Signed: \_\_\_\_\_

  
(Chairperson, AESC)

Date: \_\_\_\_\_

19/09/2011

I am satisfied that the persons listed in this application are competent to perform the procedures therein, in terms of Section 23 (1) (c) of the Veterinary and Para-Veterinary Professions Act (19 of 1982)

Signed: \_\_\_\_\_

  
(Registered Veterinarian)

Date: \_\_\_\_\_

20/09/2011

cc: Supervisor:  
Director: CAS

## **APPENDIX: B.1.**

### **Potential Publications:**

#### **Disulphide/Thiol Chemistry: A Multifaceted Versatile Tool for Macromolecular Design and Synthesis of Polyfunctional Material and Polymer for Drug Delivery** Abstract

The review highlights recent interests and applications of disulphide and thiol chemistry in creating contemporary macromolecular designs. Due to the chemical nature of disulphides and thiols a wide range of chemical species react with these functional groups to yield a variety of polymers extending their applications in chemical, biological, physical, material engineering and material sciences. The review aims to illustrate the versatility and demonstrate the potential of thiol-based chemistries. The focus is on exploring bio-cleavable disulphides and linking by “clicking” thiols via thiol/other functional group exchange reactions. Thiol synthesis, modification and functionalization are demonstrated to be highly attractive and efficient in polymer and material science. The review also illustrates the remarkable pliability of synthetic and natural approaches to designing, optimizing and functionalizing nanostructures and conjugates by thiol chemistry modification. The examples quoted in the review illustrate the power and versatility of thiols for site specific functionalization, the construction of complex macromolecules and the generation of both biodegradable disulphides and non-biodegradable bonds. In addition, the ability of thiols to react with various functional groups found in a variety of polymer science materials and biological entities such as peptide and related structures will also be demonstrated. In spite of the fact that research efforts in thiol chemistry are still at the early stages, it is likely that its true potential will be developed.

**Keywords:** Bio-cleavable disulphides, disulphide chemistry, macromolecules, nanostructures, thiol chemistry

## APPENDIX: B.2.

### Optimisation of the Novel Polyfunctionalised Drug Carrier System.

Teboho Kgesa, Yahya E. Choonara, Valence M.K. Ndesendo, Lisa du Toit and Pradeep Kumar, Viness Pillay\*<sup>1</sup>

<sup>1</sup>University of the Witwatersrand, Faculty of Health Sciences, Department of Pharmacy and Pharmacology, Johannesburg, South Africa, 2050

Correspondence to: [Viness.Pillay@wits.ac.za](mailto:Viness.Pillay@wits.ac.za)

#### ABSTRACT

As part of the developing novel drug delivery systems, thiol-based chemical reactions are distinctive role players in stabilizing macromolecules for use in material science especially in polymer interactions. This research focused on the construction, characterisation and optimisation of the thiol conjugated complex for sustained oral drug delivery. An interphase, co-particulate homogenization technique and lyophilisation guided through a Box Behnken experimental design was employed in the synthesis, characterisation and optimization of the 15 thiol carrier drug delivery systems. The results demonstrate the successful conjugation of the protein to the drug as demonstrated by the FTIR and differential scanning calorimetry results. The effects of different factor levels on the characterisation *in vitro* physicochemical performances of the thiol carrier drug delivery systems were explored. Drug loading was achieved (38-46±7.2mg). Overall amount of drug release in 24 hour was measured by the mean dissolution time value which ranged between 3.015-7.12 hours and demonstrated zero-order drug release profiles. The formulation demonstrated significant levels of the zeta potential which ranged between  $-13.6 \pm 0.53$  and  $-29.4 \pm 0.31$ mV. The size of the particles were measured (99.78±7.23 and 255.6± 23.73). The particles were mostly spherical in shape. Statistical constraints were simultaneously set to obtain levels of independent variables that optimised the thiol carrier drug delivery system. The investigation demonstrates the potential use of natural proteins in designing, optimising and functionalising nanostructures and conjugates by thiol chemistry modification. In conclusion, our validated method was successfully applied to pharmacokinetic studies of thiol containing bioactives in plasma samples.

**KEYWORDS:** Thiol, disulphide bonds, ovalbumin, captopril, conjugate.